A Dissertation of the Doctor of Philosophy

Targeting glucose metabolism as an anticancer strategy in ovarian cancer

당 대사 조절을 통한 난소암 특이적 세포사멸 유도 및 항암제 내성 극복 연구

February 2016

Seoul National University

Department of Agricultural Biotechnology

Biomodulation Major

HyeRan Gwak

Abstract

There has been a growing interest in cancer metabolism for targeted therapeutic approach for cancer, however; we still do not fully understand the signatures of metabolic alterations and modulating factors. In current studies, we provide novel insights of glucose metabolism and regulations in ovarian cancer. Resveratrol (RSV), a natural compound from grapes, selectively impairs glucose uptake via disruption of GLUT1 localization via suppression of the action of Akt in ovarian cancer cells. Inhibition of glucose uptake by RSV leads disruption of protein N-linked glycosylation (NLG) through suppression of hexosamine biosynthetic pathway, which regulated by GSK3β. Akt/GSK3β axis involves in RSV induced NLG disruption in ovarian cancer cells. Moreover, disruption of NLG by RSV leads to endoplasmic reticulum (ER) stress-mediated apoptosis in a cancer-specific manner.

Mimicking glucose availabilities enhance cisplatin responses and suppress membrane expression of ATP-binding cassette

transporters (ABC transporters), resulting from N-linked glycosylation (NLG) defect in drug-resistant ovarian cancer cells. NLG of ABC transporters is regulated by GSK3β activation through AMPK cascade in response to glucose limitation. Moreover, glucose deficiency attenuates the ovarian cancer stem-like cells (CSC) phenotypes, sphere forming capacities and stemness related gene expressions. Associated with that, glucose restriction suppresses Wnt/β-catenin signaling through decrease of β-catenin nuclear expression by GSK3β activation. Our findings provide evidence that glucose plays a pivotal role in controlling drug resistance in ovarian cancer. Hence, better understanding of differences in metabolic phenotypes between cancer cells and normal cells might offer to novel anticancer strategies.

Keyword : Ovarian cancer, Chemoresistance, Glucose metabolism, Glycosylation, ER stress, Resveratrol

Student Number : 2010-22849

Aberration

RSV; resveratrol

2-NBDG; [2-[N-(7-nitrobenz-2-oxa-1,3-diazol-4-yl)amino]-2-deoxyglucose

G.F; glucose-free media

GLUT1; glucose transporter 1

CA-Akt; constantly activated Akt

OSE; normal ovarian epithelial cells

PBMC; pheripheral blood mononuclear cells

RBC; red blood cells

NLG; N-linked glycosylation

TM; tunicamycin

ER; endoplasmic reticulum

PERK; protein kinase R (PKR)-like endoplasmic reticulum kinase

IRE1α; inositol-requiring enzyme 1α

ATF6α; activating transcription factor 6α

GADD153; growth arrest and DNA damage induced gene-153

GSK3β; glycogen synthase kinase-3

ENTPD5; ectonucleoside triphosphate diphosphohydrolase 5

CDDP; cisplatin

ABC transporters; ATP-binding cassette transporters

AMPK; 5' adenosine monophosphate-activated protein kinase

Table of Contents

Chapter 1. Introduction

1.1. Ovarian cancer

Ovarian cancer is the most lethal gynecologic cancers in world wide. There are no significant symptoms and detection methods for early detection, so it diagnoses late stage and majority patients with ovarian cancer experienced recurrence and failure of second treatment. More strikingly, the ovarian cancer-related death rates have not been changed for past forty years (1, 2). The lack of successful treatment strategies led the wide genome analysis for finding targeted molecule for better clinical outcome of ovarian cancer. Based on the TCGA data, p53 mutations are appeared in 96% high-grade serous (HGS) ovarian cancer samples; and BRCA mutations are observed. And also there are some other significantly mutated genes are appeared, but only less than 10% of HGS-ovarian cancer samples. Interestingly, PI3K/RAS pathways are deregulated overall 50% in HGS-ovarian cancer samples (3). PI3K/RAS signaling is suggested the central dogma of the cancer metabolism and its mutations are strongly associated with chemoresistance and poor prognosis in ovarian cancer (4, 5).

1.2. Cancer metabolism

Reprogramming of cancer metabolism elucidates as a new caner hallmark and a potent therapeutic target (6). However, dysregulated metabolism in cancer therapy has not been specifically subjected yet,

even though highly related in clinical area (7). For energy generation, glucose is the main energy source for cancer cells. Cancer reprogrammed their glucose metabolism to aerobic glycolysis (Warburg effect) for fast energy generation and proliferation (8). The metabolic changes are common feature of cancerous cells and it seems to be absolutely required for malignant transformation. This shift makes cancer cells to acquire high rate of glucose uptake and as a consequence, metabolic regulatory mechanisms are highly up-regulated (7, 9). Preference of glucose utilization, tumor metabolic parameter [^{18}F] fluorodeoxyglucose (FDG) positron emission tomography (PET), is an effective in diagnostic tool for cancer (10). The aberrant glucose metabolism in cancer is committed by many oncogenes, such as *PI3K/AKT/mTOR*. These signaling are the most altered oncogenic signaling cascades in cancers (11, 12). With these characteristics of cancers, epidemiological data suggest that metabolic disorders, such as diabetes and obesity are the risk factor of cancer and reduce cancer-related mortality (13-16).

1.3. Protein glycosylation

Glucose does not act as an only for energy production but also it has a role as a signaling regulator through protein modification, such as glycosylation and acetylation (17). N-linked glycosylation (NLG) only

occurs in mammalian cells and it has important roles in maturation, quality control of proteins, cell adhesion and signaling. NLG regulations are controlled by the presence of glucose and uridine diphosphate-N-acetylglucosamine, which is glucose metabolite through hexosamine biosynthetic pathway. In various cell-surface proteins, growth factor receptor (GFRs) and nutrient transporters are need to be N-linked glycosylated for their capacities to bind to the plasma membranes of the cells (17, 18). Interestingly, changes in the NLG patterns are frequently observed in various types of cancer and these phenomena lead the tumor progression, such as aberrant glycosylated GFRs constantly activate without genetic alterations (19, 20). However, the understanding of the biological relevance between the cellular metabolism and glycosylation are poorly defined.

1.4. Endoplasmic reticulum stress

The endoplasmic reticulum (ER) is the main subcellular compartment involved in protein and lipid synthesis and maturation, and cell death (21). By nutrients depletion, redox imbalance, and other stimuli easily interrupt protein modification and with accumulation of malfunction protein, induced unfolded protein responses (UPR) by activating three major ER stress sensors, protein kinase RNA-like ER kinase (PERK), inositol-requiring enzyme 1α (IRE-1α), and activating

transcription factor (ATF) 6α. These ER stress sensors trigger cellular adaptation to accumulation of the malfunction proteins that restores normal cell function or induces programmed cell death. One of the mechanisms underlying the shift of ER stress from adaptive to pro-apoptotic responses are enhancement the expression of ATF4 and GADD153 (also known as CHOP, *DDIT3*) (21). However, the signal kinetics that activates ER stress under various conditions is still remained unclear.

1.5. Glucose metabolism in Ovarian cancer

Epidemiological data suggested that ovarian cancer patients with high levels of glucose in serum have been experienced disease recurrence and poor survival rate. And ovarian cancer patient with type 2 diabetes have poor prognosis (22). Based on these observations, glucose is suggested prognostic marker and therapeutic target for ovarian cancer (23). With metabolic abnormalities, ovarian cancer highly demands on glucose uptake and these phenomena are associated with glycan expression (17, 24). In cancer, membrane-associated glycans (mucins) are overexpressed and these unique features are suggested as diagnosis tools and therapeutic targets (25, 26). Monitoring CA125 (cancer associated glycan) in blood serum levels is useful for diagnostic tool, therapeutic response and progression of

ovarian cancer (27, 28). However, the expression profile and the function of glycan in ovarian cancer have not been analyzed yet. Previous studies suggested that regulation of glucose metabolism could be the key to overcome the chemoresistance in ovarian cancer; however we still not fully understand how glucose metabolism acts in the ovarian cancer (29-31).

1.6. References

1. Bast RC, Jr., Hennessy B, Mills GB. The biology of ovarian cancer: new opportunities for translation. Nat Rev Cancer. 2009;9(6):415-28.
2. Park B, Park S, Kim TJ, Ma SH, Kim BG, Kim YM, et al. Epidemiological characteristics of ovarian cancer in Korea. Journal of gynecologic oncology. 2010;21(4):241-7.
3. Bell D, Berchuck A, Birrer M, Chien J, Cramer DW, Dao F, et al. Integrated genomic analyses of ovarian carcinoma. Nature. 2011;474(7353):609-15.
4. Dobbin ZC, Landen CN. The Importance of the PI3K/AKT/MTOR Pathway in the Progression of Ovarian Cancer. International journal of molecular sciences. 2013;14(4):8213-27.
5. Jung G, Lee Y, Oh S, Byun J, Ryu I, Kim S, et al. Comparison of 18F-FDG PET/CT and CT or MRI for the Preoperative Staging of Ovarian Cancer. Am J Roentgenol. 2007;188(5).
6. Hanahan D, Weinberg RA. Hallmarks of cancer: the next generation. Cell. 2011;144(5):646-74.
7. Zhao Y, Butler EB, Tan M. Targeting cellular metabolism to improve cancer therapeutics. Cell death & disease. 2013;4:e532.
8. Sandulache VC, Ow TJ, Pickering CR, Frederick MJ, Zhou G, Fokt I, et al. Glucose, not glutamine, is the dominant energy source required for proliferation and survival of head and neck squamous carcinoma cells. Cancer-Am Cancer Soc. 2011;117(13):2926-38.
9. Cancer: Blocking tumour sugar metabolism. Nature. 2012;483(7391):512-.
10. Gwak H, Haegeman G, Tsang BK, Song YS. Cancer-specific interruption of glucose metabolism by resveratrol is mediated through inhibition of Akt/GLUT1 axis in ovarian cancer cells. Mol Carcinog. 2014.
11. Engelman JA. Targeting PI3K signalling in cancer: opportunities, challenges and limitations. Nat Rev Cancer. 2009;9(8):550-62.
12. Fruman DA, Rommel C. PI3K and cancer: lessons, challenges and opportunities. Nat Rev Drug Discov. 2014;13(2):140-56.
13. Vigneri P, Frasca F, Sciacca L, Pandini G, Vigneri R. Diabetes and cancer. Endocr-Relat Cancer. 2009;16(4):1103-23.
14. Gallagher EJ, LeRoith D. Obesity and Diabetes: The Increased Risk of Cancer and Cancer-Related Mortality. Physiol Rev. 2015;95(3):727-48.
15. Cantiello F, Cicione A, Salonia A, Autorino R, De Nunzio C, Briganti A, et al. Association between metabolic syndrome, obesity, diabetes mellitus and oncological outcomes of bladder cancer: a systematic review. International journal of urology : official journal of the Japanese Urological Association. 2015;22(1):22-32.
16. Garg SK, Maurer H, Reed K, Selagamsetty R. Diabetes and cancer: two

diseases with obesity as a common risk factor. Diabetes Obes Metab. 2014;16(2):97-110.
17. Wellen KE, Thompson CB. A two-way street: reciprocal regulation of metabolism and signalling. Nat Rev Mol Cell Bio. 2012;13(4):270-U1.
18. Dennis JW, Nabi IR, Demetriou M. Metabolism, Cell Surface Organization, and Disease. Cell. 2009;139(7):1229-41.
19. Lau KS, Dennis JW. N-Glycans in cancer progression. Glycobiology. 2008;18(10):750-60.
20. Miwa HE, Koba WR, Fine EJ, Giricz O, Kenny PA, Stanley P. Bisected, complex N-glycans and galectins in mouse mammary tumor progression and human breast cancer. Glycobiology. 2013;23(12):1477-90.
21. Hetz C, Chevet E, Harding HP. Targeting the unfolded protein response in disease. Nat Rev Drug Discov. 2013;12(9):703-19.
22. Bakhru A, Buckanovich RJ, Griggs JJ. The impact of diabetes on survival in women with ovarian cancer. Gynecol Oncol. 2011;121(1):106-11.
23. Lamkin DM, Spitz DR, Shahzad MM, Zimmerman B, Lenihan DJ, Degeest K, et al. Glucose as a prognostic factor in ovarian carcinoma. Cancer-Am Cancer Soc. 2009;115(5):1021-7.
24. Palorini R, Cammarata F, Balestrieri C, Monestiroli A, Vasso M, Gelfi C, et al. Glucose starvation induces cell death in K-ras-transformed cells by interfering with the hexosamine biosynthesis pathway and activating the unfolded protein response. Cell death & disease. 2013;4.
25. Christiansen MN, Chik J, Lee L, Anugraham M, Abrahams JL, Packer NH. Cell surface protein glycosylation in cancer. Proteomics. 2014;14(4-5):525-46.
26. Singh AP, Senapati S, Ponnusamy MP, Jain M, Lele SM, Davis JS, et al. Clinical potential of mucins in diagnosis, prognosis, and therapy of ovarian cancer. Lancet Oncol. 2008;9(11):1076-85.
27. Theriault C, Pinard M, Comamala M, Migneault M, Beaudin J, Matte I, et al. MUC16 (CA125) regulates epithelial ovarian cancer cell growth, tumorigenesis and metastasis. Gynecol Oncol. 2011;121(3):434-43.
28. Chauhan SC, Kumar D, Jaggi M. Mucins in ovarian cancer diagnosis and therapy. Journal of ovarian research. 2009;2(1).
29. Priebe A, Tan LJ, Kueck WA, He G, Kwok R, Opipari A, et al. Glucose deprivation activates AMPK and induces cell death through modulation of Akt in ovarian cancer cells. Gynecologic Oncology. 2011;122(2):389-95.
30. Liu PP, Liao J, Tang ZJ, Wu WJ, Yang J, Zeng ZL, et al. Metabolic regulation of cancer cell side population by glucose through activation of the Akt pathway. Cell Death Differ. 2014;21(1):124-35.
31. Munoz-Pinedo C, El Mjiyad N, Ricci JE. Cancer metabolism: current perspectives and future directions. Cell death & disease. 2012;3:e248.

Chapter 2.

Cancer-specific interruption of glucose metabolism by resveratrol is mediated through inhibition of Akt/GLUT1 axis in ovarian cancer cells

Abstract

The metabolic phenotype of cancer is considered an ideal target for anticancer therapy. In ovarian cancer, glucose transporter 1 (GLUT1) is overexpressed and positron emission tomography (PET) using [18^{F}] fluorodeoxyglucose (FDG), as a metabolic tumor parameter, has been found to be an effective diagnostic tool. In this study, we have characterized the selective cytotoxicity of resveratrol (RSV) in ovarian cancer cells through glucose metabolism regulation via GLUT1 modulation. We have demonstrated that, in contrast to primary normal ovarian epithelial cells, RSV selectively inhibited glucose uptake and induced apoptosis irrespective of p53 status *in vitro*. RSV had no affect on GLUT1 mRNA and protein expressions but interrupted intracellular GLUT1 trafficking to the plasma membrane. Suppressed plasma membrane GLUT1 localization in ovarian cancer was found to be associated with the inhibition of Akt activity by RSV, as confirmed by the action of the Akt inhibitors (LY294002 and Akt inhibitor IV), as well as overexpression of a constitutive active form of Akt. Taken together, these findings suggested that RSV induced apoptosis in ovarian cancer cells by impairing glucose uptake, a process involving Akt-regulated plasma membrane GLUT1 trafficking.

2.1. Introduction

Ovarian cancer is the most lethal gynecologic malignancy. The five year survival rate for advanced disease is just thirty percent. The fatality of this disease results mainly from two factors: 1) late stage diagnosis, and 2) relapse with resistance to subsequent chemotherapy. The most common genetic changes in ovarian cancer are p53 mutation and upregulation of the PI3K/Akt/mTOR pathways. These genetic alterations are closely linked to chemoresistance and metabolic remodeling in cancer (1, 2).

Cancer cells reprogram their energy metabolism in favor of the glycolysis-dominant mechanism to ensure rapid energy generation for cell proliferation. These metabolic changes are common features of cancer cells and seem to be required for malignant transformation. This shift enables cancer cells to acquire a high rate of glucose uptake, and as a consequence, the glucose transporter (GLUT) gene is highly up-regulated (3, 4).

With this metabolic characteristic, the glucose analogue, [18^{F}] fluorodeoxyglucose (FDG) positron emission tomography (PET), is effective in diagnostic localization of ovarian cancer (5, 6). The

standardized uptake value (SUV) of FDG in ovarian cancer is associated with GLUT1 expression and correlated with aggressive tumor behavior and overall survival of patients (7, 8). Epidemiological data suggest that dysregulation of glucose metabolism in ovarian cancer could be a therapeutic strategy and a key to overcome the chemoresistance (9, 10).

Many dietary phytochemicals have been demonstrated to have cancer-specific, cytotoxic actions through modulation of multiple targets, including those of metabolic pathways. Resveratrol (RSV), a phytochemical present in various fruits including grapes, has been studied for its anticancer effects *in vivo* and *in vitro* (11). Recent studies described that RSV inhibited the glucose metabolism and induced autophagy (12, 13). However, the mechanism(s) by which RSV induces cytotoxicity in ovarian cancer cells, particularly in relation to altered energy metabolism, remain unclear. Here, we hypothesized that RSV inhibits glucose metabolism and induces apoptosis in a cancer cell-specific manner, a process involving the regulation of GLUT1.

2.2. Materials and methods

2.2.1. Ovarian cancer cell lines and culture conditions

Human ovarian cancer cell lines PA-1 (p53 wild type), OVCAR3, MDAH2774 (p53 mutant) and SKOV3 (p53 null) used in this study were from ATCC. With the exception of PA-1, these cell lines were grown in RPMI 1640 (WelGENE, Seoul, Korea) at 37˚C in 5% CO_2 and humidified atmosphere. PA-1 was cultured in MEM (WelGENE, Seoul, Korea). All culture media were supplemented with 10% fetal bovine serum (FBS) (Gibco-BRL, Gaithersberg, MD) and 100 μg/mL penicillin-streptomycin (P/S) (Invitrogen, Carlsbard, CA).

2.2.2. Normal ovarian epithelial cell culture

For normal ovarian surface epithelial cells, we followed the IRB-approved protocol (C-1307-008-502). Normal ovarian epithelial cells were isolated with Dispase (Gibco-BRL, Gaithersberg, MD) from fresh ovarian tissue (14). Isolated normal epithelial cells were maintained in MCDB105 and M199 (1:1) media, containing 10% FBS and 100 μg/mL P/S at 37˚C in 5% CO_2 and humidified atmosphere. All experimental procedures were performed within third passages of culture.

2.2.3. Peripheral blood mononuclear cells and red blood cell isolation

For human PBMC (Peripheral blood mononuclear cells) and RBC (red blood cell) isolation, we followed the IRB-approved protocol (C-1307-008-502). The buffy coats from healthy donors were used for normal control. We isolated PBMC and RBC by a density gradient centrifugation on Ficoll-Paque^{TM} PREMIUM, according to the manufacturer's protocol. Cells were maintained in RPMI 1640 media containing 10% FBS and 100 μg/mL P/S.

2.2.4. Reagents and antibodies

Stock solutions of resveratrol and fasentin (Sigma-Aldrich, St. Louis, MO), LY294002 (Cayman, MI), and Akt Inhibitor IV (Calbiochem, San Diego) were freshly prepared in dimethyl sulfoxide (DMSO; 0.001%) and used at the final concentrations indicated. Thiazolyl blue tetrazolium bromide (MTT) (Amresco, Solon, OH) and Ficoll-Paque^{TM} PREMIUM (GE Healthcare, NJ) were used for this study. Glucose - free media was purchased from Gibco-BRL. GLUT1, Akt and phospho-Akt (Ser473) were purchased from Santa Cruz Biotechnology (Santa Cruz, CA) and phospho-Akt (Thr308), phospho-mTOR, phospho-P70S6K, phospho-4EBP1 (Ser 65 and Thr37/46) and pan Cadherin were purchased from Cell Signaling (Danvers, MA). The α-tubulin antibody was obtained from Sigma-Aldrich. Alexa Fluor

conjugated anti-rabbit antibody was obtained from Invitrogen (Carlsbad, CA).

2.2.5. Glucose uptake assay

Glucose uptake was assessed using 2-NBDG [2-[N-(7-nitrobenz-2-oxa-1,3-diazol-4-yl)amino]-2-deoxyglucose (Cayman, MI) (15). Briefly, cells were plated (up to 24 h) onto coverglass-bottom dish (SPL Lifesciences, Gyeonggi-do, Korea) and then cultured (6 h) with or without Resveratrol (50 μM), LY294002 (20 μM), and Akt inhibitor IV (1 μM). The cells were then incubated in the dark with 2-NBDG (50 μM; 30 min) at 37˚C in 5% CO_2 humidified atmosphere. Before measurement each plate was washed with PBS (phosphate buffered saline) and images were captured by confocal microscopy (excitation/emission = 488/535 nm). Original magnification was 400X for all panels.

For flow cytometric analysis of 2-NBDG uptake, cells were plated (up to 24 h) onto 6-well plate and then treated (6 h) with resveratrol (50 μM), fasentin (50 μM) or DMSO. The cells were then incubated in the dark with 2-NBDG (50 μM; 30 min) at 37˚C in 5% CO_2 humidified atmosphere. Before measurement each cells were detached with EDTA (Ethylenediaminetetraacetic acid, 5mM) and washed twice with cold PBS and cells were analyzed with flow

cytometer with FITC channel, respectively.

For PBMC and RBC assessment, cells were incubated (6 h) in 5 ml of RPMI-1640 with or without RSV (50 μM) and co-incubated (30 min) with 2-NBDG (50 μM). They were washed twice with HBSS and analyzed by flow cytometry.

2.2.6. Cell viability assay

Cell viabilities were evaluated by the MTT assay. Cells were seeded in 96-well plate. After overnight incubation, RSV (50 μM) containing media or glucose-free media were adjusted to a final volume of 100 μl/well for indicated time. The cells were incubated with 50 μl MTT (2mg/ml; 3 h, 37˚C) in 5% CO_2 in humidified atmosphere and subsequently solubilized in DMSO (100 μl). The optical density at 540 nm was determined, using an enzyme linked immunesorbent assay reader.

2.2.7. Flow cytometric analysis

Apoptotic cell death was determined by flow cytometric analysis, using the Annexin V-FITC apoptosis detection kit (BD Pharmingen, CA, USA). Cells were prepared according to the manufacturer's protocol and analyzed within 1 h.

.

2.2.8. Immunofluorescence microscopy.

Cells were plated onto 8-well chamberslide (Lab-Tek, NUNC, Wiesbaden, Germany) and incubated with the test agents. The cells were fixed with 4% paraformaldehyde, permeabilized with 0.2% of Triton X-100, and blocked with 5% of goat serum. The anti-GLUT1 antibody (1:250), Alexa Fluor conjugated anti-rabbit antibody (1:250) and the membrane specific dye (CellMask™ Deep Red Plasma membrane Stain, Invitrogen) were used for GLUT1 membrane localization. Imaging was performed using a Zeiss Pascal 5 confocal imaging system (Carl Zeiss MicroImaging). Original magnification was 400X for all panels, respectively.

2.2.9. RT-PCR

Total RNA was isolated with the TRIZOL reagent (Life Technologies, Gaithersburg, MD) and cDNAs were synthesized from 1 μg total RNA, using M-MLV reverse transcriptase (Invitrogen, Carlsbad, CA) with random oligomer priming. PCR was performed with specific primers GLUT1 sense 5’ – GCA AGT CCT TTG AGA TGC TGA TCC – 3’, antisense 5’ – GCC GAC TCT CTT CCT TCA TCT CC – 3’ and sense 5′-GCC ATG GAG CCC AGC AGC AAG-3′, antisense 5′- CAC TTG GGA ATC AGC CCC CAG - 3′ (16, 17), GLUT2 sense 5' - CGT CTC CTT TGA CAT TTC CTT C - 3',

antisense 5'- GGT GGA GAA AAC AGC CTA GAG AT - 3' (18), GLUT3 sense 5′- AAA GTC CCT GAG ACC CGT GGC AGG -3′, antisense 5′ - AAG ATC CAA CAA ACC GCA GCC TTG - 3′ (19), GLUT4 sense 5' - GCA CCG CCA GGA CAT TGT TG - 3', antisense 5' - CGC AGA ATT CCC CCC TCA GCA GCG AGT GA - 3' (20) and ß-actin sense 5'- ACA CTG CCA TCT ACG AGC - 3', antisense 5'- AGG GGC CGG ACT CGT CAT ACT - 3' using the following amplification conditions: denaturation (94˚C, 30 sec), annealing (60˚C, 30 sec), and extension (72˚C, 1 min) followed by 36 cycles (72˚C,10 min).

2.2.10. Western blotting

Protein lysates were prepared as described previously (21). In brief, after cell extraction, proteins were separated by SDS/PAGE (6 to 12% gel, depending on specific protein assessed) followed by electrotransfer on to nitrocellulose membranes and probed with the indicated antibodies.

2.2.11. Transient transfection

Human constitutively active Akt containing plasmid (CA-Akt) was generously provided by Prof. Kangyeol Choi (Yeonsei University, Korea) (22). All cell lines were transiently transfected using Mirus

reagent (Mirus Bio LLC, Madison), according to the manufactures' protocols.

2.2.12. Statistical analysis

Statistical analysis was performed with the PASW statistics 18 software, including the Student T-test. Statistical significant differences were considered as* *$p<0.05$, **$P<0.01$ and ***$P<0.001$*.

2.3. Results

2.3.1. RSV inhibits glucose uptake in ovarian cancer cells

Clinical and experimental studies strongly suggest the importance of glucose metabolism in ovarian cancer (9). Previous studies demonstrated that resveratrol (RSV) inhibited glucose metabolism and induced autophagy (12, 13). However, the mechanisms of RSV effects on glucose metabolism in ovarian cancer remain unclear. Here, we characterized the selective cytotoxicity of RSV in ovarian cancer cells through glucose uptake dysregulation. First, we examined the ability of RSV to inhibit glucose uptake in four human ovarian cancer cell lines with various genetic backgrouds [PA-1 (wild type), SKOV3 (null), OVCAR3 and MDAH2774 (mutant)] with the fluorescently labeled glucose probe [2-[N-(7-nitrobenz-2-oxa-1,3-diazol-4-yl)amino]-2-deoxyglucose (2-NBDG) (15). RSV (50 μM) significantly suppressed glucose uptake in all four cell lines within 6 hours of treatment (Fig 1A) (23). Associated with the inhibition of glucose uptake, RSV significantly reduced cell viability in a time–dependent manner when compared with control (DMSO treated). Glucose starvation by culturing the ovarian cancer cells in glucose free media also decreased cell viabilities (Fig 1B). Apoptosis response in

the four ovarian cancer cell lines (as determined by Annexin V/PI staining) was induced in a time - dependent (24 to 48 hours) manner by RSV (50 μM) and glucose starvation (Fig 1C). These data demonstrated that glucose is an essential metabolite to ovarian cancer proliferation and RSV impaired glucose consumption and induced cell death in ovarian cancer cells.

A.

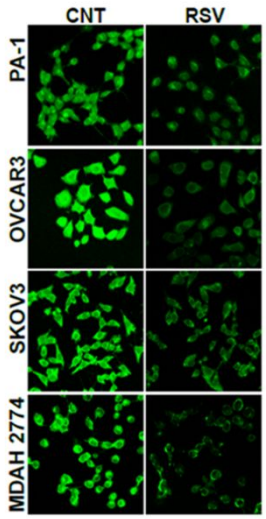
CNT
RSV
PA-1
OVCAR3
SKOV3
MDAH 2774

B.

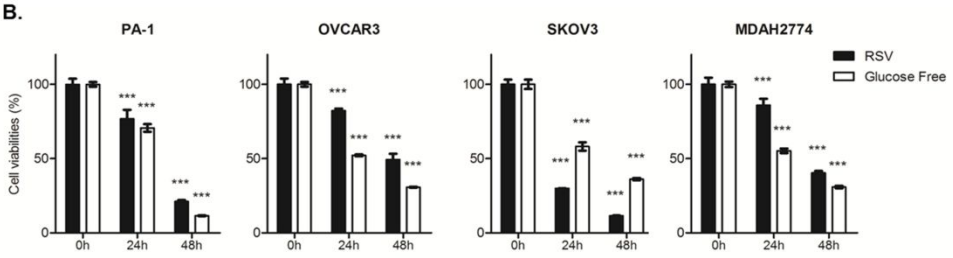
PA-1
OVCAR3
SKOV3
MDAH2774
RSV
Glucose Free
Cell viabilities (%)
0h
24h
48h

C. (1)

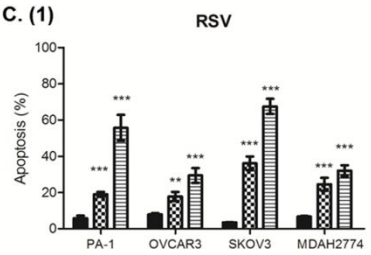
RSV
Apoptosis (%)
PA-1
OVCAR3
SKOV3
MDAH2774

(2)

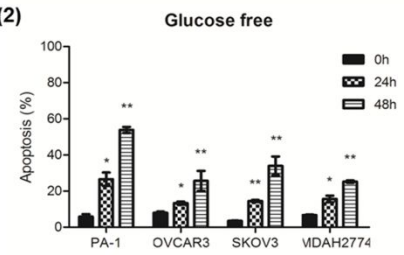
Glucose free
0h
24h
48h
Apoptosis (%)
PA-1
OVCAR3
SKOV3
MDAH2774

Figure 1. Effects of RSV on the glucose uptake and the cell death.

A. Glucose uptake inhibition effect of RSV in ovarian cancer cells. All four ovarian cancer cell lines were treated with RSV (50 μM) or DMSO as a control for 6 hours and co-treated with 2-NBDG (50 μM) for 30min. Then intracellular level of 2-NBDG was measured with confocal microscopy. Original magnification 400X for all panels.

B. Growth inhibition effect of RSV in ovarian cancer cells. Each cancer cell line was treated with RSV (50 μM), glucose-free media or DMSO (control) for 0 to 48 hours. After the indicated times, cell viability was validated with the MTT assay. All experiments were repeated in triplicate and data were expressed as mean ± SEM. ****P<0.001,* control versus RSV or glucose free media treatment.

C. Induction of apoptosis by RSV in ovarian cancer cells. Four ovarian cancer cell lines were incubated with 1) RSV (50 μM) or 2) glucose free media and corresponding DMSO controls for 0 to 48 hours. Annexin V/PI staining was performed to assess apoptotic cell death. All experiments were repeated in triplicate and data were expressed as mean ± SEM. * *p<0.05, **P<0.01, and ***P<0.001,* control versus RSV or glucose free media treatment.

2.3.2. Plasma membrane localization of GLUT1 is attenuated with RSV treatment

To determine the mechanism of the dysregulation of glucose uptake by RSV, gene expression of the glucose transporters GLUT1 to GLUT4 in samples with ovarian cancer patients and normal ovarian epithelial (Fig 2A) as well as ovarian cancer cells was compared with normal ovarian surface epithelial cells (Fig 2B). GLUT1 mRNA expressions are significantly up-regulated in ovarian cancer cells than normal ovarian surface epithelia (OSE; Fig 2A, 2B). Thus we focused on GLUT1 regulation by RSV in ovarian cancer cells in subsequent studies. Although RSV had no significant effects on the levels of GLUT1 mRNA and protein expression (Fig 2C), GLUT1 plasma membrane localization was reduced in all cancer cells treated with RSV (50 μM) but not by glucose starvation (Fig 2D). To confirm the dysregulation of GLUT1 plasma membrane trafficking in ovarian cancer cells, plasma membrane protein were isolated for the evaluation of GLUT1 trafficking. Membrane bound GLUT1 expression was significant reduced by RSV treatment, a response consistent with our immunocytochemical results (Fig 2E). These data suggest that RSV suppresses GLUT1 translocation to cytoplasmic membrane and thus glucose uptake of ovarian cancer cells.

A.

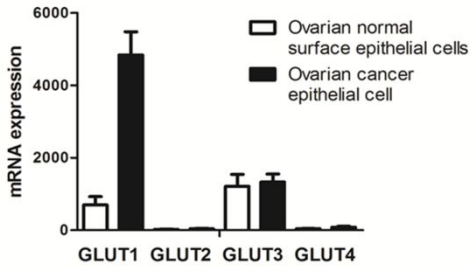
6000
4000
2000
0
mRNA expression
Ovarian normal surface epithelial cells
Ovarian cancer epithelial cell
GLUT1
GLUT2
GLUT3
GLUT4

B.

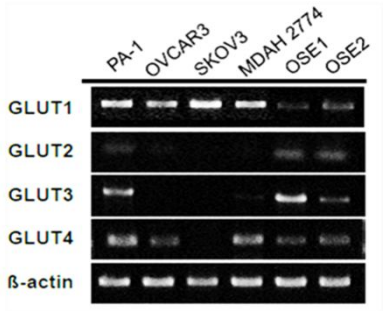
PA-1
OVCAR3
SKOV3
MDAH 2774
OSE1
OSE2
GLUT1
GLUT2
GLUT3
GLUT4
ß-actin

C. (1)

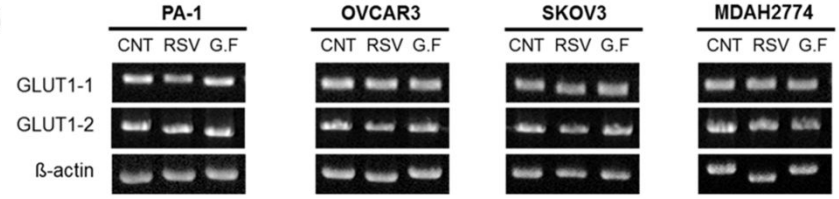
PA-1
OVCAR3
SKOV3
MDAH2774
CNT RSV G.F
GLUT1-1
GLUT1-2
ß-actin

(2)

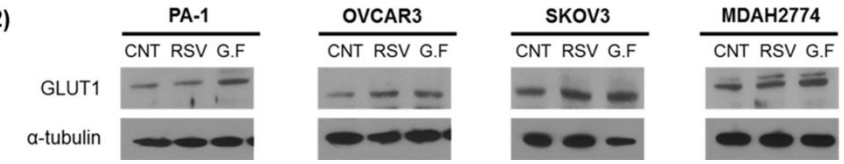
PA-1
OVCAR3
SKOV3
MDAH2774
CNT RSV G.F
GLUT1
α-tubulin

D.

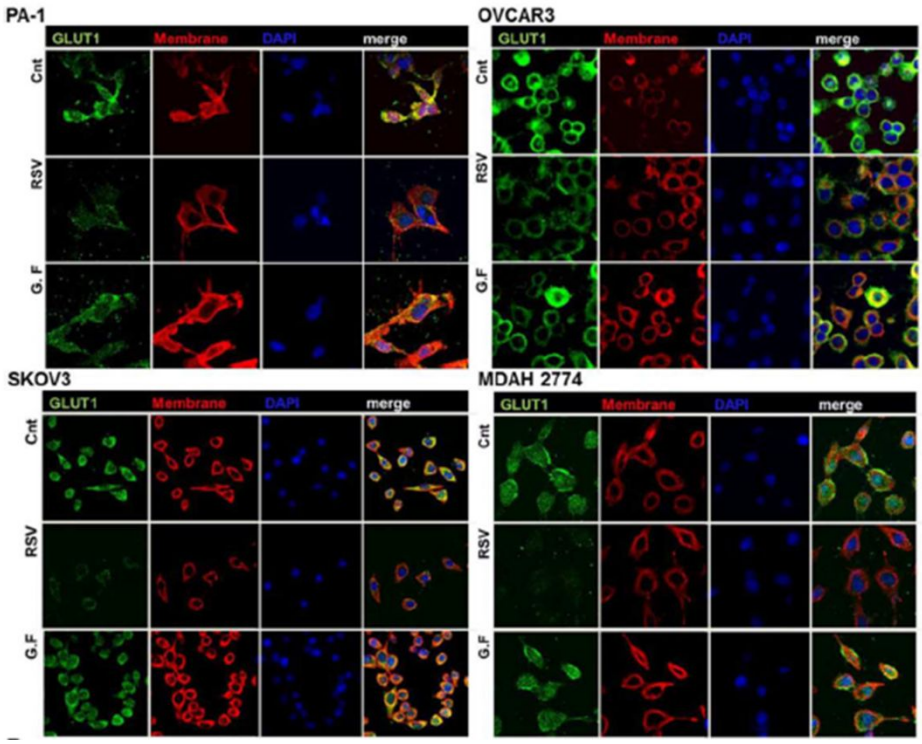
PA-1
OVCAR3
SKOV3
MDAH 2774
GLUT1
Membrane
DAPI
merge
Cnt
RSV
G.F

E.

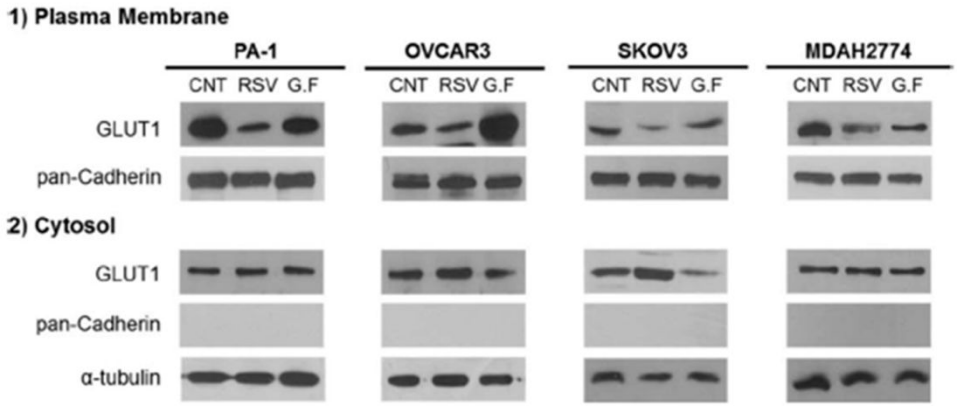
1) Plasma Membrane
PA-1
OVCAR3
SKOV3
MDAH2774
CNT RSV G.F
GLUT1
pan-Cadherin
2) Cytosol
GLUT1
pan-Cadherin
α-tubulin

Figure 2. Inhibition of GLUT1 membrane localization by RSV.

A. Upregulation of GLUT1 in ovarian cancer. The glucose transporter family (GLUT1 to GLUT4) gene expression was validated from online-available data (GEO, GDS3592). (n=12)

B. Upregulation of GLUT1 in ovarian cancer. The glucose transporter family gene expression was validated in ovarian cancer cell lines and primary cultured normal ovarian epithelial cells by RT-PCR.

C. GLUT1 mRNA and protein expressions under RSV treatment in ovarian cancer cells. Each cancer cell line was incubated with RSV (50 μM), glucose - free media (G.F) or DMSO (control) containing media for 24 hours. After incubation, 1) RT-PCR and 2) Western blotting was performed.

D. Inhibition of GLUT1 membrane trafficking by RSV in ovarian cancer cells. GLUT1 membrane localization was verified in response to RSV and glucose – free media (G.F) by confocal microscopy. Green; GLUT1, red; plasma membrane, and blue; DAPI. Original magnification 400X for all panels.

E. Membrane bounded GLUT1 inhibited by RSV in ovarian cancer cells. Each cancer cell line was co-incubated with RSV,

DMSO containing media or glucose - free media (G.F), for 24 hours and Western blotting was performed with protein, isolated from the plasma membrane or the cytosol.

2.3.3. Akt regulates GLUT1 membrane localization in ovarian cancer cells

It has been reported that PI3K/Akt signaling regulates glucose metabolism through modulation of glucose transporter activity and glycolytic enzyme in cancer cells (24). Based on these observations, we assessed the Akt/mTOR signaling cascades in four ovarian cancer cell lines to explore the mechanism by which RSV decreases GLUT1 membrane trafficking. Akt/mTOR activation was suppressed by RSV treatment in a time-dependent manner (control, 12 h to 48 h), as evidenced by a decreased expression of phospho-Akt at Ser 473 and Thr 308 and of phospho-mTOR (Fig 3A).

First, for understanding the contribution of Akt to the GLUT1 translocation, we examined the influence of two inhibitors of the PI3K-Akt pathway in ovarian cancer cells [LY294002 (20 μM), an inhibitor of PI3K and Akt inhibitor IV (1 μM), and inhibitor of Akt]. GLUT1 membrane trafficking (Fig 3B) and glucose uptake were significantly reduced by both inhibitors (Fig 3C) as were cell viability, a response associated with increased apoptosis (Fig 3D). Although apoptosis in OVCAR3 were not affected by the inhibitors, previous studies have shown glucose starvation induces autophagy in ovarian cancer cells, raising the possibility that OVCAR3 might undergo another cell death

mechanism with dysregulated glucose metabolism (13). In contrast, inhibition of mTOR by Rapamycin (100 nM) failed to significantly influence on glucose uptake through GLUT1 dysregulation (Spl Fig 1), suggesting that Akt regulates glucose metabolism in ovarian cancer cells through GLUT1 translocalization to the plasma membrane.

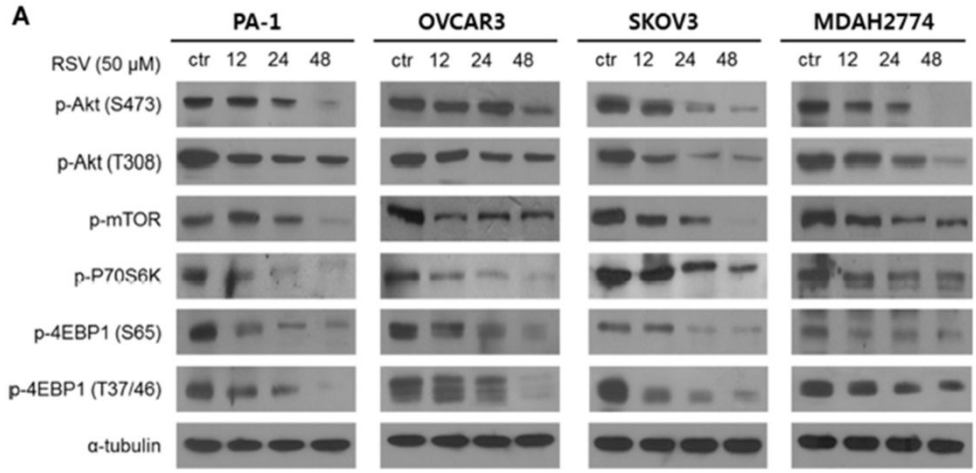
A
PA-1
OVCAR3
SKOV3
MDAH2774
RSV (50 μM)
ctr 12 24 48
p-Akt (S473)
p-Akt (T308)
p-mTOR
p-P70S6K
p-4EBP1 (S65)
p-4EBP1 (T37/46)
α-tubulin

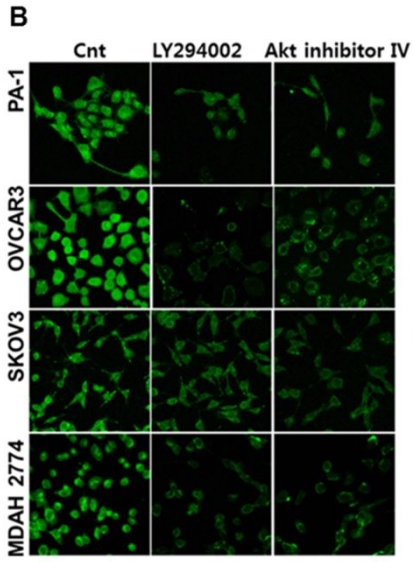
B
Cnt
LY294002
Akt inhibitor IV
PA-1
OVCAR3
SKOV3
MDAH 2774

C

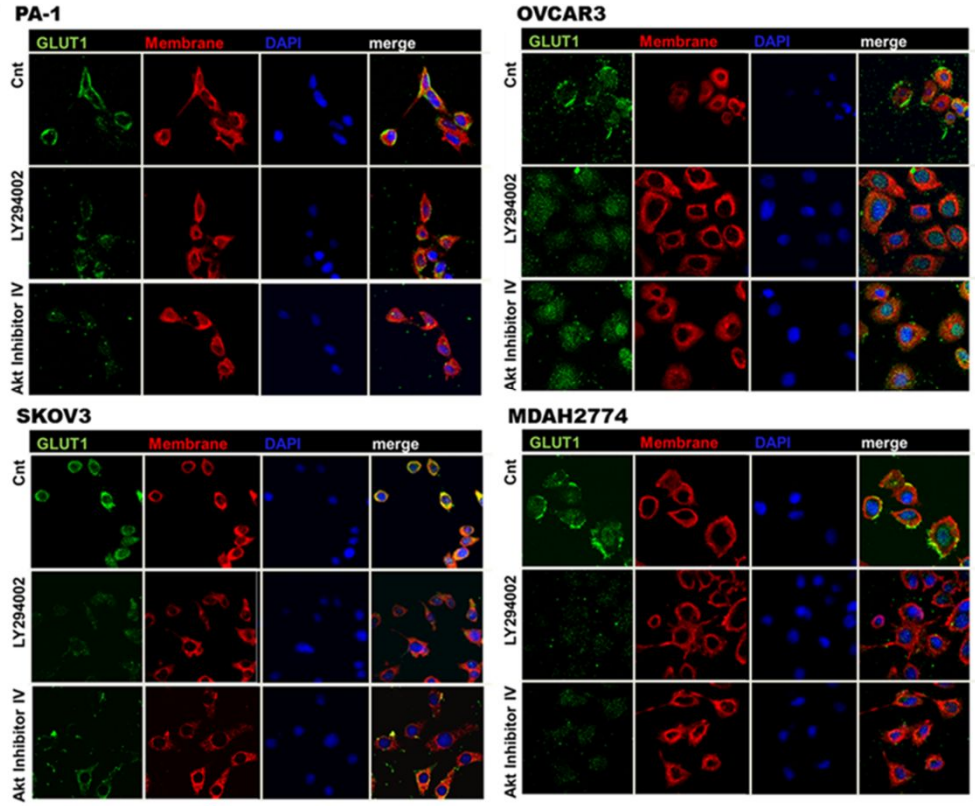
PA-1
OVCAR3
SKOV3
MDAH2774
GLUT1
Membrane
DAPI
merge
Cnt
LY294002
Akt Inhibitor IV

D. (1)

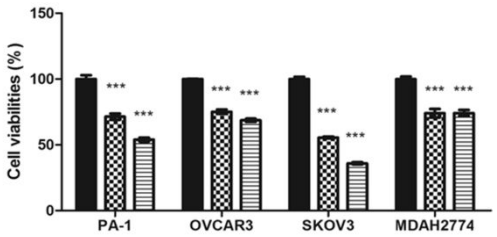
Cell viabilities (%)
150
100
50
0
***
PA-1
OVCAR3
SKOV3
MDAH2774

(2)

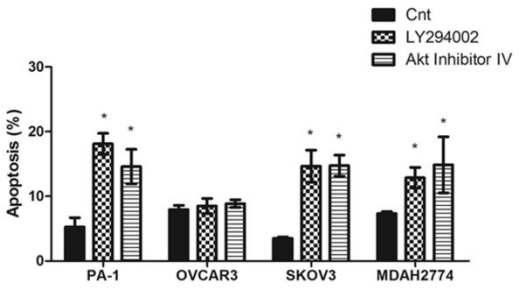
Cnt
LY294002
Akt Inhibitor IV
Apoptosis (%)
30
20
10
0
*
PA-1
OVCAR3
SKOV3
MDAH2774

Figure 3. GLUT1 membrane localization regulated by Akt. Two types of Akt inhibitors, LY294002 (20 μM) and Akt inhibitor IV (1 μM) were used to verify the effect of Akt on GLUT1 membrane localization.

A. Akt inhibition effect of RSV in ovarian cancer cells. After 12 to 48 hours of treatment RSV (50 μM), Akt activation (Ser473 and Thr308) and downstream molecules were assessed by Western blotting.
B. Akt inhibitiors' effect of GLUT1 localization in ovarian cancer cells. After 24 hours of treatment with LY294002 and Akt inhibitor IV in four ovarian cancer cell lines, GLUT1 membrane localization was assessed with confocal microscopy. Original magnification 400X for all panels.
C. Glucose uptake inhibition effect of Akt inhibitors. Glucose uptake was analyzed with 2-NBDG after 6 hours of treatment with LY294002 and Akt inhibitor IV. Original magnification 400X for all panels.
D. Cell death effects of Akt inhibition. After 24 hours of treatment with the Akt inhibitors, 1) MTT assay and 2) Annexin V/PI staining were used for demonstrating cell death. All experiments were repeated in triplicate and data were expressed as mean ± SEM. * $p<0.05$, *and* *** $P<0.001$, control versus Akt inhibitors.

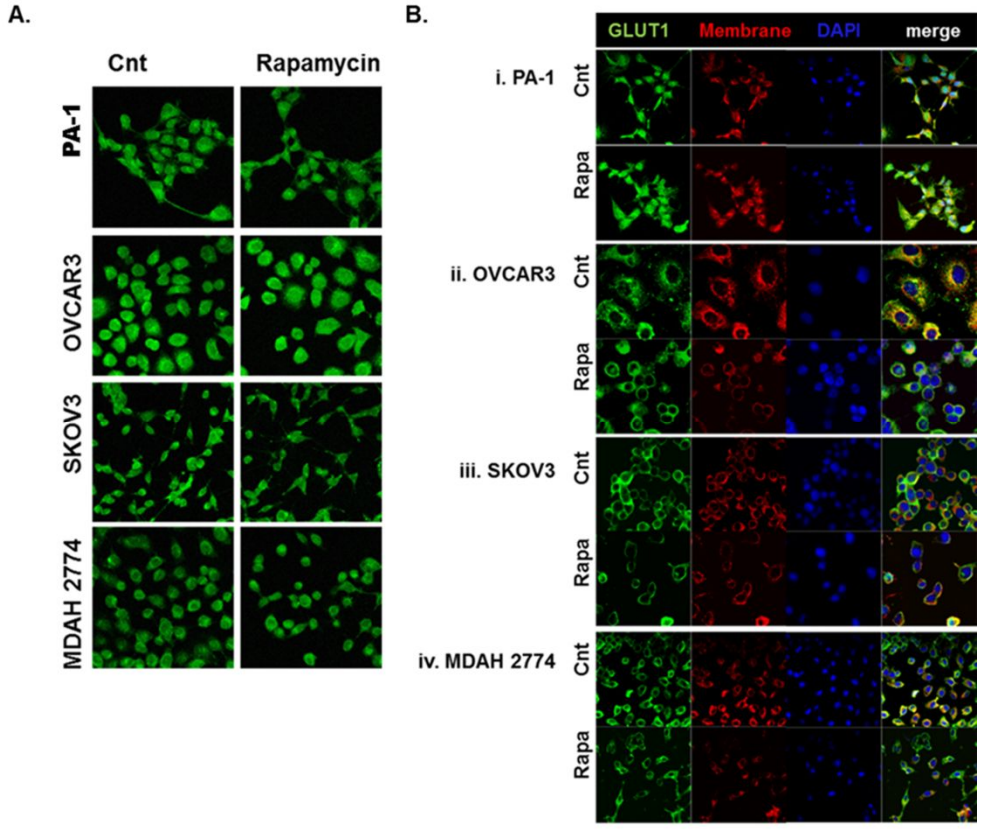
A.
Cnt
Rapamycin
PA-1
OVCAR3
SKOV3
MDAH 2774
B.
GLUT1
Membrane
DAPI
merge
i. PA-1
ii. OVCAR3
iii. SKOV3
iv. MDAH 2774
Cnt
Rapa

Supplementary figure 1. Effect of mTOR inhibition on ovarian cells. Rapamycin (Rapa, 100nM, a mTOR inhibitor) was used to evaluate the mTOR function in glucose uptake and GLUT1 localization in ovarian cancer cell lines

A. Rapamycin did not interrupt glucose uptake in ovarian cancer cells. All four ovarian cancer cell lines were treated with Rapamycin (100 nM) or DMSO as a control for 6 hours and co-treated with 2-NBDG (50 μM) for 30min. Then the intracellular level of 2-NBDG was measured with confocal microscopy (excitation/emission = 485/535nm.

B. Rapamycin did not alter GLUT1 membrane trafficking in ovarian cancer cells. GLUT1 membrane localization was not affected Rapamycin treatment, as shown by confocal microscopy. Green; GLUT1, red; plasma membrane, and blue; DAPI.

2.3.4. Akt is a strong candidate for GLUT1 regulation

To further confirm that RSV impairs glucose uptake through Akt-mediated GLUT1 localization, we examined the influence of forced expression of a constitutively activated Akt (CA-Akt) on the responsiveness of ovarian cancer cells to RSV. First, we verified Akt activation in response to RSV treatment in CA-Akt overexpressed cells. As shown in Fig 4A, RSV treatment did not suppress Akt activation in CA-Akt-overexpressing cells. Moreover, ovarian cancer cells with activated Akt (CA-Akt) did not exhibit altered membrane bound GLUT1 level even in the presence of RSV (Fig 4B). The modulation of RSV-attenuated intracellular GLUT1 trafficking to plasma membrane by Akt activation was associated with decreased ability of the cells to undergo apoptotic cell death (Fig 4C). Taken together, these data suggest an important role of Akt in GLUT1 regulation in ovarian cancer cells.

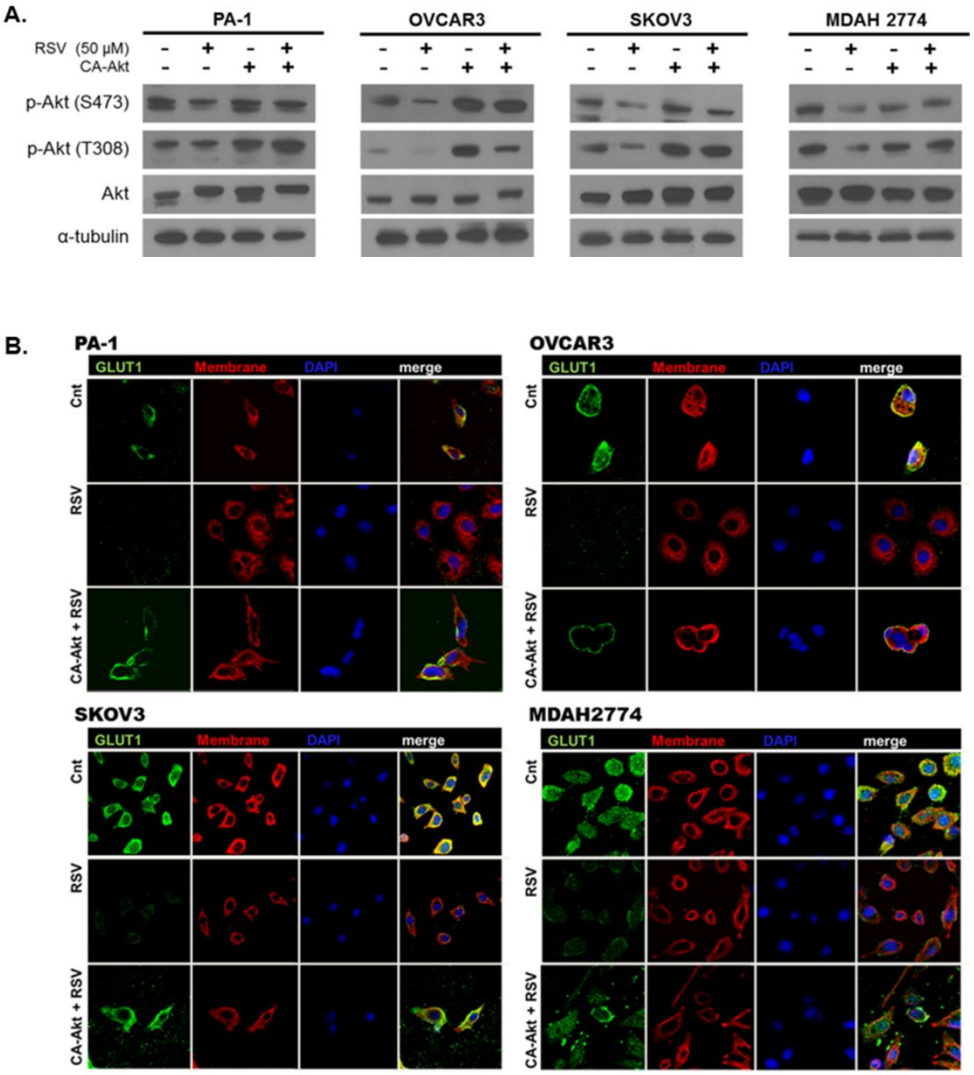
A.
PA-1
OVCAR3
SKOV3
MDAH 2774
RSV (50 μM)
CA-Akt
p-Akt (S473)
p-Akt (T308)
Akt
α-tubulin
B.
PA-1
OVCAR3
SKOV3
MDAH2774
GLUT1
Membrane
DAPI
merge
Cnt
RSV
CA-Akt + RSV
C.
Cnt
RSV
CA-Akt
CA-Akt + RSV
Apoptosis (%)
100
80
60
40
20
0
**
*
*
*
PA-1
OVCAR3
SKOV3
MDAH2774

Figure 4. RSV regulates GLUT1 localization through Akt activation. Four ovarian cancer cell lines were transfected with CA-Akt vector and control vector (2.5 μg) prior to RSV treatment. After transfection, RSV (50 μM) was treated for 24 hours.

A. The phosphorylated Akt expression was verified in CA-Akt overexpressing cell by Western blotting.
B. GLUT1 membrane trafficking was assessed with confocal microscopy 24 hours after RSV treatment in CA-Akt transfected cells. Original magnification 400X for all panels.
C. Apoptotic cell death was assessed with Annexin V/ PI straining 24 hours after RSV treatment in CA-Akt transfected cells. All experiments were repeated three times and data were expressed as mean ± SEM. * $p<0.05$, *and* ** $P<0.01$, RSV *versus* CA-Akt+RSV.

2.3.5. Dysregulated glucose uptake by RSV induces cancer cell – specific apoptosis

RSV inhibited glucose uptake and induced apoptotic cell death in various ovarian cancer cells and these effects could affect on normal cells. Here, we evaluated the effects of RSV on healthy counterpart [normal ovarian surface epithelial cells, PBMC (peripheral blood mononuclear cells) and RBC (red blood cells)]. In freshly isolated normal ovarian surface epithelial cells (OSE), RSV (50 μM) did not affect the glucose uptake (6 h, Fig 5A) and cell viability (24 h, Fig 5C), while cisplatin (24 h, 10 μM), a chemotherapeutic agent for ovarian cancer, reduced the viabilities of OSE (Fig 5C). Moreover, the plasma membrane-bound GLUT1 content in OSE was not affected by the presence of RSV (Fig 5B). Since GLUT1 is predominantly expressed in human erythrocyte, we analyzed glucose uptake capacity in fresh isolated PBMC and RBC in response to RSV (50 μM), using 2-NBDG (50 μM). RSV treatment did not affect glucose uptake in PBMC and RBC (Fig 5D). These findings suggested that RSV modulated glucose metabolism via inhibition of GLUT1 translocation in a cancer cell - specific manner.

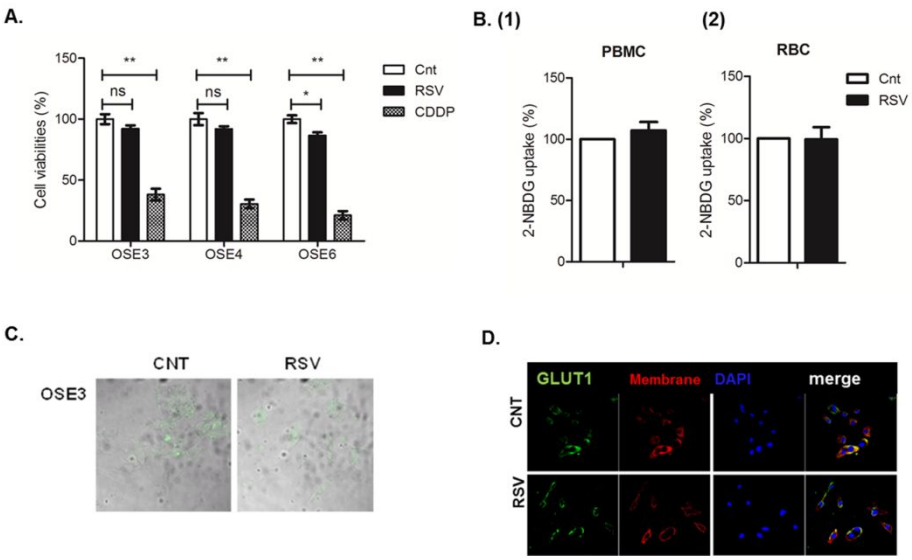
A.
Cell viabilities (%)
150
100
50
0
**
ns
**
ns
**
*
OSE3
OSE4
OSE6
Cnt
RSV
CDDP
B. (1)
PBMC
2-NBDG uptake (%)
150
100
50
0
(2)
RBC
2-NBDG uptake (%)
150
100
50
0
Cnt
RSV
C.
CNT
RSV
OSE3
D.
GLUT1
Membrane
DAPI
merge
CNT
RSV

Figure 5. Effects of RSV in normal cells. Primary cultured human ovarian epithelial cells (OSE), human PBMC and erythrocyte were used to determine the effect of RSV (50 μM) on normal cells.

A. Cisplatin (CDDP, 10 μM) was used to determine the cytotoxicity of standard chemo-agent on normal OSE. Twenty four hours after treatment with RSV (50 μM), CDDP or DMSO, OSE viability was validated using the MTT assay (n=3). All experiments were repeated triplet and data was expressed as mean ± SEM. *$P<0.05$, control versus RSV treatment (OSE6) and **$P<0.01$, control versus CDDP treatment.

B. Glucose uptake measured in human 1) PBMC and 2) erythrocytes after treatment with RSV (50 μM) for 6 hours, using 2-NBDG (50 μM). Data was expressed as mean ± SEM (n=4).

C. Glucose uptake assay, using 2-NBDG (50 μM), was performed in normal ovarian epithelial cells (OSE) in response to RSV treatment for 6 hours.

D. Membrane - bound GLUT1 of OSE 6 was shown by confocal microscopy 24 hours after RSV treatment. Original magnification 400X for all panels.

2.4. Discussion

Reprogramming of cancer metabolism emerges as a new cancer hallmark and a potent therapeutic target (25). However, dysregulated metabolism in cancer therapy has not as yet been specifically described, even though it is highly related to the clinical area (26). Here, we first demonstrated that RSV inhibits glucose uptake through interruption of plasma membrane trafficking of GLUT1 in ovarian cancer cells. This phenomenon was regulated by Akt inhibition in response to RSV. This response is independent of the status of p53, the most commonly altered in ovarian cancer (Fig 2). Moreover, in normal cells (normal ovarian surface epithelial cells, peripheral blood mononucleated cells and red blood cells), there are no compelling effects of RSV even though glucose is an essential metabolite in mammalian cells (Fig 5) (27).

Over 70 % of ovarian cancer patients carry genetic alterations in p53 and components of the PI3K-Akt-mTOR pathway, and is significantly associated with the chemoresistance and poor survival rate (2, 28, 29). The PI3K-Akt signaling cascades are activated by oncogenic stimuli and promote cell survival. In addition, Akt is believed to be responsible for the cancer cell metabolic phenotype, as it

activates glycolysis by regulating the activities of glucose transporters (GLUT) and glycolytic enzymes (24). Previous studies demonstrated that, Akt governed cell survival and increase nutrient uptake via GLUT1 regulation in various cancer cells (30, 31). In addition, chronic suppression of GSK-3ß, downstream molecule of Akt, increase glucose uptake in various cell types though GLUT1 regulation (32). These findings are consistent with our observation that glucose uptake through GLUT1 membrane trafficking and cell survival are Akt-dependent mechanisms (Fig 4).

With the metabolic abnormality of cancer, the glucose analogue [18^{F}] fluoro-deoxy-glucose (FDG) in cancer imaging is effective diagnostic tool for many cancer types (33). PET/CT using FDG accumulation for ovarian cancer diagnosis is effective for detection and localization of cancer (5). In ovarian cancer, glucose transporter 1 (GLUT1) and hexokinase are up-regulated (34, 35) and these genetic alterations lead to a dramatic increase in the rate of the first two steps of glucose metabolism and are sufficient to explain the substantial FDG accumulation detected in cancer by PET scanning. These metabolic alterations are related with malignant transformation and prognosis of patients (7). Targeting GLUT1 regulation with RSV in ovarian cancers may offer an efficient anticancer strategy since GLUT1

mRNA was significantly up-regulated in ovarian cancer tissues and various ovarian cancer cells but not in normal tissues and primary-cultured normal ovarian epithelial cells (Fig 2). Although the function of glucose transporter family in ovarian cancer cells is yet unclear, we found GLUT3 mRNA expression was slightly up-regulated in PA-1 and OSE1. Recent studies based on big data analysis suggest that it may be associated with poor survival in various tumor types, including ovarian carcinoma (36). After all epidemiological data show clear correlations with GLUT1 and ovarian cancer progression (3, 7-10), GLUT1-mediated suppression of glucose metabolism by RSV provides the evidence for efficacy of metabolic therapy (Fig 4).

Resveratrol, a phytoalexin, is described as an anticancer agent (11). However, the specific target of RSV remains unclear. Here, we reported that the anti-cancer mechanism of RSV is in part related to the regulation of glucose metabolism via interruption of GLUT1 translocation to the plasma membrane through the inhibition of Akt activation. The glycolytic phenotype of cancer is well documented and for therapeutic intervention, glycolytic inhibitors have been tested in clinical trials in combination with standard chemotherapeutic agents, such as paclitaxel (4, 37). Epidemiological data suggest that the regulation of glucose metabolism could potentially be exploited as a

way to overcome chemoresistance and give rise to the beneficial effects of standard chemotherapy (10, 38). Although metabolic alteration in cancer is one of the major clinical interests, use of the GLUT1 inhibitors have not been tested for cancer therapeutic agents. Here we propose that RSV-induced GLUT1 modulation via Akt inactivation could be a potent cancer targeted strategy and might be a key to overcome the chemoresistant ovarian cancer.

2.6. References

1. Bast RC, Jr., Hennessy B, Mills GB. The biology of ovarian cancer: new opportunities for translation. Nat Rev Cancer. 2009;9(6):415-28.

2. Yap TA, Carden CP, Kaye SB. Beyond chemotherapy: targeted therapies in ovarian cancer. Nat Rev Cancer. 2009;9(3):167-81.

3. Vander Heiden MG. Targeting cancer metabolism: a therapeutic window opens. Nat Rev Drug Discov. 2011;10(9):671-84.

4. Ward PS, Thompson CB. Metabolic reprogramming: a cancer hallmark even warburg did not anticipate. Cancer cell. 2012;21(3):297-308.

5. Chung HH, Kwon HW, Kang KW, Kim JW, Park NH, Song YS, et al. Preoperative [F-18]FDG PET/CT predicts recurrence in patients with epithelial ovarian cancer. Journal of gynecologic oncology. 2012;23(1):28-34.

6. Jung G, Lee Y, Oh S, Byun J, Ryu I, Kim S, et al. Comparison of 18F-FDG PET/CT and CT or MRI for the Preoperative Staging of Ovarian Cancer. Am J Roentgenol. 2007;188(5).

7. Kurokawa T, Yoshida Y, Kawahara K, Tsuchida T, Okazawa H, Fujibayashi Y, et al. Expression of GLUT-1 glucose transfer, cellular proliferation activity and grade of tumor correlate with [F-18]-fluorodeoxyglucose uptake by positron emission tomography in epithelial tumors of the ovary. International journal of cancer Journal international du cancer. 2004;109(6):926-32.

8. Semaan A, Munkarah AR, Arabi H, Bandyopadhyay S, Seward S, Kumar S, et al. Expression of GLUT-1 in epithelial ovarian carcinoma: correlation with tumor cell proliferation, angiogenesis, survival and ability to predict optimal cytoreduction. Gynecol Oncol. 2011;121(1):181-6.

9. Lamkin DM, Spitz DR, Shahzad MM, Zimmerman B, Lenihan DJ, Degeest K, et al. Glucose as a prognostic factor in ovarian carcinoma. Cancer-Am Cancer Soc. 2009;115(5):1021-7.

10. Kellenberger LD, Bruin JE, Greenaway J, Campbell NE, Moorehead RA, Holloway AC, et al. The role of dysregulated glucose metabolism in epithelial ovarian cancer. Journal of oncology. 2010;2010:514310.

11. Kundu JK, Surh YJ. Cancer chemopreventive and therapeutic potential of resveratrol: Mechanistic perspectives. Cancer Lett. 2008;269(2):243-61.

12. Kueck A, Opipari AW, Jr., Griffith KA, Tan L, Choi M, Huang J, et al. Resveratrol inhibits glucose metabolism in human ovarian cancer cells. Gynecol Oncol.

2007;107(3):450-7.
13. Opipari AW. Resveratrol-induced Autophagocytosis in Ovarian Cancer Cells. Cancer Res. 2004;64(2):696-703.
14. Shepherd TG, Theriault BL, Campbell EJ, Nachtigal MW. Primary culture of ovarian surface epithelial cells and ascites-derived ovarian cancer cells from patients. Nature protocols. 2006;1(6):2643-9.
15. Millon SR, Ostrander JH, Brown JQ, Raheja A, Seewaldt VL, Ramanujam N. Uptake of 2-NBDG as a method to monitor therapy response in breast cancer cell lines. Breast Cancer Res Treat. 2011;126(1):55-62.
16. Rumsey SC, Kwon O, Xu GW, Burant CF, Simpson I, Levine M. Glucose transporter isoforms GLUT1 and GLUT3 transport dehydroascorbic acid. The Journal of biological chemistry. 1997;272(30):18982-9.
17. Hudson CC, Liu M, Chiang GG, Otterness DM, Loomis DC, Kaper F, et al. Regulation of hypoxia-inducible factor 1 alpha expression and function by the mammalian target of rapamycin. Molecular and cellular biology. 2002;22(20):7004-14.
18. Tsuruda T, Hatakeyama K, Nagamachi S, Sekita Y, Sakamoto S, Endo GJ, et al. Inhibition of Development of Abdominal Aortic Aneurysm by Glycolysis Restriction. Arterioscl Throm Vas. 2012;32(6):1410-+.
19. Li LF, Zhou SH, Zhao K, Wang SQ, Wu QL, Fan J, et al. Clinical Significance of FDG Single-Photon Emission Computed Tomography: Computed Tomography in the Diagnosis of Head and Neck Cancers and Study of Its Mechanism. Cancer Biother Radio. 2008;23(6):701-14.
20. Montel-Hagen A, Blanc L, Boyer-Clavel M, Jacquet C, Vidal M, Sitbon M, et al. The Glut1 and Glut4 glucose transporters are differentially expressed during perinatal and postnatal erythropoiesis. Blood. 2008;112(12):4729-38.
21. Kim SH, Kim SH, Kim YB, Jeon YT, Lee SC, Song YS. Genistein Inhibits Cell Growth by Modulating Various Mitogen-Activated Protein Kinases and AKT in Cervical Cancer Cells. Natural Compounds and Their Role in Apoptotic Cell Signaling Pathways. 2009;1171:495-500.
22. Hwang SO, Lee GM. Effect of Akt overexpression on programmed cell death in antibody-producing Chinese hamster ovary cells. J Biotechnol. 2009;139(1):89-94.
23. Wood TE, Dalili S, Simpson CD, Hurren R, Mao XL, Saiz FS, et al. A novel inhibitor of glucose uptake sensitizes cells to FAS-induced cell death. Molecular cancer therapeutics. 2008;7(11):3546-55.

24. Cairns RA, Harris IS, Mak TW. Regulation of cancer cell metabolism. Nat Rev Cancer. 2011;11(2):85-95.
25. Hanahan D, Weinberg RA. Hallmarks of cancer: the next generation. Cell. 2011;144(5):646-74.
26. Zhao Y, Butler EB, Tan M. Targeting cellular metabolism to improve cancer therapeutics. Cell death & disease. 2013;4:e532.
27. Teiten MH, Mack F, Debbab A, Aly AH, Dicato M, Proksch P, et al. Anticancer effect of altersolanol A, a metabolite produced by the endophytic fungus Stemphylium globuliferum, mediated by its pro-apoptotic and anti-invasive potential via the inhibition of NF-kappa B activity. Bioorgan Med Chem. 2013;21(13):3850-8.
28. Carden CP, Stewart A, Thavasu P, Kipps E, Pope L, Crespo M, et al. The association of PI3 kinase signaling and chemoresistance in advanced ovarian cancer. Molecular cancer therapeutics. 2012;11(7):1609-17.
29. No JH, Jeon YT, Park IA, Kim YB, Kim JW, Park NH, et al. Activation of mTOR signaling pathway associated with adverse prognostic factors of epithelial ovarian cancer. Gynecol Oncol. 2011;121(1):8-12.
30. Wieman HL, Wofford JA, Rathmell JC. Cytokine stimulation promotes glucose uptake via phosphatidylinositol-3 kinase/Akt regulation of Glut1 activity and trafficking. Mol Biol Cell. 2007;18(4):1437-46.
31. Wofford JA, Wieman HL, Jacobs SR, Zhao Y, Rathmell JC. IL-7 promotes Glut1 trafficking and glucose uptake via STAT5-mediated activation of Akt to support T-cell survival. Blood. 2008;111(4):2101-11.
32. Buller CL, Loberg RD, Fan MH, Zhu QH, Park JL, Vesely E, et al. A GSK-3/TSC2/mTOR pathway regulates glucose uptake and GLUT1 glucose transporter expression. Am J Physiol-Cell Ph. 2008;295(3):C836-C43.
33. Bar-Shalom R, Yefremov N, Guralnik L, Gaitini D, Frenkel A, Kuten A, et al. Clinical performance of PET/CT in evaluation of cancer: Additional value for diagnostic Imaging and patient management. Journal of Nuclear Medicine. 2003;44(8):1200-9.
34. Rudlowski C, Moser M, Becker AJ, Rath W, Buttner R, Schroder W, et al. GLUT1 mRNA and protein expression in ovarian borderline tumors and cancer. Oncology. 2004;66(5):404-10.
35. Suh DH, Kim MA, Kim H, Kim MK, Kim HS, Chung HH, et al. Association of overexpression of hexokinase II with chemoresistance in epithelial ovarian cancer. Clin Exp Med. 2013.

36. Flavahan WA, Wu QL, Hitomi M, Rahim N, Kim Y, Sloan AE, et al. Brain tumor initiating cells adapt to restricted nutrition through preferential glucose uptake. Nat Neurosci. 2013;16(10):1373-+.
37. Tennant DA, Duran RV, Gottlieb E. Targeting metabolic transformation for cancer therapy. Nat Rev Cancer. 2010;10(4):267-77.
38. Banerjee S, Kaye SB. New strategies in the treatment of ovarian cancer: current clinical perspectives and future potential. Clin Cancer Res. 2013;19(5):961-8.

Chapter 3.

Resveratrol triggers ER stress-mediated apoptosis by disrupting N-linked glycosylation of proteins in ovarian cancer cells

Abstract

Malignant tumors have a high glucose demand and alter cellular metabolism to survive. Herein, focusing on the utility of glucose metabolism as a therapeutic target, we found that RSV induced endoplasmic reticulum (ER) stress-mediated apoptosis by interrupting protein glycosylation in a cancer-specific manner. Our results indicated that RSV suppressed hexosamine biosynthetic pathway and interrupted protein glycosylation through GSK3β activation. Application of either biochemical intermediates of hexosamine pathway or small molecule inhibitors (lithium chloride and SB216763) reversed the effects of RSV which disrupts protein glycosylation. Furthermore, ER UDPase, ENTPD5 (ectonucleoside triphosphate diphosphohydrolase 5) modulated protein glycosylation via Akt suppression in response to RSV. With inhibition or overexpression of Akt functions, we confirmed that the glycosylation activities were dependent on the ENTPD5 expressions and regulated by the action of Akt. RSV-mediated disruption of protein glycosylation leads to the induction of cellular apoptosis as indicated by the up-regulation of GADD153, followed by the activation of ER-stress sensors (PERK, IRE1α and ATF6α). Thus, our results provide a novel insight into cancer cell metabolism and protein glycosylation as the therapeutic potential of targeting glucose metabolism for cancers.

3.1. Introduction

Growing evidence suggests that malignant transformation is associated with changes in several branches of metabolism. To cope with the heightened energy requirement for accelerated cell growth and proliferation, cancer cells resort to increase glucose metabolism [1, 2]. Such oncogenic-transformed glucose metabolism opens a new therapeutic window for cancer treatment.

Glucose not only acts as fuel for energy production but also acts as a signaling regulator for protein modification such as glycosylation and acetylation [3]. In cancer, changes in glycosylation patterns are frequently observed to be causative factors driving the progression and chemoresistance [4-6]. Particularly, N-linked glycosylation (NLG) plays a critical role in protein maturation and the quality control of mature proteins. Additionally, NLG is critical for growth factor receptors (GFR) and nutrient transporters, binding to the plasma membrane of cells [3, 7]. Impaired protein glycosylation often leads to disrupt protein maturation and folding, which in turn leads to accumulation of aberrant proteins and unfolded protein responses (UPR) in the endoplasmic reticulum (ER). The UPR-mediated ER stress response can trigger either an adaptive survival response or cell death [8, 9].

Our previous findings indicated that resveratrol (RSV) selectively toxic to ovarian cancer cells by inhibition of glucose uptake [10]. However, it has not been clarified whether the apoptotic death induced by RSV is merely owing to the energy deprivation or any other mechanisms downstream of glucose metabolism. Previous studies have shown that deregulated glucose metabolism impairs protein glycosylation [3, 11]. Moreover, the disruption of protein glycosylation could causes of ER stress and ER stress-mediated apoptosis [9]. Thus, we hypothesized that the metabolic stressor, RSV might interrupt protein N-linked glycosylation and induces ER stress-mediated apoptosis in ovarian cancer cells. Our results indicate here, the disruption of glucose metabolism by RSV impairs protein N-linked glycosylation (NLG) and subsequent ER stress-mediated apoptosis in ovarian cancer cells.

3.2. Materials and Methods

3.2.1. Ovarian cancer cell lines and culture conditions

Human ovarian cancer cell lines; PA-1 (p53 wild type), MDAH2774 (p53 mutant) and SKOV3 (p53 null) that were used in this study are from ATCC. MDAH2774 and SKOV3 cell lines were grown in RPMI 1640 (WelGENE, Seoul, Korea) whereas PA-1 cell line was grown in MEM (WelGENE, Seoul, Korea) at 37˚C in 5% CO_2 and humidified atmosphere. All culture media were supplemented with 10% fetal bovine serum (FBS) (Gibco-BRL, Gaithersburg, MD) and 100 μg/mL of penicillin-streptomycin (P/S) (Invitrogen, Carlsblad, CA).

3.2.2. Peripheral blood mononuclear cells and red blood cell isolation

The Seoul National University Hospital Institutional Review Board approved all experiments that were conducted using normal samples from healthy donors (IRB No. C-1307–008-502). Peripheral blood mononuclear cells (PBMC) and red blood cells (RBC) were used as normal control cells. They were isolated from the buffy coats using Ficoll-Paque gradient (GE Healthcare, NJ) centrifugation as described previously [10]. PBMC were maintained in RPMI 1640 media containing 10% FBS and 100 μg/mL of P/S.

3.2.3. Reagents and antibodies

Stock solutions of resveratrol (Sigma Aldrich, St. Louis, MO), tunicamycin (Sigma Aldrich), LY294002, SB21673 (Cayman, MI), and Akt Inhibitor IV (Calbiochem, San Diego) were freshly prepared in dimethyl sulfoxide (DMSO; 0.001%) and used at the final concentrations as indicated. Glucose-free media (Gibco-BRL), uridine diphosphate N-acetylglucosamine, fructose-6-phosphate, LiCl were from Sigma Aldrich and thiazolyl blue tetrazolium bromide (MTT) was from Amresco (olon, OH). Antibodies to GADD153, GRP78/BiP, PERK, phospho-PERK, phospho-GSK3β (Y216), Akt and phospo-Akt (S473) were purchased from Santa Cruz Biotechnology (Santa Cruz, CA). Antibodies to IRE1α, phospho-Akt (T308), GSK3β, and phospho-GSK3β (S9) were purchased from Cell Signaling (Danvers, MA). ATF6α-antibodies were obtained from Enzo (Enzo Life Sciences, NY) and Anti-ENTPD5 and α-tubulin antibody were obtained from Sigma-Aldrich (St. Louis, MO).

3.2.4. Cell death analysis assay

Cells were seeded on to 96-well plates in medium constituted with or without glucose. After the addition of RSV, tunicamycin or DMSO (control) at the indicated concentrations, cells were incubated with 50 μl MTT (2mg/ml) for 4 hours at 37°C in 5% CO_2 in humidified

atmosphere. Medium was removed and the cells were solubilized in DMSO (100 μl). The optical density at 540 nm was determined using the Multiskan Spectrum spectrophotometer (Thermo Scientific, Hudson, NH).

For PBMC viabilities, cells were pipetted into 2 ml of medium constituted with or without glucose in the round-bottom polystyrene tubes and pretreated with RSV, tunicamycin, or DMSO (control) for indicated lengths of time. After the pretreatment, cells were incubated with 1 ml MTT (2mg/ml) for 4 hours at 37°C in 5% CO_2 in humidified atmosphere. At 4 hrs, cells were pelleted down by centrifugation at 1500 rpm for 10 min and solubilized in DMSO (200 μl). The optical density at 540 nm was determined.

For measurement of apoptotic cell death in ovarian cancer cells, we performed flow cytometric analysis using Annexin-V and PI staining (BD Pharmingen, CA) according to the manufacturer's protocol.

3.2.5. Hemolysis analysis

RBCs were washed with HBSS buffer twice and maintained with or without glucose, RSV, and tunicamycin for 12 hours. Hemolysis by 0.1 % of TritonX-100 was used as a positive control.

After treatment, cells were centrifuge at 600 g for 6 minutes and the supernatants were collected for the determination of optical density at 500 nm.

3.2.6. Western blotting and Lectin blotting

Protein preparation and immunoblot analyses were carried out according to previously published procedures [12] In brief, proteins were subjected to SDS-PAGE under reducing conditions then transferred onto nitrocellulose membranes. The blotted membranes were blocked with 5% nonfat dried milk and then incubated with the respective antibodies. GAPDH was used as a loading control.

Lectin blotting was performed as described previously [13] N-linked glycans were detected using concanavalin A (Con A, Sigma Aldrich) binding). After 30 min of blocking with 5 % skimmed milk, blots were incubated with 5 μg/ml of Con A in 5% skimmed milk overnight in an agitating incubator.

3.2.7. Small interfering RNA transfection

The siRNA-targeting GADD153 (DDIT3) gene sequence was as followed; 5'-GAGAAUGAACGGCUCAAGCAGGAAA- 3'. Scrambled RNA (mBiotech, Gyeonggido, Korea) was used as a

negative control [14]. Prior to RSV (50 μM) treatment, all cancer cells were transfected with the siRNA oligonucleotides with G-Fectin (Genolution Pharmaceuticals, Inc., Seoul, Korea) according to manufacturer protocol. The final concentration of siRNA was 50 nmol/ml.

3.2.8. Transient and stable transfection

Constitutively active human Akt (CA-Akt) was overexpressed in ovarian cancer cells using pCMV5 plasmid encoding CA-Akt as described previously [10]. Stable expression of the CA-Akt in ovarian cancer cells was generated by transfecting CA-Akt-encoding plasmid in respective cells using Mirus reagent (1 mg/ml; Mirus Bio LLC, Madison) and selecting stably expressing clones with G418 (500 μg/ml; Geneticin, Invitrogen).

3.2.9. Statistical analysis

All the data are presented as mean ± SEM. Statistical analysis was performed using PASW statistics 18 software. Differences of data were analyzed by 1-ANOVA and the Student T-test. Statistical significant differences were considered as* $p<0.05$, **$P<0.01$ and ***$P<0.001$.

3.3. Results

3.3.1. Interruption of protein N-linked glycosylation by resveratrol in ovarian cancer cells

We previously demonstrated that RSV interrupts glucose uptake via Akt/GLUT1 axis in ovarian cancer cells [10]. Herein, we hypothesized that disruption of glucose metabolism by RSV interrupted protein NLG. We employed various ovarian cancer cell lines with different genetic background (PA-1; p53-wild type, SKOV3; null, and MDAH 2774; mutant). To determine the effect of RSV on protein NLG, a lectin binding assay using concanavalin A (Con A) was carried out. Con A specifically detects N-linked glycosylated proteins through its binding to Asn-linked glycan of protein. Tunicamycin (TM) was used as a positive control, since TM (5 μg/ml) is an established inhibitor of NLG [15]. And artificial metabolic stress *in vitro* through glucose-deprivation exerted a similar reduction in NLG (Fig 1A). Reduction protein NLG closely correlated with the decreased cell viabilities and induced apoptosis of ovarian cancer cells following the treatment with the respective reagents (Fig1 B, C). As shown in figure 1D, RSV-treatment did not elicit these effects in the primarily cultured normal cells such as peripheral blood mononuclear cells (PBMC) and red blood cells (RBC). However, both the deprivation of glucose and

treatment with TM decreased cell viabilities in normal cells than RSV, which did not affect the normal cells during the 24 hour treatment period. These data demonstrate that RSV disrupted protein NLG and induce cell death in a cancer cell-specific manner.

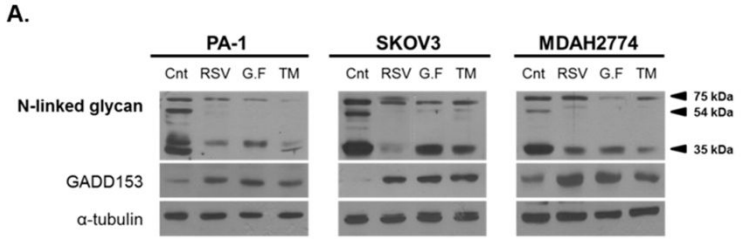
A.
PA-1
SKOV3
MDAH2774
Cnt RSV G.F TM
N-linked glycan
GADD153
α-tubulin
75 kDa
54 kDa
35 kDa

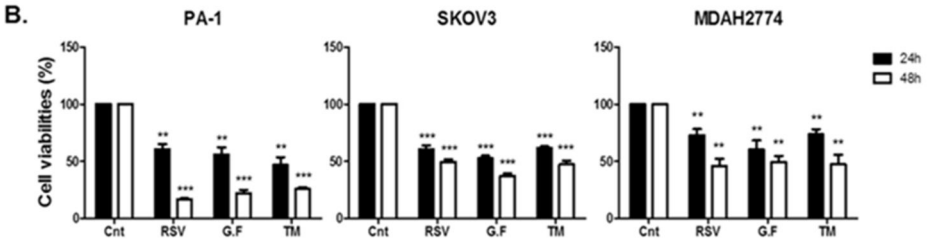
B.
PA-1
SKOV3
MDAH2774
Cell viabilities (%)
24h
48h
Cnt
RSV
G.F
TM

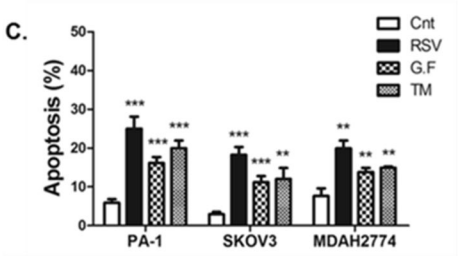
C.
Apoptosis (%)
Cnt
RSV
G.F
TM
PA-1
SKOV3
MDAH2774

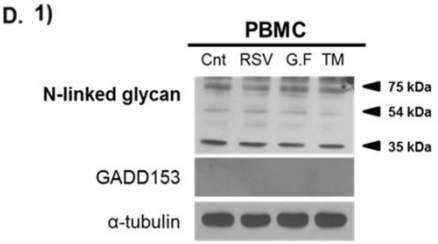
D. 1)
PBMC
Cnt RSV G.F TM
N-linked glycan
GADD153
α-tubulin
75 kDa
54 kDa
35 kDa

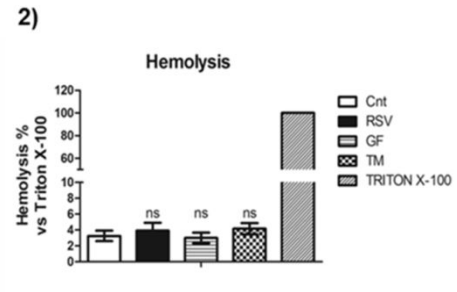
2)
Hemolysis
Hemolysis % vs Triton X-100
Cnt
RSV
GF
TM
TRITON X-100
ns

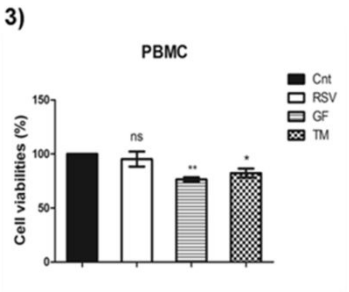
3)
PBMC
Cell viabilities (%)
Cnt
RSV
GF
TM
ns

Figure 1. Inhibition of N-linked glycosylation and cancer specific-cytotoxicity of RSV. Effect of RSV on N-glycosylation and cytotoxicity were monitored in ovarian cancer cells (PA-1, SKOV3 and MDAH2774) and primary cultured-normal cells (PBMC; peripheral blood mononuclear cells and RBC; red blood cells). Glucose free media (G.F) and tunicamycin (TM, 5 μg/ml, N-glycosylation inhibitor) were used as positive controls for the inhibition of glycosylation.

A. Suppression of protein N-liked glycosylation by RSV. Cells were RSV (50 μM), G.F, TM or DMSO (control) was treated for 24 hours. N-linked glycan were detected with lectin blot assay with Con A (5 μg/ml) and GADD153 expressions were monitored by immunoblot analysis. α-tubulin served as a loading control.

B. Growth inhibition effects of RSV in ovarian cancer cells. Ovarian cancer cells were treated with RSV, G.F, TM or DMSO (control) for 24 to 48 hours and cell viabilities were measured by MTT assay. Results represented as mean ± SEM of three independent experiments. ** $P < 0.01$ and *** $P<0.001$, control vs RSV, G.F or TM treatment.

C. Induction of apoptosis by RSV. Annexin V/PI-based flow cytometric analysis was conducted after 24 hours treatment

with RSV, G.F, TM or DMSO (control) in ovarian cancer cells. Data represented as mean ± SEM of three independent experiments. ** $P < 0.01$ and *** $P<0.001$, control vs RSV, G.F or TM treatment.

D. Effects of RSV on the normal cells. RBC and PBMC from heath donors were treated with RSV, G.F, TM or DMSO (control). 1) Effects of RSV on the protein N-linked glycosylation in PBMC. N-linked glycans in the PBMC were detected with Lectin blot assay with Con A (5 μg/ml) and GADD153 expressions were assessed by immunoblot analysis. 2) Effects of RSV on RBC. Hemolysis was determined after 12 hours of treatment with RSV, G.F, TM, DMSO (control) or TRITON-X100 (0.01%, positive control) by spectrophotometer at 500 nm. 3) Effects of RSV on PBMC. Viabilities of PBMC were determined using MTT assay after 24 hours of treatment with RSV, G.F, TM or DMSO (control). Results represented as mean ± SEM from the PBMCs from five different individuals. * $P < 0.01$, ** $P < 0.01$, control vs RSV, G.F or TM treatment.

3.3.2. Resveratrol induces ER stress-mediated apoptosis.

Disruption of protein NLG causes the accumulation of aberrant proteins in the endoplasmic reticulum (ER), which in turn activates unfolded protein responses (UPR) in the ER conferring severe stress [3, 8]. ER stress is monitored by three major ER stress sensors, protein kinase RNA-like ER kinase (PERK), inositol-requiring enzyme 1α (IRE-1α), and activating transcription factor 6α (ATF6α). Activation of ER stress sensors triggers cellular adaptation to stressful conditions, thereby restoring normal cellular function or inducing programmed cell death. Increased expression of GADD153 (also known as CHOP, *DDIT3*) and ATF4 is involved in the events leading to apoptosis following ER stress [8]. Since RSV-treatment results disrupted protein NLG as well as induced of apoptosis in ovarian cancer cells (Fig 1A, C), we investigated whether RSV treatment causes ER-stress mediates apoptosis. We monitored the expression of GADD153 (a key mediator of ER stress-mediated apoptosis) in ovarian cancer cells following treated with of RSV (50 μM), glucose free media or TM (5 μg/ml). These treatment in ovarian cancer cells showed NLG inhibition and increased GADD153 expression (Fig 1A); however, this was not observed in normal controls (Fig 1D. 1). As shown in Figure 2A, induction of GADD153 was followed by activation of the ER stress

signature proteins, PERK, IRE1α and ATF6α in time-dependent manner (6 - 48h) in response to RSV treatment. The effects of RSV seemed predominant on PERK and ATF6α. And a key marker of ER stress, GRP78/BiP was decreased. The underlying temporal relationship remains unclear.

Next, to verify the role of GADD153 in RSV-induced apoptosis, we used small interfering RNA (siRNA) transfection prior to RSV treatment in each ovarian cancer cell. With siRNA transfection, GADD153 protein expressions were significantly decreased, and correspondingly, RSV-induced apoptotic cell death was reversed (Fig 2B). Taken together, these results demonstrate that that RSV induces ER stress-mediated apoptosis in ovarian cancer cells with different genetic background.

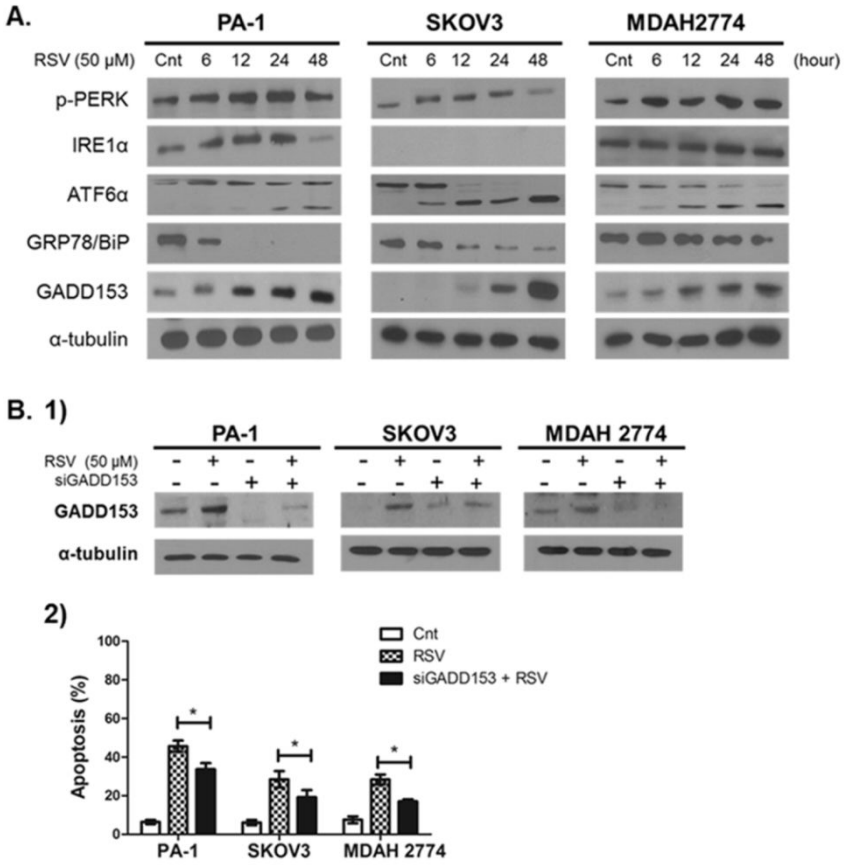
A.
PA-1
SKOV3
MDAH2774
RSV (50 μM)
Cnt 6 12 24 48
(hour)
p-PERK
IRE1α
ATF6α
GRP78/BiP
GADD153
α-tubulin
B. 1)
PA-1
SKOV3
MDAH 2774
RSV (50 μM)
siGADD153
GADD153
α-tubulin
2)
Cnt
RSV
siGADD153 + RSV
Apoptosis (%)
100
80
60
40
20
0
PA-1
SKOV3
MDAH 2774

Figure 2. Induction of ER stress-mediated apoptosis by RSV.

A. After RSV (50 μM) treatment for 6 to 48 hours in all ovarian cancer cell lines, ER stress signatures were evaluated by immunoblot analysis.

B. All ovarian cancer cells were transfected with GADD153 targeted siRNA (50 ng/ ml) or negative control siRNA (50 ng/ ml) prior to RSV (50 μM) treatment for 24 hours. (1) GADD153 expressions were measured with immunoblot analysis and (2) apoptotic cell death was analyzed by flow cytometric analysis with Annexin V/PI staining. Data represented as mean ± SEM of three independent experiments. * $P < 0.05$, control siRNA transfected cells with RSV treatment vs siGADD153 transfected cells with RSV treatment.

3.3.3. Resveratrol inhibits glycan synthesis via hexosamine pathway with GSK3-ß activation

Expressions of membrane-associated glycans and protein glycosylation activities are known to be dependent on the intracellular levels of glucose and hexosamine biosynthetic pathway, which is regulated by GSK3β [11, 16]. Fructose-6-phosphate (F6P) and uridine diphosphate *N*-acetylglucosamine (UDP-GlcNAc) are intermediate metabolites of hexosamine pathway, so we evaluated effects of RSV on the glycan synthesis and GADD153 expression with supplying UDP-GlcNAc (10 mM) and F6P (10 mM). As shown in Figure 3A, supplementation of these cells with UDP-GlcNAc (10 mM) and F6P (10 mM) reversed the effect of RSV on the protein NLG suppression and GADD153 induction. These results suggest that RSV affects the protein N-linked glycosylation via hexosamine biosynthetic pathway.

Recent studies have shown that GSK3β regulates enzymatic activation related with hexosamine pathway and protein NLG in cancer [11]. With that notion, we further investigated whether RSV regulated the action of GSK3β in ovarian cancer cells. As shown in Figure 3B, RSV treatment activated GSK3β through suppression of the inhibitory S9-phosphorylation GSK3β without affecting the expressions of Y216 phosphorylated form (active form of GSK3β). Next, we examined whether the activation of GSK3β is required for RSV-induced

disruption of protein NLG. To interrogate the role of GSK3β activation in protein NLG and ER stress induction in response to RSV, we used two different inhibitors of GSK3β, lithium chloride (Li, 20 mM) and SB216763 (SB, 10 μM). ER stress was monitored by GADD153 induction. Inhibition of GSK3β function using either of the inhibitors, RSV-induced protein NLG suppression and GADD153 induction were reversed (Fig 3C). These data demonstrate that RSV modulated glycan synthesis by GSK3β activation in ovarian cancer.

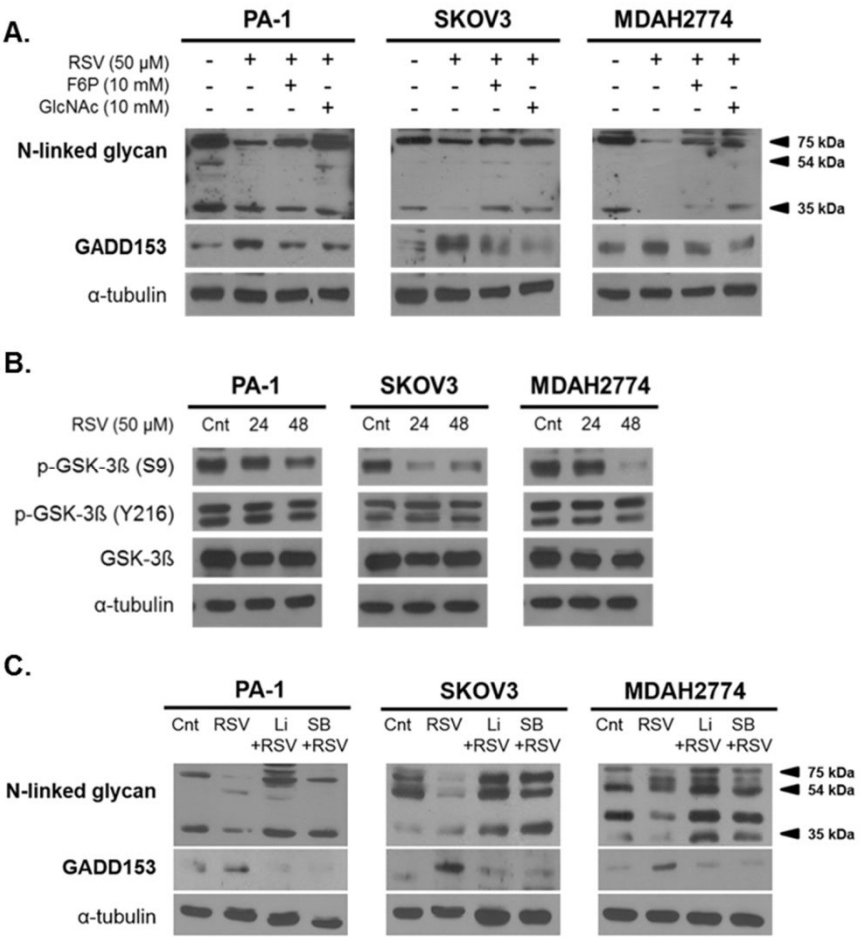
A.
PA-1
SKOV3
MDAH2774
RSV (50 μM)
F6P (10 mM)
GlcNAc (10 mM)
N-linked glycan
GADD153
α-tubulin
75 kDa
54 kDa
35 kDa
B.
PA-1
SKOV3
MDAH2774
RSV (50 μM)
Cnt 24 48
p-GSK-3ß (S9)
p-GSK-3ß (Y216)
GSK-3ß
α-tubulin
C.
PA-1
SKOV3
MDAH2774
Cnt RSV Li +RSV SB +RSV
N-linked glycan
GADD153
α-tubulin
75 kDa
54 kDa
35 kDa

Figure 3. Inhibition of N-liked glycan synthesis via GSK3β activation in response to RSV.

A. Interruption of glycan synthesis by RSV. Supplementary with fructose-6-phosphate (F6P, 10 mM) or uridine diphosphate N-acetylglucosamine (UDP-GlcNAc, 10 mM) along with RSV (50 μM, 24h) was used to evaluate the RSV-mediated interruption of N-linked glycan synthesis. N-linked glycan and GADD153 expressions were monitored by lectin blotting and immunoblot analysis respectively.

B. Activation of GSK3β by RSV. After 24 to 48 hours of treatment of RSV (50 μM) in ovarian cancer cells, activated GSK3β (phosphorylated at Y216) and inhibited GSK3β (phosphorylated at S9) were assessed by immunoblot analysis.

C. Regulation of N-linked glycan synthesis by GSK3β. Ovarian cancer cells were pre-treated with two kinds of GSK3β inhibitors [lithium chloride (Li, 20 mM) and SB216763 (SB, 10 μM)] for 3 hours and co-treated with RSV (50 μM) for 24 hours.

3.3.4. Akt incorporated protein glycosylation through ENTPD5.

Recent studies have indicated a critical role for Akt in protein glycosylation. Activated Akt enhances protein glycosylation via ENTPD5 (ER UDPase, entonucleoside triphosphate diphosphohydrolase 5), an enzyme located in the endoplasmic reticulum that regulates protein glycosylation via UDP-GlcNAc synthase [17, 18]. Since our previous studies showed that RSV impairs glucose uptake by Akt suppression [10], we postulated that RSV might inhibit ENTPD5 through Akt inhibition. Immunoblot assay indicated that RSV significantly down-regulated ENTPD5 expressions, in parallel with the inhibition of Akt activation (Fig 4A). To confirm if the ENTPD5 expression is dependent on the active status of Akt in ovarian cancer cells, we used two different small molecular inhibitors of Akt (LY294002; 20 μM and Akt inhibitor IV; 1 μM). As shown in figure 4B, ENTPD5 and NLG expression was decreased in response to Akt inhibition. A corollary increase in GADD153, indicating ER stress mediated apoptosis, was also observed. However, overexpression of constitutively activated Akt (CA-Akt) reversed RSV-induced suppression of ENTPD5, protein NLG, and GADD153 expressions (Fig 4C; Fig S1C). Thus, attenuation of Akt-activity could be correlated with NLG as well as ER-stress mediated apoptosis in response to RSV.

The interplay between GSK3β and Akt in cancer cells following RSV-treatment have not been determined. Our results demonstrate that RSV treatment (50 μM) activated GSK3β through suppression of GSK3β inhibition form (phosphorylated at S9) (Fig 3B) and suppressed the Akt activation (Fig 4A). To define the relationship between these kinases, we first evaluated whether inhibition of GSK3β affected the activation of Akt or *vice versa*. Inhibition of GSK3β with either lithium chloride (20 mM) or SB216763 (10 μM), did not affect RSV- induced attenuation of Akt activities (Fig. S1A), whereas inhibition of Akt with small molecular inhibitor LY294002 (20 μM) or Akt inhibitor IV (1 μM) drastically suppressed the inhibitory S9 phosphorylation of GSK3β in all ovarian cancer cells (Spl Fig. 1B). Even in the presence with RSV (50 μM), the overexpression of CA-Akt reversed the inhibitory S9-phosphorylation of GSK3β expressions (Spl Fig. 1C). Taken together, the data implied that RSV-induced attenuation of Akt activity led to the activation of GSK3β, resulting in the inhibition of protein NLG and ER stress-mediated apoptosis.

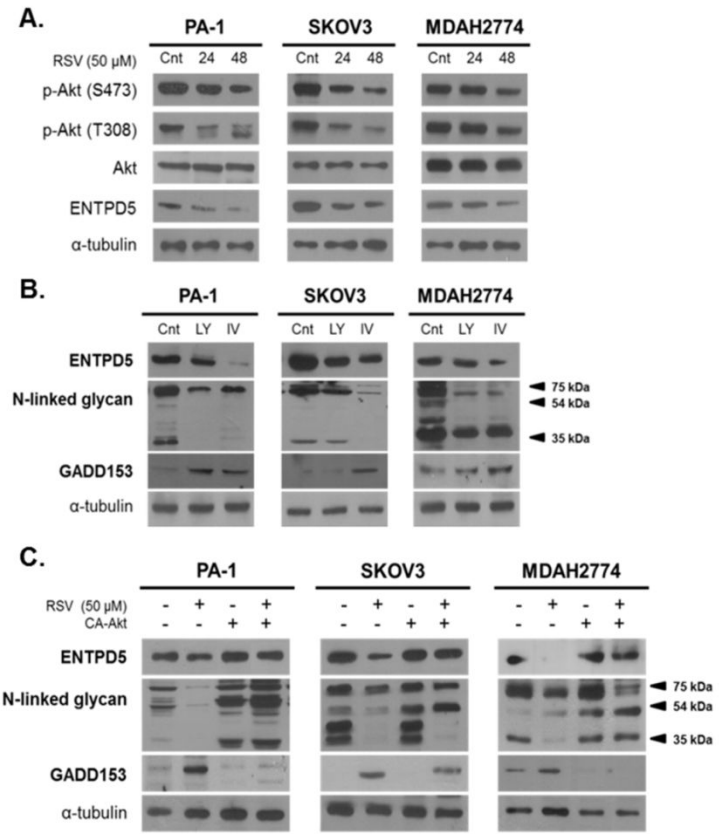
A.
PA-1
SKOV3
MDAH2774
RSV (50 μM)
Cnt 24 48
p-Akt (S473)
p-Akt (T308)
Akt
ENTPD5
α-tubulin
B.
PA-1
SKOV3
MDAH2774
Cnt LY IV
ENTPD5
N-linked glycan
GADD153
α-tubulin
75 kDa
54 kDa
35 kDa
C.
PA-1
SKOV3
MDAH2774
RSV (50 μM)
CA-Akt
ENTPD5
N-linked glycan
GADD153
α-tubulin
75 kDa
54 kDa
35 kDa

Figure 4. Dysregulation of protein N-liked glycosylation via Akt/ENTPD5 axis by RSV.

A. Inhibition of Akt by RSV. After 24 to 48 hours of RSV (50 μM) treatment, active Akt (phosphorylated at S473 and T308) and ENTPD5 expressions were assessed by immunoblot analysis.

B. Role of Akt on the protein N-linked glycosylation. Two types of Akt inhibitors, LY294002 (LY, 20 μM) and Akt inhibitor IV (IV, 1 μM) were treated in all ovarian cancer cells for 24 hours and N-linked glycan were measured by lectin blotting and related protein expressions were determined by immunoblot analysis.

C. Disruption of protein N-linked glycosylation through Akt suppression by RSV. All ovarian cancer cell lines were transfected with control vector and CA-Akt vector (2.5 mg) prior to 24 hours of RSV treatment (50 μM). In transfected cells, N-linked glycan were measured by lectin blotting and related molecules were evaluated by immunoblot analysis.

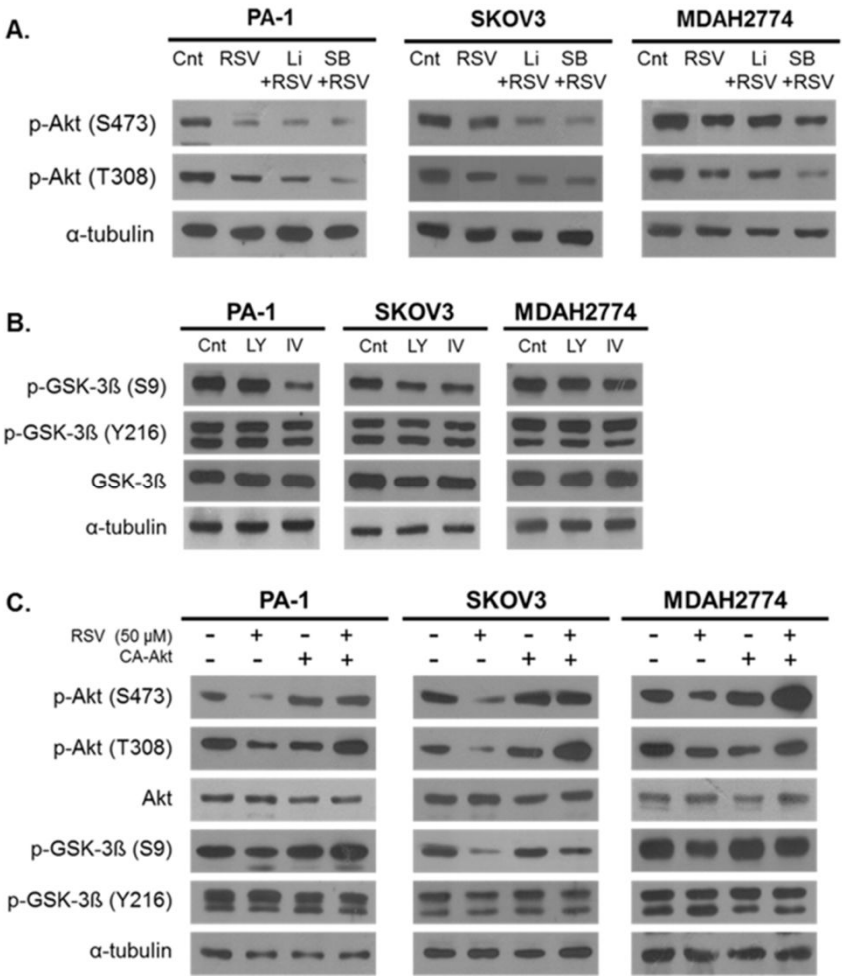
A.
PA-1
SKOV3
MDAH2774
Cnt
RSV
Li +RSV
SB +RSV
p-Akt (S473)
p-Akt (T308)
α-tubulin
B.
PA-1
SKOV3
MDAH2774
Cnt
LY
IV
p-GSK-3ß (S9)
p-GSK-3ß (Y216)
GSK-3ß
α-tubulin
C.
PA-1
SKOV3
MDAH2774
RSV (50 μM)
CA-Akt
p-Akt (S473)
p-Akt (T308)
Akt
p-GSK-3ß (S9)
p-GSK-3ß (Y216)
α-tubulin

Supplementary figure 1. RSV activates GSK3β by suppression of the Akt activity in ovarian cancer cells.

A. Effect of GSK3β inhibition on the activation of Akt in response to RSV. Ovarian cancer cells were pretreated with GSK3β inhibitor, lithium chloride (Li, 20 mM) or SB216763 (SB, 10 μM) for three hours, following incubated with RSV (50 μM) for 24 hours. Activated Akt (phosphorylated at S473 and T308) was monitored by immunoblot analysis.

B. Role of Akt on the activation of GSK3β in ovarian cancer cells. With two types of Akt inhibitors; LY294002 (LY, 20 μM) and Akt inhibitor IV (IV, 1 μM), the inhibited configuration of GSK3β (phosphorylated at S9) as well as the activated form (phosphorylated at Y216) were monitored by immunoblot analysis.

C. Dependence of the GSK3β activation on the Akt in response to RSV. Each of the ovarian cancer cells were transfected with CA-Akt vector or control vector (2.5 mg) prior to 24 hours of RSV (50 μM) treatment. The activated Akt and the GSK3β were monitored by immunoblot analysis.

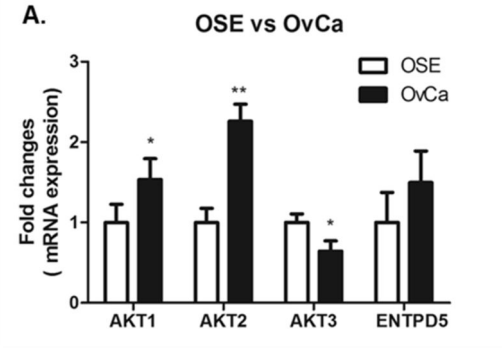
A.
OSE vs OvCa
OSE
OvCa
Fold changes
(mRNA expression)
3
2
1
0
*
**
*
AKT1
AKT2
AKT3
ENTPD5

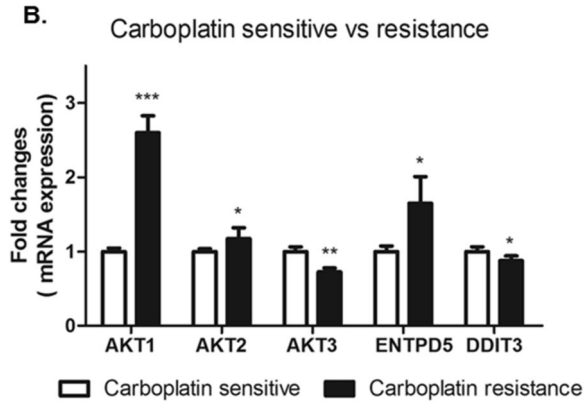
B.
Carboplatin sensitive vs resistance
Fold changes
(mRNA expression)
3
2
1
0
***
*
**
*
*
AKT1
AKT2
AKT3
ENTPD5
DDIT3
Carboplatin sensitive
Carboplatin resistance

Supplementary figure 2. Analysis of human ovarian cancer data sets available through GEO.

A. Akt1, Akt2 and ENTPD5 mRNA expressions were highly upregulated in ovarian cancer epithelial cells. Based on the microarray data set, differences in mRNA expression levels of Akt1, Akt2, and ENTPD5 in ovarian normal surface epithelia (OSE) and ovarian cancer epithelial cells (OvCa) were analyzed. Data represents results derived from twelve individual patients per group (n=12 per group); results are presented as Mean ± SEM with * $P < 0.05$, ** $P < 0.01$ *for* OSE vs OvCa.

B. Akt1, Akt2, and ENTPD5 mRNA expressions were significantly upregulated otherwise DDIT3 (human gene name of GADD153) was down-regulated in chemoresistant ovarian cancer tissue. Based on the micro array data set, mRNA expressions of carboplatin sensitive and resistance ovarian cancer tissues were analyzed. Results are presented as Mean ± SEM for nine persons per group (n=9 per group) with * $P < 0.01$, ** $P < 0.01$, *** $P < 0.001$ *for* sensitive vs resistant.

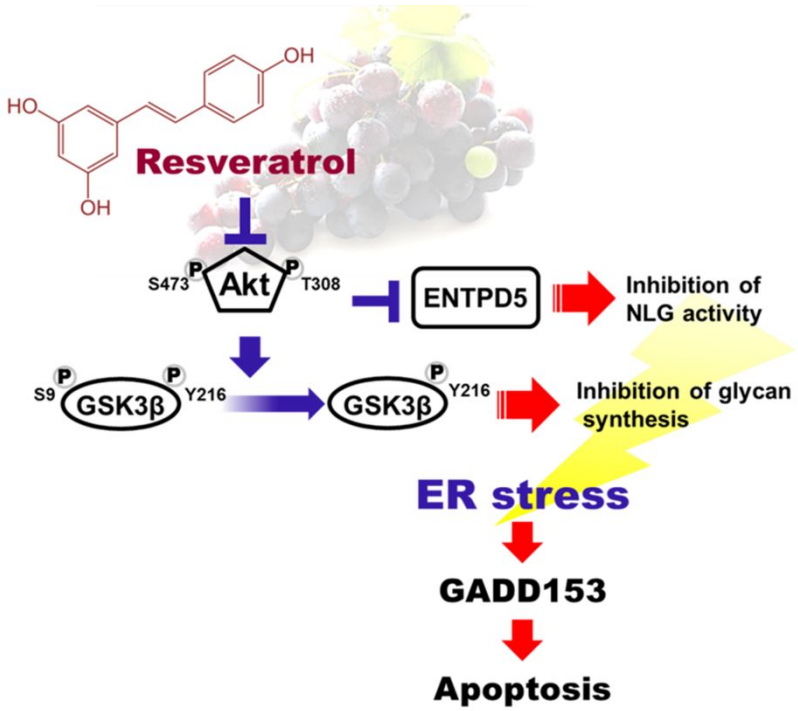

Figure 5. Resveratrol induces ER stress-mediated apoptosis through disruption of protein N-linked glycosylation via Akt/GSK3β axis.

3.4. Discussion

Altered glycosylation is a universal feature of cancer cells, and certain glycan structures are well-known markers of tumor progression [6]. Interestingly, malignant cells commonly exhibit increased expression of complex N-linked glycans on their surface with metabolic alterations [19, 20]. However, the functions and underpinning mechanisms of protein glycosylation in cancer are poorly understood. In current study, we described how metabolic disruption affected ovarian cancer cells in relation to protein NLG and ER stress-mediated apoptosis by RSV.

Previous studies have shown that RSV impairs glucose consumption via Akt/GLUT1 axis in cancer [10, 21]. Limited on glucose availability has been correlated decreased of hexosamine biosynthetic flux which can disrupt of protein glycosylation [11, 16]. Herein, we demonstrated that the supplementation with metabolic intermediates of the hexosamine biosynthesis pathway reverses the disruption of protein NLG by RSV (Fig 3). The hexosamine pathway is regulated by various enzymatic activities and GSK3β has been shown to inhibit the enzymatic activities of glycogen synthase through a hexosamine biosynthetic mechanism [22, 23]. Activated GSK3β by RSV suppressed protein NLG and induced ER stress- mediated cellular

apoptosis, which was confirmed using two small molecule inhibitors (Fig 3, Spl Fig 1). Even though the role of GSK3β in cancer has been disputed, the concept of the metabolic regulator of its mechanisms must be determined [22, 24].

PI3K/Akt is frequently altered in oncogenic pathways and is a key modulator of metabolic functions in malignant cells [25, 26]. Based on TCGA data, more than 45 % of patients show genetic alterations in PI3K/Akt-associated genes [27]. Overexpression of PI3K/Akt related genes are observed in ovarian cancer tissues and the expressions of these genes are more pronounced in ovarian cancer tissue samples obtained from carboplatin resistance patients (Spl. Fig 2) [28, 29]. A previous study clearly shows that the hyper-activation of Akt enhances aerobic glycolysis through protein glycosylation and ATP consumption by ENTPD5 upregulation [17]. These findings strongly correlate with our results in which RSV-mediated suppression of protein NLG depended on the inhibition of Akt/ ENTPD5 (Fig 4), which are upregulated in tissues from ovarian cancer patients and who were experienced carboplatin resistance (Spl. Fig 2) [28, 29].

Recent advances in strategies for manipulating ER stress response pathway in preclinical models of chronic diseases including cancer, metabolic disorder, brain, and heart ischemia have showed promising evidence for their therapeutic potential [8]. Epidemiologic

data have suggested that the ER stress signatures strongly correlate with tumor progressions and the chemoresistance of various cancers including ovarian cancer. High expression of GRP78/BiP in cancer patients has been correlated with shorter disease-free survival, whereas GADD153 (also called as CHOP, *DDIT3*) has been shown to have the opposite effect [30-33]. GADD153 (*DDIT3*) mRNA expression was significantly down-regulated in ovarian cancer with carboplatin resistance (Spl. Fig 2B) while there were no significant changes in GRP78/BiP levels (data not shown). Following the inhibition of protein N-linked glycosylation (NLG) by RSV, ovarian cancer cells experiences severe ER stress caused by RSV and metabolic disruption in a cancer-specific manner (Fig 1, 2).

With metabolic abnormalities, cancers have a high glucose demand which is associated with membrane-associated glycan expression [3, 11]. In cancer, membrane-associated glycans (mucins) are overexpressed, which can be used as diagnosis tools and therapeutic targets [6, 34]. However, the expression profile and function of glycan in various cancers have not been analyzed. In accordance with our findings, RSV-mediated suppression of Akt leads to the activation of GSK3β and consequently inhibition protein NLG and ER-stress mediated apoptotic cell in a cancer cell-specific manner (Fig 5). The regulation of protein glycosylation and glycan expression via GSK3β

coupled to Akt actions as demonstrated by RSV-treatment. These findings could represent a novel therapeutic model for cancers and might provide the strategies for overcoming chemoresistance.

3.5. References

[1] L. Galluzzi, O. Kepp, M.G. Vander Heiden, G. Kroemer, Metabolic targets for cancer therapy (vol 12, pg 829, 2013), Nat Rev Drug Discov, 12 (2013) 965-965.

[2] V.C. Sandulache, T.J. Ow, C.R. Pickering, M.J. Frederick, G. Zhou, I. Fokt, M. Davis-Malesevich, W. Priebe, J.N. Myers, Glucose, not glutamine, is the dominant energy source required for proliferation and survival of head and neck squamous carcinoma cells, Cancer-Am Cancer Soc, 117 (2011) 2926-2938.

[3] K.E. Wellen, C.B. Thompson, A two-way street: reciprocal regulation of metabolism and signalling, Nat Rev Mol Cell Bio, 13 (2012) 270-U271.

[4] K.S. Lau, J.W. Dennis, N-Glycans in cancer progression, Glycobiology, 18 (2008) 750-760.

[5] H.E. Miwa, W.R. Koba, E.J. Fine, O. Giricz, P.A. Kenny, P. Stanley, Bisected, complex N-glycans and galectins in mouse mammary tumor progression and human breast cancer, Glycobiology, 23 (2013) 1477-1490.

[6] M.N. Christiansen, J. Chik, L. Lee, M. Anugraham, J.L. Abrahams, N.H. Packer, Cell surface protein glycosylation in cancer, Proteomics, 14 (2014) 525-546.

[7] J.W. Dennis, I.R. Nabi, M. Demetriou, Metabolism, Cell Surface Organization, and Disease, Cell, 139 (2009) 1229-1241.

[8] C. Hetz, E. Chevet, H.P. Harding, Targeting the unfolded protein response in disease, Nat Rev Drug Discov, 12 (2013) 703-719.

[9] C. Hetz, The unfolded protein response: controlling cell fate decisions under ER stress and beyond, Nat Rev Mol Cell Bio, 13 (2012) 89-102.

[10] H. Gwak, G. Haegeman, B.K. Tsang, Y.S. Song, Cancer-specific interruption of glucose metabolism by resveratrol is mediated through inhibition of Akt/GLUT1 axis in ovarian cancer cells, Mol Carcinog, (2014).

[11] R. Palorini, F. Cammarata, C. Balestrieri, A. Monestiroli, M. Vasso, C. Gelfi, L. Alberghina, F. Chiaradonna, Glucose starvation induces cell death in K-ras-transformed cells by interfering with the hexosamine biosynthesis pathway and activating the unfolded protein response, Cell death & disease, 4 (2013).

[12] H.S. Moon, B. Kim, H. Gwak, D.H. Suh, Y.S. Song, Autophagy and protein kinase RNA-like endoplasmic reticulum kinase (PERK)/eukaryotic initiation factor 2 alpha kinase (eIF2alpha) pathway protect ovarian cancer cells from metformin-induced apoptosis, Mol Carcinog, (2015).

[13] B.Y. Ma, K. Yoshida, M. Baba, M. Nonaka, S. Matsumoto, N. Kawasaki, S. Asano, T. Kawasaki, The lectin Jacalin induces human B-lymphocyte apoptosis through glycosylation-dependent interaction with CD45, Immunology, 127 (2009) 477-488.

[14] A. Saha, T. Kuzuhara, N. Echigo, M. Suganuma, H. Fujiki, New Role of (-)-Epicatechin in Enhancing the Induction of Growth Inhibition and Apoptosis in Human Lung Cancer Cells by Curcumin, Cancer prevention research, 3 (2010) 953-962.

[15] V.H. Bull, B. Thiede, Proteome analysis of tunicamycin-induced ER stress, Electrophoresis, 33 (2012) 1814-1823.

[16] A.L. Huber, J. Lebeau, P. Guillaumot, V. Petrilli, M. Malek, J. Chilloux, F. Fauvet, L. Payen, A. Kfoury, T. Renno, E. Chevet, S.N. Manie, p58(IPK)-Mediated Attenuation of the Proapoptotic PERK-CHOP Pathway Allows Malignant Progression upon Low Glucose, Molecular cell, 49 (2013) 1049-1059.

[17] M. Fang, Z.R. Shen, S. Huang, L.P. Zhao, S. Chen, T.W. Mak, X.D. Wang, The ER UDPase ENTPD5 Promotes Protein N-Glycosylation, the Warburg Effect, and Proliferation in the PTEN Pathway, Cell, 143 (2010) 711-724.

[18] F. Liu, K. Iqbal, I. Grundke-Iqbal, C.X. Gong, Involvement of aberrant glycosylation in phosphorylation of tau by cdk5 and GSK-3 beta, Febs Lett, 530 (2002) 209-214.

[19] M.M. Fuster, J.D. Esko, The sweet and sour of cancer: Glycans as novel therapeutic targets, Nat Rev Cancer, 5 (2005) 526-542.

[20] W. Romero-Fernandez, D.O. Borroto-Escuela, M.P. Alea, Y. Garcia-Mesa, P. Garriga, Altered trafficking and unfolded protein response induction as a result of M-3 muscarinic receptor impaired N-glycosylation, Glycobiology, 21 (2011) 1663-1672.

[21] A. Kueck, A.W. Opipari, Jr., K.A. Griffith, L. Tan, M. Choi, J. Huang, H. Wahl, J.R. Liu, Resveratrol inhibits glucose metabolism in human ovarian cancer cells, Gynecol Oncol, 107 (2007) 450-457.

[22] J.A. McCubrey, N.M. Davis, S.L. Abrams, G. Montalto, M. Cervello, J. Basecke, M. Libra, F. Nicoletti, L. Cocco, A.M. Martelli, L.S. Steelman, Diverse roles of GSK-3: tumor promoter-tumor suppressor, target in cancer therapy, Advances in biological regulation, 54 (2014) 176-196.

[23] P. Cohen, S. Frame, The renaissance of GSK3, Nat Rev Mol Cell Bio, 2 (2001) 769-776.

[24] F. Takahashi-Yanaga, Activator or inhibitor? GSK-3 as a new drug target, Biochemical pharmacology, 86 (2013) 191-199.

[25] M.G. Vander Heiden, Targeting cancer metabolism: a therapeutic window opens, Nat Rev Drug Discov, 10 (2011) 671-684.
[26] R.A. Cairns, I.S. Harris, T.W. Mak, Regulation of cancer cell metabolism, Nat Rev Cancer, 11 (2011) 85-95.
[27] D. Bell, A. Berchuck, M. Birrer, J. Chien, D.W. Cramer, F. Dao, R. Dhir, P. DiSaia, H. Gabra, P. Glenn, A.K. Godwin, J. Gross, L. Hartmann, M. Huang, D.G. Huntsman, M. Iacocca, M. Imielinski, S. Kalloger, B.Y. Karlan, D.A. Levine, G.B. Mills, C. Morrison, D. Mutch, N. Olvera, S. Orsulic, K. Park, N. Petrelli, B. Rabeno, J.S. Rader, B.I. Sikic, K. Smith-McCune, A.K. Sood, D. Bowtell, R. Penny, J.R. Testa, K. Chang, H.H. Dinh, J.A. Drummond, G. Fowler, P. Gunaratne, A.C. Hawes, C.L. Kovar, L.R. Lewis, M.B. Morgan, I.F. Newsham, J. Santibanez, J.G. Reid, L.R. Trevino, Y.Q. Wu, M. Wang, D.M. Muzny, D.A. Wheeler, R.A. Gibbs, G. Getz, M.S. Lawrence, K. Cibulskis, A.Y. Sivachenko, C. Sougnez, D. Voet, J. Wilkinson, T. Bloom, K. Ardlie, T. Fennell, J. Baldwin, S. Gabriel, E.S. Lander, L. Ding, R.S. Fulton, D.C. Koboldt, M.D. McLellan, T. Wylie, J. Walker, M. O'Laughlin, D.J. Dooling, L. Fulton, R. Abbott, N.D. Dees, Q. Zhang, C. Kandoth, M. Wendl, W. Schierding, D. Shen, C.C. Harris, H. Schmidt, J. Kalicki, K.D. Delehaunty, C.C. Fronick, R. Demeter, L. Cook, J.W. Wallis, L. Lin, V.J. Magrini, J.S. Hodges, J.M. Eldred, S.M. Smith, C.S. Pohl, F. Vandin, B.J. Raphael, G.M. Weinstock, R. Mardis, R.K. Wilson, M. Meyerson, W. Winckler, G. Getz, R.G.W. Verhaak, S.L. Carter, C.H. Mermel, G. Saksena, H. Nguyen, R.C. Onofrio, M.S. Lawrence, D. Hubbard, S. Gupta, A. Crenshaw, A.H. Ramos, K. Ardlie, L. Chin, A. Protopopov, J.H. Zhang, T.M. Kim, I. Perna, Y. Xiao, H. Zhang, G. Ren, N. Sathiamoorthy, R.W. Park, E. Lee, P.J. Park, R. Kucherlapati, D.M. Absher, L. Waite, G. Sherlock, J.D. Brooks, J.Z. Li, J. Xu, R.M. Myers, P.W. Laird, L. Cope, J.G. Herman, H. Shen, D.J. Weisenberger, H. Noushmehr, F. Pan, T. Triche, B.P. Berman, D.J. Van den Berg, J. Buckley, S.B. Baylin, P.T. Spellman, E. Purdom, P. Neuvial, H. Bengtsson, L.R. Jakkula, S. Durinck, J. Han, S. Dorton, H. Marr, Y.G. Choi, V. Wang, N.J. Wang, J. Ngai, J.G. Conboy, B. Parvin, H.S. Feiler, T.P. Speed, J.W. Gray, D.A. Levine, N.D. Socci, Y. Liang, B.S. Taylor, N. Schultz, L. Borsu, A.E. Lash, C. Brennan, A. Viale, C. Sander, M. Ladanyi, K.A. Hoadley, S. Meng, Y. Du, Y. Shi, L. Li, Y.J. Turman, D. Zang, E.B. Helms, S. Balu, X. Zhou, J. Wu, M.D. Topal, D.N. Hayes, C.M. Perou, G. Getz, D. Voet, G. Saksena, J.N.H. Zhang, H. Zhang, C.J. Wu, S. Shukla, K. Cibulskis, M.S. Lawrence, A. Sivachenko, R. Jing, R.W. Park, Y. Liu, P.J. Park, M. Noble, L. Chin, H. Carter, D. Kim, R. Karchin, P.T. Spellman, E. Purdom, P. Neuvial, H. Bengtsson, S. Durinck, J.

Han, J.E. Korkola, L.M. Heiser, R.J. Cho, Z. Hu, B. Parvin, T.P. Speed, J.W. Gray, N. Schultz, E. Cerami, B.S. Taylor, A. Olshen, B. Reva, Y. Antipin, R. Shen, P. Mankoo, R. Sheridan, G. Ciriello, W.K. Chang, J.A. Bernanke, L. Borsu, D.A. Levine, M. Ladanyi, C. Sander, D. Haussler, C.C. Benz, J.M. Stuart, S.C. Benz, J.Z. Sanborn, C.J. Vaske, J. Zhu, C. Szeto, G.K. Scott, C. Yau, K.A. Hoadley, Y. Du, S. Balu, D.N. Hayes, C.M. Perou, M.D. Wilkerson, N. Zhang, R. Akbani, K.A. Baggerly, W.K. Yung, G.B. Mills, J.N. Weinstein, R. Penny, T. Shelton, D. Grimm, M. Hatfield, S. Morris, P. Yena, P. Rhodes, M. Sherman, J. Paulauskis, S. Millis, A. Kahn, J.M. Greene, R. Sfeir, M.A. Jensen, J. Chen, J. Whitmore, S. Alonso, J. Jordan, A. Chu, J.H. Zhang, A. Barker, C. Compton, G. Eley, M. Ferguson, P. Fielding, D.S. Gerhard, R. Myles, C. Schaefer, K.R.M. Shaw, J. Vaught, J.B. Vockley, P.J. Good, M.S. Guyer, B. Ozenberger, J. Peterson, E. Thomson, C.G.A.R. Network, Integrated genomic analyses of ovarian carcinoma, Nature, 474 (2011) 609-615.

[28] D. Peters, J. Freund, R.L. Ochs, Genorne-wide transcriptional analysis of carboplatin response in chemosensitive and chemoresistant ovarian cancer cells, Molecular cancer therapeutics, 4 (2005) 1605-1616.

[29] N.J. Bowen, L.D. Walker, L.V. Matyunina, S. Logani, K.A. Totten, B.B. Benigno, J.F. McDonald, Gene expression profiling supports the hypothesis that human ovarian surface epithelia are multipotent and capable of serving as ovarian cancer initiating cells, Bmc Med Genomics, 2 (2009).

[30] L.M. Fan, J. Su, H. Dong, M. Wei, M.H. Cui, [Inhibition of GRP78 expression reverses cisplatin resistance in human ovarian cancer], Zhonghua yi xue za zhi, 93 (2013) 1341-1344.

[31] F. Delie, P. Petignat, M. Cohen, GRP78 Protein Expression in Ovarian Cancer Patients and Perspectives for a Drug-Targeting Approach, Journal of oncology, 2012 (2012) 468615.

[32] Y.Z. Zheng, Z.G. Cao, X. Hu, Z.M. Shao, The endoplasmic reticulum stress markers GRP78 and CHOP predict disease-free survival and responsiveness to chemotherapy in breast cancer, Breast Cancer Res Tr, 145 (2014) 349-358.

[33] N. Mujumdar, Z. Chen, S. Banerjee, V. Sangwan, S.M. Vickers, A.K. Saluja, Glucose-Regulated Protein 78 (Grp78) Inhibition Causes Cell Death in Pancreatic Cancer Cells, Pancreas, 41 (2012) 1388-1389.

[34] A.P. Singh, S. Senapati, M.P. Ponnusamy, M. Jain, S.M. Lele, J.S. Davis, S. Remmenga, S.K. Batra, Clinical potential of mucins in diagnosis, prognosis, and therapy of ovarian cancer, Lancet Oncol, 9 (2008) 1076-1085.

Chapter 4.

Glucose restriction enhances therapeutic responses via attenuation of ABC transporters and stemness via GSK3β/β-catenin signaling in ovarian cancer cells

Abstract

Alterations in glucose metabolism are one of the hallmarks of ovarian cancer, and these phenomena have strong correlation with drug resistance. Herein, we first demonstrated the function of glucose in cisplatin (CDDP)-resistant ovarian cancer cells. Lack of glucose availabilities enhanced CDDP responses in chemoresistant ovarian cancer cells. On the other hand, high glucose conditions (20 mM) had opposite effect. Glucose restriction suppressed membrane expression of ATP-binding cassette transporters (ABC transporters), resulting from glycosylation defect. Glycosylation of ABC transporters was regulated by GSK3β activation through AMPK cascade in response to glucose limitation. Moreover, glucose deficiency attenuated the ovarian cancer stem-like cells (CSC) phenotypes, sphere forming capacities and stemness related gene expressions. Associated with that, glucose restriction suppressed Wnt/β-catenin signaling through decrease of β-catenin nuclear expression by GSK3β activation. Our findings provide evidence that glucose plays a pivotal role in controlling drug resistance in ovarian cancer.

4.1. Introduction

Ovarian cancer is the most lethal gynecologic oncology in worldwide. Despites of enormous efforts to prevent the disease and to improve the therapeutic responses, overall survival has not been changed and remains the leading cause of death form gynecological malignancies for past decades (1, 2). Most of ovarian cancer patients diagnose at the advanced stage and two-third of them experienced disease recurrence and chemoresistance (3, 4). For ovarian cancer treatment, targeted therapies have failed to incorporate into standard treatment caused by lack of understanding new oncogenic driver, except mutations in *TP53*. Therefore platinum-based therapy remains the standard of care since 1970s (3). Currently, the primary goal of ovarian cancer treatment is enhanced the sensitivity of standard chemotherapy and restrained the recurrence (4, 5).

Even though there are limited understanding of ovarian cancer, glucose metabolism suggest as a prognostic marker and therapeutic targets. Epidemiological data suggested that highly demands on glucose consumption and overexpression of glucose transporter 1 (GLUT1) in ovarian cancer patients affect the survival and response to chemotherapy (6, 7). The correlations of alteration in glucose metabolism in ovarian cancer, tumor metabolic parameter [^{18}F]

fluorodeoxyglucose (FDG) using positron emission tomography (PET) scan is an useful diagnostic tool for primary and recurrent ovarian cancer (7-9).

Previous studies suggested that regulation of glucose metabolism could be the key to overcome the chemoresistance in ovarian cancer; however we still not fully understand how glucose metabolism acts in the ovarian cancer progression (10-12). Previous our findings indicate that targeting glucose metabolism induces cancer-specific programmed cell death in ovarian cancer cells, restraint with glycan synthase and protein glycosylation (9). Cancers display variety alterations in protein glycosylation compared with normal counterparts. Glycosylation of proteins participate in numerous biological process involves in cancer, such as inter- and intracellular signaling and cellular metabolism (13, 14). Moreover, loss of glycosylation of multi-drug efflux pumps, such as ATP-binding cassette transporters, might lead mislocalization and disrupt their activities (15). Herein, we postulated that glucose might be the key modulator of chemoresistance via regulation of multidrug resistance efflux pumps in ovarian cancers.

4.2. Materials and Methods

4.2.1. Cell culture conditions and tumor sphere formation assay

Human ovarian cancer cell lines; PA-1 (p53 wild type), OVCAR3 (p53 mutant) and SKOV3 (p53 null) were obtained from ATCC. All ovarian cancer cell lines were grown in RPMI 1640 (WelGENE, Seoul, Korea) at 37˚C in 5% CO_2 and humidified atmosphere. All culture media were supplemented with 10% fetal bovine serum (FBS) (Gibco-BRL, Gaithersburg, MD) and 100 μg/mL of penicillin-streptomycin (P/S) (Invitrogen, Carlsblad, CA). For tumor sphere formation assay, cells were grown in poly-HEMA coated plate with sphere medium and daily-added growth factors [20 ng/mL fibroblast growth factor (FGF), 20 ng/mL EGF; Sigma-Aldrich] as described previously (16). After 21days of culture, the number and sized of spheres were counted.

4.2.2. Reagents and antibodies

Stock solutions of cisplatin (Enzo life science) were prepared in (Dimethylformamide; 0.001%), and tunicamycin (Sigma Aldrich), SB21673 (Cayman, MI), and compound C (Calbiochem, San Diego) were freshly prepared in dimethyl sulfoxide (DMSO; 0.001%) and used at the final concentrations as indicated. Glucose-free media (Gibco-

BRL), glucose (Sigma Aldrich) and LiCl (Sigma Aldrich) were used for this study. Thiazolyl blue tetrazolium bromide (MTT) was from Amresco (olon, OH). Cycloheximide (Sigma Aldrich) used for determine the protein stabilities (17). Antibodies to ABCG2, phospho-GSK3β (Y216), Lamin B, and phospo-Akt (S473) were purchased from Santa Cruz Biotechnology (Santa Cruz, CA). Antibodies to p-glycoprotein, phospho-Akt (T308), phospho-mTOR, phospho-P70S6K, GSK3β, phospho-GSK3β (S9), β-catenin and pan Cadherin were purchased from Cell Signaling (Danvers, MA). GAPDH (AB frontier) was used as a loading control. Alexa Fluor conjugated anti-rabbit and anti-mouse antibodies were obtained from Invitrogen (Carlsbad, CA).

4.2.3. Cell death analysis

Cell viabilities were analyzed by MTT assay according to previously published procedures (9). For measurement of apoptotic cell death in ovarian cancer cells, we performed flow cytometric analysis using Annexin-V and PI staining (BD Pharmingen, CA) according to the manufacturer's protocol.

4.2.4. qRT-PCR

Total RNA was isolated with the TRIZOL reagent (Life Technologies, Gaithersburg, MD) and cDNAs were synthesized from 1

μg total RNA, using M-MLV reverse transcriptase (Invitrogen, Carlsbad, CA) with random oligomer priming. PCR was performed with specific primers (Table 1) and we followed the PCR conditions according to previously published procedures. GAPDH served as a control.

Table 1. Primer pairs for qRT-PCR analysis

Gene	Forward	Reverse	Ref
ABCB1	5'-CATGCAGATTAT GCGGATCAA-3'	5'-TTTGTTGTGCTG TAGGAAGCTCA-3'	(18)
ABCG2	5'-CTGAGATCCTGA GCCTTTGG-3'	5'-TGCCCATCACAA CATCATCT-3'	(19)
ALDH1A1	5'-ATGGATGCTTCC GAGAGG-3'	5'-GCCACATACACC AATAGGTTC-3'	(20)
SOX2	5'-TTGCTGCCTCTT TAGACTAGGA-3'	5'-CTGGGGCTCAA ACTTCTCTC-3'	(16)
Oct4	5'-GCCGGTTACAGA ACCACACT-3'	5'-GTGGAGGAAGCT GACAACAA-3'	(21)
BMI1	5'-ATGTGTGTGCTT TGTGGAG-3'	5'-AGTGGTCTGGTC TTGTGAAC-3'	(19)
Nanog	5'-ATGCCTGTGATT TGTGGGCC-3'	5'-GCCAGTTGTTTT TCTGCCAC-3'	(22)
GAPDH	5'-ACCACAGTCCAT GCCATCAC-3'	5'-TCCACCACCCTG TTGCTGTA-3'	(20)

4.2.5. Isolation of glycol-conjugated proteins and membrane-associated proteins

Glycol-conjugated proteins were isolated with Glycoprotien Isolation Kit, Con A (Thermo scientific, IL) and for membrane associated protein isolations, we used Membrane protein extraction kit (Biovision, CA). The extractions were performed according to the manufacturer's instructions.

4.2.6. Western blotting and Lectin binding assay

Protein preparation and immunoblot analyses were carried out according to previously published procedures (9). In brief; proteins were subjected to SDS-PAGE under reducing conditions then transferred onto nitrocellulose membranes. The blotted membranes were blocked with 5% nonfat dried milk and then incubated with the respective antibodies. GAPDH was used as a loading control.

Lectin blotting was performed as described previously [13]. N-linked glycans were detected using concanavalin A (Con A, Sigma Aldrich) binding. After 30 min of blocking with 5 % skimmed milk, blots were incubated with 5 μg/ml of Con A in 5% skimmed milk overnight in an agitating incubator.

4.2.7. Immunocytochemistry

Cells were plated onto 8-well chamberslide (SPL. Seoul. Korea) and incubated with the test media and agents. The cells were fixed with 4% paraformaldehyde, permeabilized with 0.2% of Triton X-100, and blocked with 5% of goat serum. The anti-P-gp and anti-ABCG2 antibodies (1:250), Alexa Fluor conjugated anti-rabbit and anti-mouse antibodies (1:250) and the membrane specific dye (CellMask™ Deep Red Plasma membrane Stain (Invitrogen) were used for membrane

localization of P-gp and ABCG2. Imaging was performed using a Confocal FV1000 imaging system (Olympus).

4.2.8. Statistical analysis

All the data are presented as mean ± SEM. Statistical analysis was performed using PASW statistics 18 software. Differences of data were analyzed by 1-ANOVA and the Student T-test. Statistical significant differences were considered as* $p<0.05$, **$P<0.01$ and ***$P<0.001$.

4.3. Results

4.3.1. Expressions of P-glycoprotein and ABCG2 associates with cisplatin resistance in ovarian cancer

Multi-drug efflux pumps, ATP-binding cassette transporters (ABC transporters) are suggested as signatures for chemoresistance in various cancers (23, 24). In ovarian cancer, P-glycoprotein (*ABCB1*, also called as MDR1) and ABCG2 are closely related with resistance of platinum-based therapy (25, 26). Based on the open data analysis (GEO profile No. GD4950), we found that *ABCB1* (Fig 1A) and *ABCG2* (Fig 1B) expressions were upregulated in human samples with carboplatin (platinum-based drug) resistance from high-grade serous (HGS) ovarian cancer patient and incereased in samples from III/IV stage of HGS ovarian cancer patients [Fig 1A (2), 1B (2)] (27). We employed three different types of ovarian cancer cells to analyze effects of cisplatin (CDDP) and correlation with ABC transporters expression. SKOV3 showed most resistance to CDDP treatment and PA-1 appeared sensitive to (Fig 1C). As shown in figure 1D, in SKOV3, *ABCB1* and *ABCG2* mRNA expressions were significantly upregulated and protein expressions were correlated with it. For further evaluation the role of glucose on the CDDP resistance, we used SKOV3 cells.

A. *ABCB1* (P-glycoprotein; MDR1)

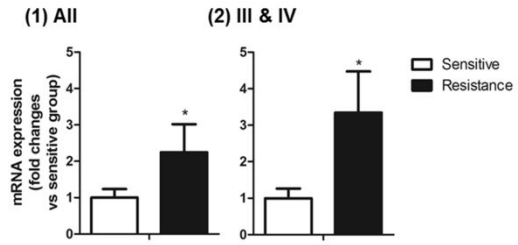

B. *ABCG2*

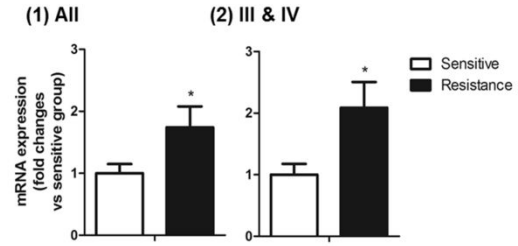

C.

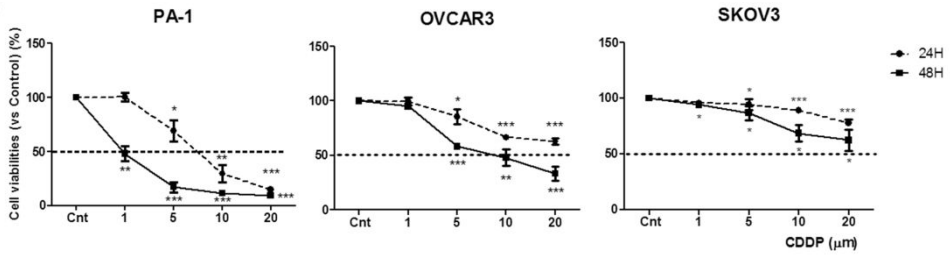

D.

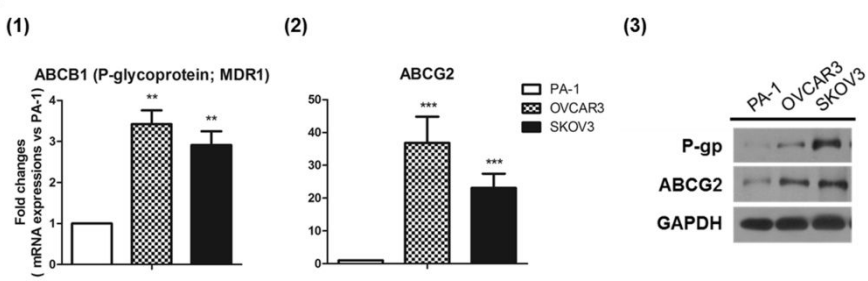

Figure 1. Association of CDDP resistance and ABC transporter expression in ovarian cancer.

A. B. Overexpression of *ABCB1* (A) and *ABCG2* (B) in human ovarian cancer tissue with platinum-based drug resistance. Gene expressions were evaluated by (1) sensitive ovarian cancer patient vs resistant patients samples (n=16), and (2) stage III /IV ovarian cancer patients with drug sensitive and resistant. (n=11). Data were represented as ± SEM with independent experiments. * P< 0.05, ovarian cancer tissue with sensitive versus resistance samples.

C. Effect of CDDP in the ovarian cancer cell viabilities. Ovarian cancer cells were treated with CDDP in a dose (1 to 20μM) and a time (24 to 48h)-dependent manner. DMF (0.01 %) was used as vehicle. Cell viabilities were measured by MTT assay and data were represented as ± SEM with three independent experiments. * P< 0.05, ** P<0.01, and *** P<0001, control versus CDDP treatment.

D. Overexpressions of *ABCB1* and *ABCG2* in CDDP resistant ovarian cancer cells. To check the basal expressions of *ABCB1* (P-glycoprotein, P-gp) and *ABCG2* in ovarian cancer cells, we performed (1, 2) qRT-PCR and (3) Western Blotting. Data were

represented as ± SEM with three independent experiments. ** P<0.01, and *** P<0.01. PA-1 versus OVCAR3 or SKOV3.

4.3.2. Glucose restriction suppresses ABC trasporters and enhances cisplatin responses in ovarain cancer cells

Glucose consumption rate of cancers are significantly different from normal tissues (28). Therefore, to study the metabolic dependencies imposed on glucose availabilities in CDDP resistant ovarian cancer cells, we applied various concentration of glucose containing media (0, 1, 10 and 20 mM). After 48 hours of treatment with these media, we checked the expressions of *ABCB1* and *ABCG2* by quantitative real-time PCR and Western blotting. As shown in figure 2A, treated with glucose free media significantly suppressed the mRNA and protein expressions of P-glycoprotein (*ABCB1*, P-gp*)* and ABCG2 in SKOV3. Parallel with these findings, CDDP in 0 mM of glucose-containing media significantly improved the CDDP-induced apoptosis (Fig 2E. 1). On the other hand, when exposed to CDDP in high glucose (20 mM)-containing media suppressed the effect of CDDP in SKOV3 (Fig 2E. 2). Our data showed that CDDP responses depended on the glucose availabilities in CDDP resistant ovarian cancer cells.

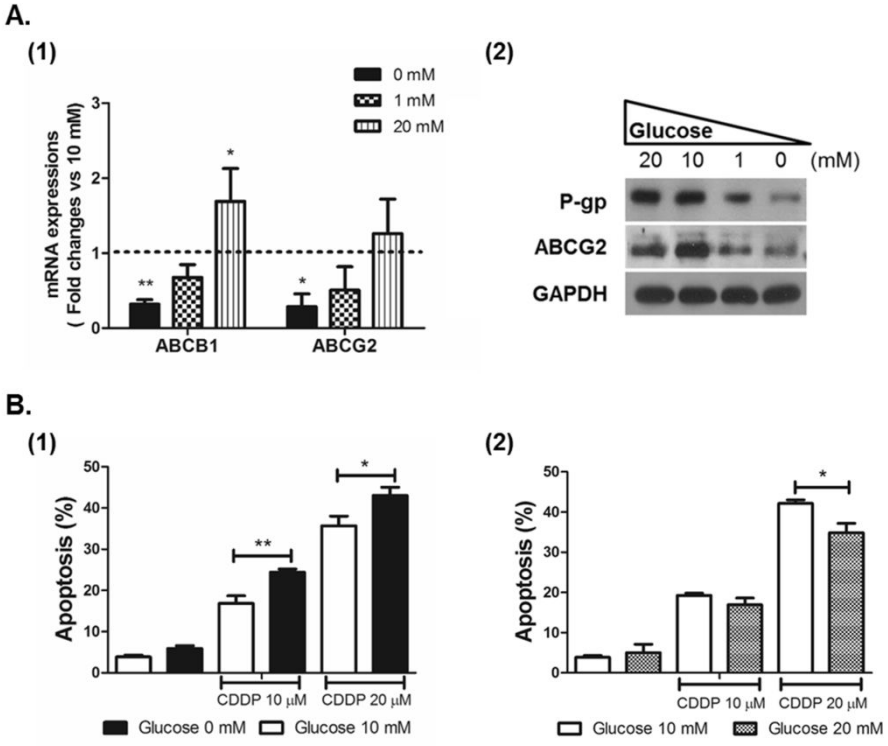
A.
(1)
0 mM
1 mM
20 mM
mRNA expressions
(Fold changes vs 10 mM)
ABCB1
ABCG2
(2)
Glucose
20 10 1 0 (mM)
P-gp
ABCG2
GAPDH
B.
(1)
Apoptosis (%)
CDDP 10 μM
CDDP 20 μM
Glucose 0 mM
Glucose 10 mM
(2)
Apoptosis (%)
CDDP 10 μM
CDDP 20 μM
Glucose 10 mM
Glucose 20 mM

Figure 2. Suppression of ABC transporters by glucose limitation.

A. Suppression of p-glycoprotein and ABCG2 by glucose restriction. After 48 hours treatment with various concentration of glucose-containing media (0 to 20 mM), (1) mRNA expressions of ABC transporters were analyzed by qRT-PCR and (2) protein expressions were assessed by Western Blotting. Data were represented as ± SEM with three independent experiments. * $P< 0.05$, and ** $P<0.01$, 10 mM of glucose versus 0 mM or 20 mM of glucose.

B. Improvement of CDDP-induced apoptosis by glucose restriction. CDDP (10 μM and 20 μM) in 0, 10 and 20 mM of glucose containing media (10 mM of glucose-containing media used as control) were treated in SKOV3 cells for 48 hours and apoptotic cell death was analyzed by Annexin V/PI staining. (1) Induction of CDDP in glucose free media. (2) Induction of CDDP in 20 mM of glucose containing media. Data were represented as ± SEM with three independent experiments. * $P< 0.05$ and ** $P<0.01$. CDDP in 10 mM versus CDDP in 0 mM or 20 mM-glucose containing media.

4.3.3. Glucose restriction disrupts ABC transporters through glycosylation failure

In previous report, glucose acts as a signaling modulator involves in protein modification (29). ABC transporters are transmembrane proteins which need to be N-linked glycosylated (NLG) (15). Therefore, we postulated that mimicking glucose availabilities induced NLG defects of ABC transporters. To address NLG disruption of ABC transporters by glucose restriction, we isolated glycol-conjugated proteins with concanavalin A (Con A) binding beads. Con A binds to Asn-linked glycan of protein, so we could isolate NLG proteins. When exposed to various concentration of glucose-containing media (0, 1, 10 and 20 mM) for 48 hours in SKOV3, glycosylated P-gp and ABCG2 were significantly decreased in glucose restriction (Fig 3A.1). Associated with these findings, glucose restriction suppressed membrane expression of P-gp and ABCG2, analyzed by isolation of membrane-bounded proteins (Fig 3A. 2) and co-expression with plasma membrane marker by immunocytochemistry (Fig 3A. 3). To identify the role of NLG in membrane expression of P-gp and ABCG2, we employed tunicamycin (TM, 5 μg/mL), as a positive control for inhibition of protein NLG. 48 hours of treatment with TM suppressed NLG and membrane expression of P-gp and ABCG2 in SKOV3 (Fig

3B).

Disruption of protein NLG decreased membrane expression and also suppresses protein stabilities (30, 31). When SKOV3 cells exposed to glucose free media or TM (5 μg/mL), total protein expressions of P-gp and ABCG2 were decreased in a time-dependent manner (Fig 3C. 1). Therefore, we investigated the effect of NLG disruption in protein stabilities of P-gp and ABCG2. Protein stabilities were analyzed using cycloheximide (CHX, an inhibitor of protein synthesis) (17). In control media (10 mM of glucose), P-gp and ABCG2 was persistently expressed within CHX treatment (20 μg/ml, 6 to 48 h), however; disruption of protein NLG by glucose free media or TM remarkably decreased expressions of ABC transporters (Fig 3C. 2). With densitometric quantification, we could address that NLG defect significantly suppressed the protein stabilities of P-gp and ABCG2 in SKOV3 cells (Fig 3C. 3). Glucose restriction suppressed the transcriptional and translational activities of P-gp and ABCG2 (Fig 2A). We did not fully understand how glucose regulated mRNA expression of ABC transporters, however; glycosylation defects significantly suppressed the stabilities of ABC transporters. Taken together, these results indicated that glucose acted as an ABC transporters regulator via NLG.

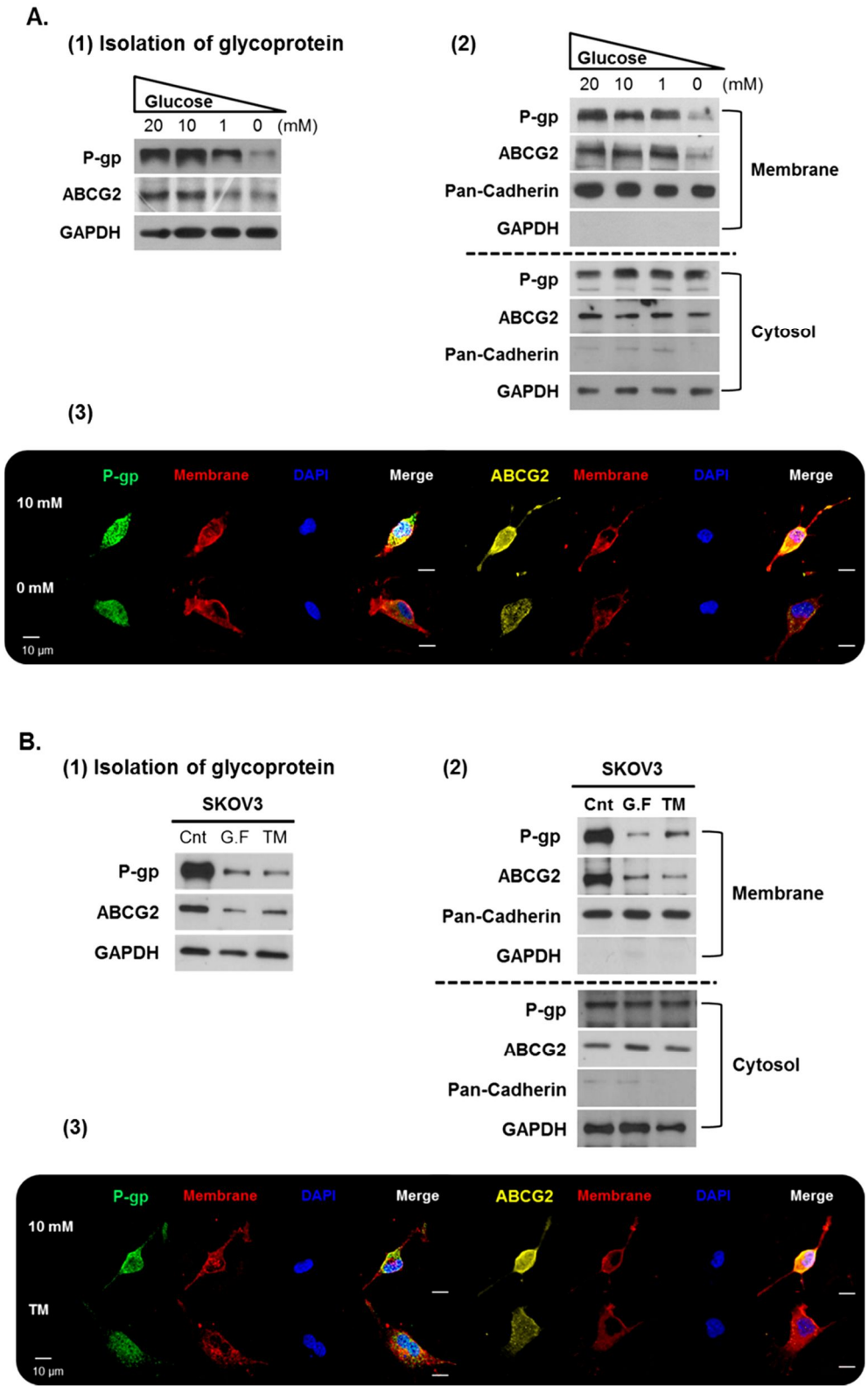
A.
(1) Isolation of glycoprotein
Glucose
20 10 1 0 (mM)
P-gp
ABCG2
GAPDH
(2)
Glucose
20 10 1 0 (mM)
P-gp
ABCG2
Pan-Cadherin
GAPDH
Membrane
P-gp
ABCG2
Pan-Cadherin
GAPDH
Cytosol
(3)
P-gp
Membrane
DAPI
Merge
ABCG2
Membrane
DAPI
Merge
10 mM
0 mM
10 μm
B.
(1) Isolation of glycoprotein
SKOV3
Cnt G.F TM
P-gp
ABCG2
GAPDH
(2)
SKOV3
Cnt G.F TM
P-gp
ABCG2
Pan-Cadherin
GAPDH
Membrane
P-gp
ABCG2
Pan-Cadherin
GAPDH
Cytosol
(3)
P-gp
Membrane
DAPI
Merge
ABCG2
Membrane
DAPI
Merge
10 mM
TM
10 μm

C.

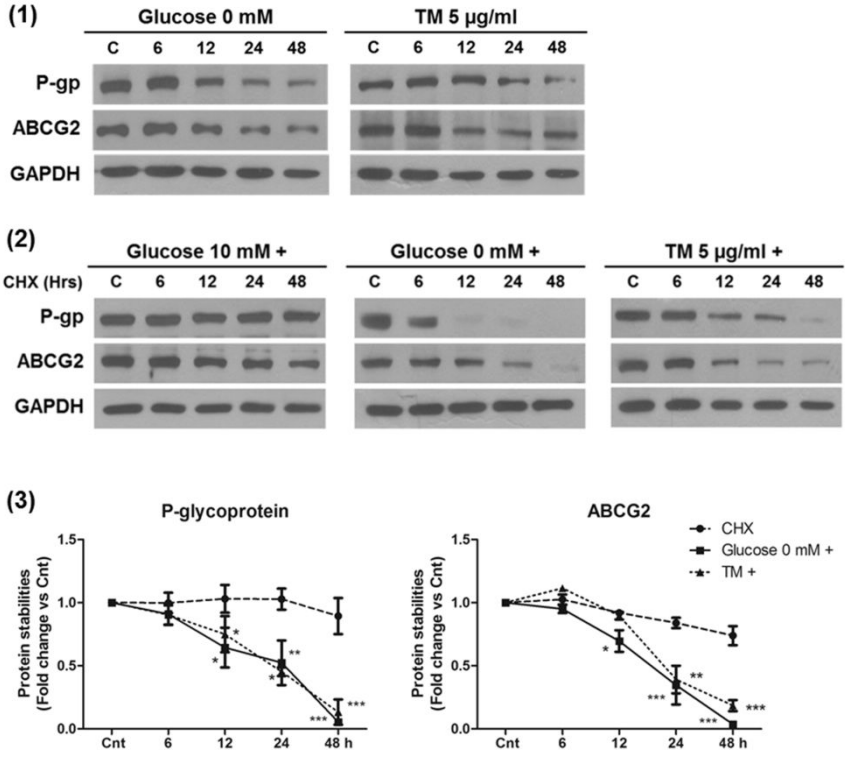
(1)
Glucose 0 mM
TM 5 μg/ml
C 6 12 24 48
C 6 12 24 48
P-gp
ABCG2
GAPDH
(2)
Glucose 10 mM +
Glucose 0 mM +
TM 5 μg/ml +
CHX (Hrs)
C 6 12 24 48
C 6 12 24 48
C 6 12 24 48
P-gp
ABCG2
GAPDH
(3)
P-glycoprotein
ABCG2
CHX
Glucose 0 mM +
TM +
Protein stabilities (Fold change vs Cnt)
1.5
1.0
0.5
0.0
Cnt 6 12 24 48 h

Figure 3. Inhibition of NLG and membrane expression of ABC transporters by glucose restriction. After 48 h treatment with various concentrations of glucose containing media (0 to 20 mM, 10 mM used as control), we analyzed the expression pattern of ABC transporters in SKOV3.

A. Suppression of NLG and membrane expression of ABC transporters in response to glucose starvation. Expression of ABC transporters in SKOV3 were analyzed by Western blot with (1) isolation of glycol-conjugated proteins, (2) fraction of membrane-bounded proteins. (3) Membrane expression of P-gp (p-glycoprotein) and ABCG2 were assessed with confocal microscopy. Green; P-gp, yellow; ABCG2, red; plasma membrane, blue; DAPI. Scale bars in this figure correspond to 10 μm.

B. Suppression of membrane expression of ABC transporters by NLG inhibition. Tunicamycin (TM, 5μg/ml) used as a positive control for NLG inhibitor. After 48 h treatment with glucose free media or TM, expression of ABC transporters were analyzed by Western blot with (1) isolation of glycol-conjugated proteins, (2) fraction of membrane-bounded proteins. (3) Membrane expression of P-gp (p-glycoprotein) and ABCG2 were assessed with confocal microscopy. Green; P-gp, yellow;

ABCG2, red; plasma membrane, blue; DAPI. Scale bars in this figure correspond to 10 μm.

C. Suppression of protein stabilities of P-gp and ABCG2 by NLG inhibition.

(1) Suppression of ABC transporters by NLG inhibition.

Glucose free media or TM was treated in SKOV3(6 to 48 h) and P-gp and ABCG2 expressions were analyzed by Western Blot.

(2, 3) Cycloheximide (CHX, 20 μg/ml) was used to determine the stabilities of ABC transporters. Pretreatment with glucose free or TM -containing media for 4 hour and applied with CHX indicated time. P-gp and ABCG2 expression was analyzed by Western blot. Plots were normalized to GAPDH and performed densitometric quantification. Data represent as ± SEM with three independent experiments, compared with control. * $P< 0.05$ and ** $P<0.01$. CHX single treatment versus 0 mM of glucose or TM co-treatment.

4.3.4. GSK3β regulates glycosylation of ABC transporters

Intracellular levels of glucose and hexosamine biosynthetic pathway strongly involves in protein NLG (30). Multi-kinase of GSK3β regulates enzyme activities involves in glycogen synthase and hexosamine biosynthetic pathway (29). Moreover, previous our finding indicates that GSK3β activation interrupts protein glycosylation in ovarian cancer cells. Here, we evaluated whether the action of GSK3β involved in glycosylation of ABC transporters in response to glucose restriction. After SKOV3 cells were expose to various concentrations of glucose-containing media (0 to 20 mM) for 48 hours, protein NLG expression profiles were assessed by lectin binding assay and related molecular events were analyzed by Western blot. As shown in figure 4A, protein NLG was significantly suppressed by glucose free media and GSK3β activated, resulting from decreased in GSK3β inhibition form (phosphorylated at S9) while its active form (phosphorylated at Y216) persistently expressed. In parallel with these events, GSK3β downstream molecule, β-catenin was reduced (Fig 4A). Next, to address the role of GSK3β on protein NLG, two different types of GSK3β inhibitors, lithium chloride (Li, 20 mM) and SB216763 (SB, 10 μM), were employed. Suppressed protein NLG patterns and β-catenin expression by glucose restriction was recovered by GSK3β inhibitors

(Fig 4B). To identify potential role of GSK3β on NLG of ABC transporters, we isolated glycol-conjugated proteins after treatment with GSK3β inhibitors. NLG defects of P-gp and ABCG2 by glucose restriction was recovered by GSK3β inhibitors (Fig 4C. 1). Additionally, we found GSK3β inhibition reversed membrane expression of P-gp and ABCG2 (Fig 4C. 2, 3), which repressed by glucose restriction. Further, to evaluate the restorations of membrane expression ABC transporters in CDDP responses, we assessed CDDP-induced apoptotic cell death in response to GSK3β inhibition. As shown in figure 4D, increased CDDP-induced apoptotic cell death by glucose restriction was attenuated by GSK3β inhibitors. Notably, glucose restriction raised CDDP-responses through disruption of ABC transporters NLG via GSK3β activation.

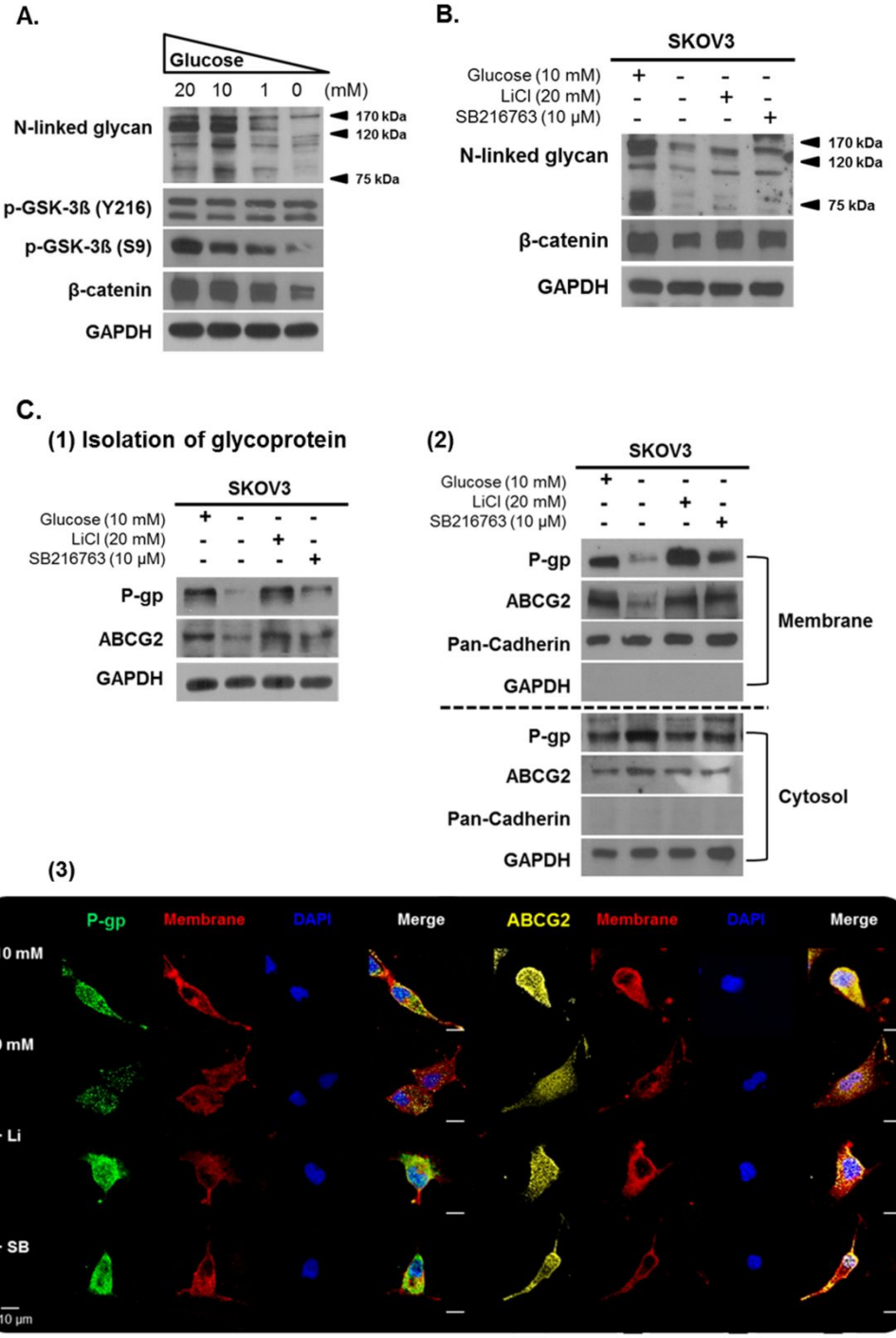
A.
Glucose
20 10 1 0 (mM)
N-linked glycan
170 kDa
120 kDa
75 kDa
p-GSK-3ß (Y216)
p-GSK-3ß (S9)
β-catenin
GAPDH
B.
SKOV3
Glucose (10 mM) + - - -
LiCl (20 mM) - - + -
SB216763 (10 μM) - - - +
N-linked glycan
170 kDa
120 kDa
75 kDa
β-catenin
GAPDH
C.
(1) Isolation of glycoprotein
SKOV3
Glucose (10 mM) + - - -
LiCl (20 mM) - - + -
SB216763 (10 μM) - - - +
P-gp
ABCG2
GAPDH
(2)
SKOV3
Glucose (10 mM) + - - -
LiCl (20 mM) - - + -
SB216763 (10 μM) - - - +
P-gp
ABCG2
Pan-Cadherin
GAPDH
Membrane
P-gp
ABCG2
Pan-Cadherin
GAPDH
Cytosol
(3)
P-gp
Membrane
DAPI
Merge
ABCG2
Membrane
DAPI
Merge
10 mM
0 mM
+ Li
+ SB
10 μm

D.

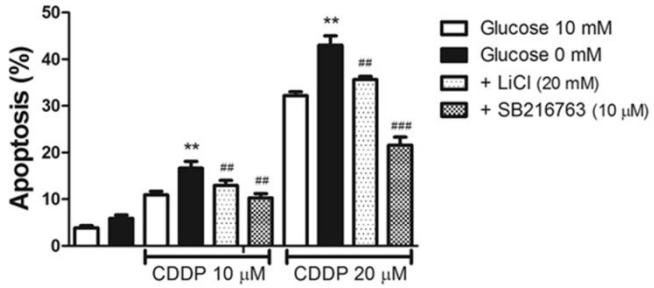
Apoptosis (%)
50
40
30
20
10
0
**
**
##
##
##
###
CDDP 10 μM
CDDP 20 μM
Glucose 10 mM
Glucose 0 mM
+ LiCl (20 mM)
+ SB216763 (10 μM)

Figure 4. Glycosylation and membrane expression of ABC transporters by GSK3β activation in responses to glucose restriction. Two types of GSK3β inhibitors [lithium chloride (Li, 20 mM) and SB216763 (SB, 10 μM)] were used for evaluate the effects of GSK3β on the regulation of ABC transporters NLG.

A. Inhibition of protein NLG by glucose starvation. SKOV3 exposed to various concentrations of glucose-containing media (0 to 20 mM) for 48 h. NLG proteins were detected with lectin binding assay with Con A (5 μg/ml) and GSK3β regularoty molecules were analyzed by Western blot.

B. Interruption of protein NLG by GSK3β activation. Apply with GSK3β inhibitors, protein NLG and related molecules were analyzed as described previously.

C. Regulation of NLG and membrane expression of ABC transporters by GSK3β. After applied with GSK3β inhibitors, expression pattens of ABC transporters were analyzed. (1) Inhibition of NLG of p-glycoprotein and ABCG2 by GSK3β activation. (2) Interruption of membrane expression of p-glycoprotein and ABCG2 by GSK3β activation. (3) Membrane expression of P-gp (p-glycoprotein) and ABCG2 were assessed with confocal microscopy. Green; P-gp, yellow; ABCG2, red;

plasma membrane, blue; DAPI. Scale bars in this figure correspond to 10 μm.

D. Effect of GSK3β on CDDP-induced apoptosis by glucose restriction in SKOV3. Pretreatment of GSK3β inhibitors as indicated concentrations for 3 hours and co-treated with CDDP (10 to 20μM)-containing glucose free media. 10 mM of glucose containing with CDDP as control group. After 48 hours of treatment, apoptotic cell death was analyzed by Annexin V/PI staining. Data were represented as ± SEM with three independent experiments. ** $P<0.01$. CDDP in glucose 10 mM versus CDDP in glucose 0 mM. $^{\#\#}$ $P<0.01$, $^{\#\#\#}P<0.001$. CDDP in glucose 0 mM versus CDDP in glucose 0 mM-containing GSK3β inhibitors.

4.3.5. AMPK cascade regulates the action of GSK3β

Herein, we found GSK3β played a key role in ABC transporters NLG and membrane expression in response to glucose mimicking. GSK3β activation is controlled by phosphorylation through Akt and p70S6K activation, at S9 site of GSK3β (GSK3β inhibition form) (32). Previous findings indicate that activated Akt and p70S6K suppresses the action of GSK3β through S9-phosphorylation, and these molecular events involves by AMPK (33, 34). Therefore, we postulated that glucose restriction activated GSK3β via AMPK cascade. As shown in figure 6A, glucose restriction activated AMPK (p-AMPK) and the actions of Akt (phosphorylated at S473 and T308) and p70S6K (p-p70S6K) were suppressed. Using AMPK inhibitor, compound C (C.C, 10 μM), we determined the role of AMPK in GSK3β activation through p-Akt and p-p70S6K regulation. AMPK inhibition reversed the molecular mechanisms related with Akt/mTOR by glucose restriction. Followed by these events, GSK3β was inhibited, monitored by increased S9-phosphorylation of GSK3β, protein NLG and β-catenin expression. To address the role of AMPK activation contributed to GSK3β-mediated NLG and membrane expression of ABC transporters, we analyzed glycosylated- and membrane expression of ABC transporters in response to AMPK inhibitor. AMPK inhibition recovered NLG and

membrane expression of P-gp and ABCG2, which were suppressed by glucose restriction (Fig 6C). These results provided glucose restriction suppressed glycosylation and membrane expressions of ABC transporters by GSK3β activation followed by AMPK cascades in CDDP-resistance ovarian cancer cells.

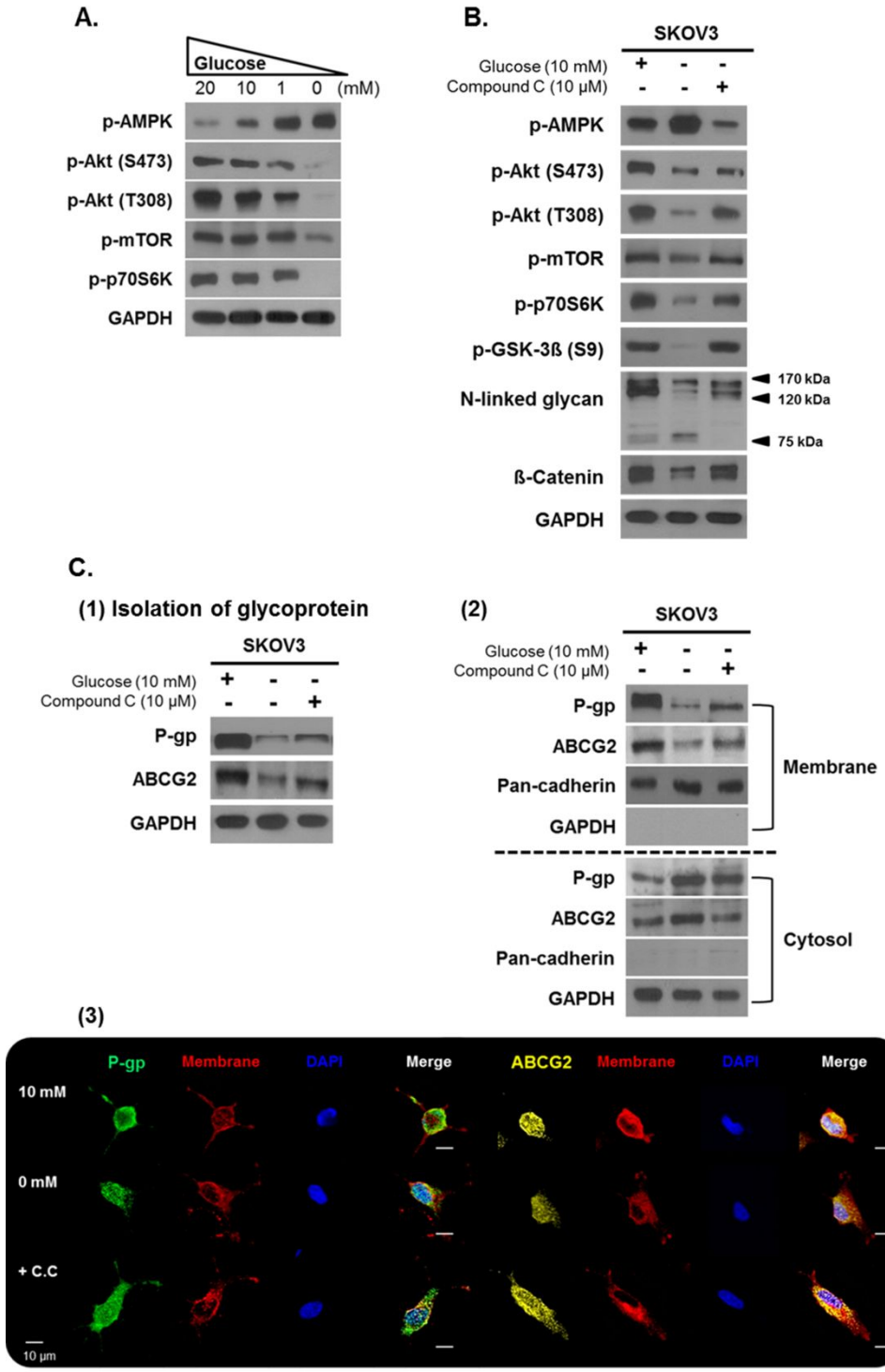
A.
Glucose
20 10 1 0 (mM)
p-AMPK
p-Akt (S473)
p-Akt (T308)
p-mTOR
p-p70S6K
GAPDH
B.
SKOV3
Glucose (10 mM)
Compound C (10 μM)
p-AMPK
p-Akt (S473)
p-Akt (T308)
p-mTOR
p-p70S6K
p-GSK-3ß (S9)
N-linked glycan
170 kDa
120 kDa
75 kDa
ß-Catenin
GAPDH
C.
(1) Isolation of glycoprotein
SKOV3
Glucose (10 mM)
Compound C (10 μM)
P-gp
ABCG2
GAPDH
(2)
SKOV3
Glucose (10 mM)
Compound C (10 μM)
P-gp
ABCG2
Pan-cadherin
GAPDH
Membrane
P-gp
ABCG2
Pan-cadherin
GAPDH
Cytosol
(3)
P-gp
Membrane
DAPI
Merge
ABCG2
Membrane
DAPI
Merge
10 mM
0 mM
+ C.C
10 μm

Figure 5. Modulation of GSK3β by AMPK activation

A. AMPK activation by glucose restriction. After 48 h of incubation with various glucose containing-media (0 to 20 mM) in SKOV3, AMPK regulatory molecules were evaluated by Western blotting.

B. Disruption of protein NLG through AMPK/GSK3β activation. AMPK inhibitor, compound C (C.C, 10 μM) was used for evaluation of the role of AMPK in protein NLG and GSK3β activation. Pretreated with C.C for 3 h and applied with glucose free media for 48 hours. The related signaling molecules were assessed by Western blot and protein NLG was analyzed by lectin binding assay.

C. Dysregulation of ABC transporters by AMPK activation. Apply with AMPK inhibitor, compound C (C.C, 10 μM), (1) glycosylated P-gp and ABCG2 and (2) membrane expression of P-gp and ABCG2 were analyzed by Western blot with isolated samples. (3) Membrane expression of P-gp (p-glycoprotein) and ABCG2 were assessed with confocal microscopy. Green; P-gp, yellow; ABCG2, red; plasma membrane, blue; DAPI. Scale bars in this figure correspond to 10 μm.

4.3.6. Glucose restriction attenuates ovarain cancer stemness through AMPK/GSK3β/ β-catenin axis.

Recent data demonstrates that glucose starvation suppresses stemness phenotypes of ovarian cancer cells (35). Herein, we found glucose restriction disrupted of ABC transporters in CDDP resistant ovarian cancer cells. ABC transporters suggest as signatures of cancer stem-like cells (CSC) and/or cancer initiating cells, which are strongly involved in chemoresistance (23, 24). To validate role of glucose on CSC phenotypes of ovarian cancer, we performed tumor sphere formation and analyzed stemness related genes. As shown figure 6A, glucose restriction significantly attenuated sphere forming capacities and suppressed expression of stemness related genes, *ALDH1A1, SOX2, Oct4, and BMI1, Nanog,* in SKOV3 (16, 18-20, 22). Additionally, high glucose-containing media enhanced size of tumor sphere and expressions of stemness related genes, *ALDH1A1* and *BMI1* (Fig 6A).

Our finding indicated that limited glucose availabilities activated GSK3β, a key regulator of β-catenin (Fig 4A) (36). Wnt signaling is well described as a critical regulator of CSC and chemoresistance in many cancers and co-transcriptional activity of β-catenin is a main molecular event in Wnt signaling (36, 37). Therefore, we speculated GSK3β activation dysregulated Wnt/β-catenin signaling

through repressed β-catenin. As shown in figure 6B, glucose restriction repressed nuclear expression of β-catenin and cyclin D1 expression, a target gene of the Wnt signaling (Fig 6B) (36). Next, we evaluated the role of GSK3β activation on β-catenin nuclear movement using GSK3β inhibitors, Li (20 mM) and SB (10 μM). GSK3β inhibition recovered nuclear expression of β-catenin and also cyclin D1, which were suppressed by glucose restriction (Fig 6C). Moreover, attenuated sphere formation and stemness related gene expressions also recovered in response to GSK3β inhibitors (Fig 6D). These data suggested that glucose restriction attenuated CSC phenotypes and these phenomena might be related with suppression of Wnt/β-catenin signlaing through GSK3β activation.

In accordance with GSK3β activation through AMPK cascade in glucose limitation (Fig 5B), we assessed β-catenin nuclear expression and CSC phenotypes by AMPK inhibitor. AMPK inhibition recovered β-catenin nuclear expression and cyclin D1, even in the absence of glucose (Fig 6E). Additionally, CSC phenotypes were restored by AMPK inhibition, sphere forming capacities and stemness related makers (Fig 6D. 2, 3). These results provided evidence that glucose restriction attenuated CSC phenotypes via AMPK/GSK3β axis in CDDP-resistant ovarian cancer cells.

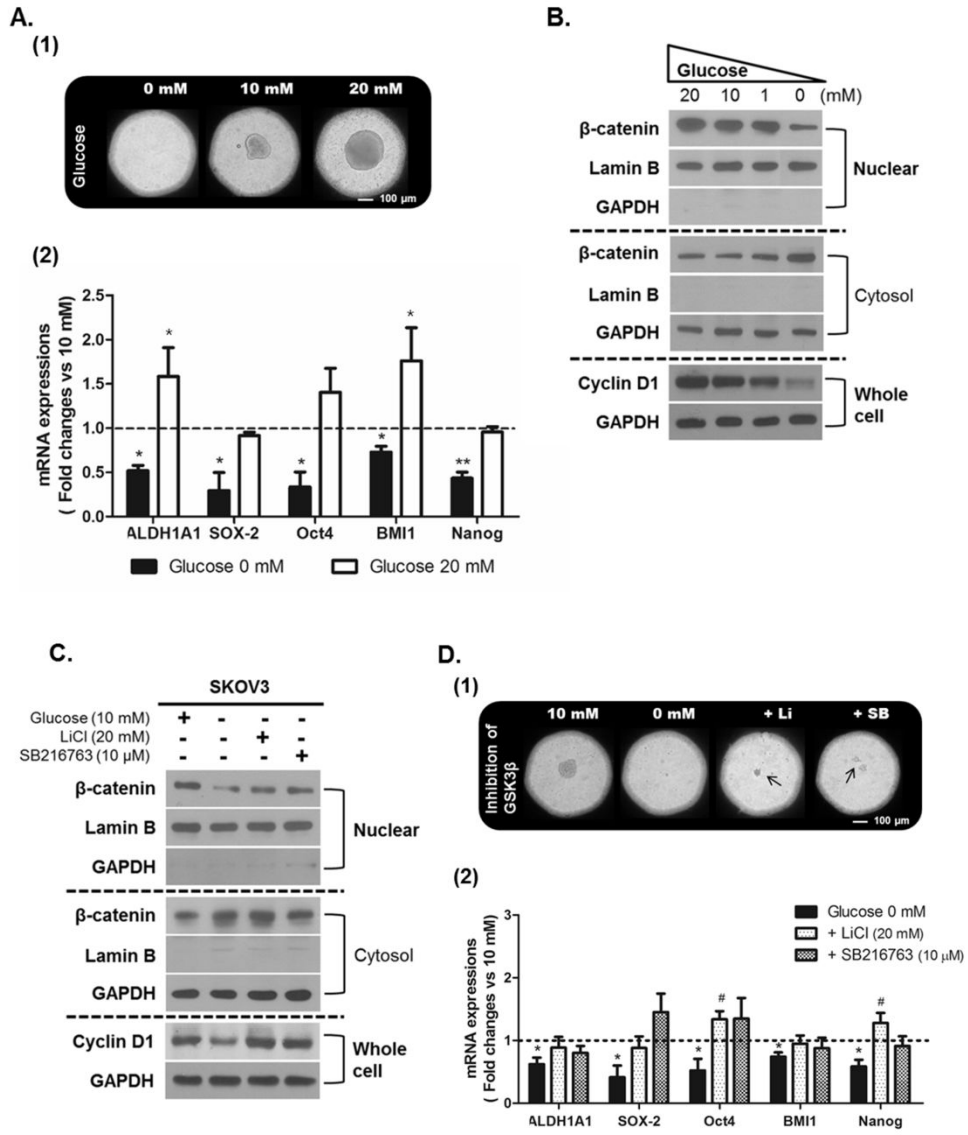
A.
(1)
0 mM
10 mM
20 mM
Glucose
100 μm
(2)
mRNA expressions
(Fold changes vs 10 mM)
2.5
2.0
1.5
1.0
0.5
0.0
ALDH1A1
SOX-2
Oct4
BMI1
Nanog
Glucose 0 mM
Glucose 20 mM
B.
Glucose
20 10 1 0 (mM)
β-catenin
Lamin B
GAPDH
Nuclear
β-catenin
Lamin B
GAPDH
Cytosol
Cyclin D1
GAPDH
Whole cell
C.
SKOV3
Glucose (10 mM)
LiCl (20 mM)
SB216763 (10 μM)
β-catenin
Lamin B
GAPDH
Nuclear
β-catenin
Lamin B
GAPDH
Cytosol
Cyclin D1
GAPDH
Whole cell
D.
(1)
Inhibition of GSK3β
10 mM
0 mM
+ Li
+ SB
100 μm
(2)
mRNA expressions
(Fold changes vs 10 mM)
Glucose 0 mM
+ LiCl (20 mM)
+ SB216763 (10 μM)
ALDH1A1
SOX-2
Oct4
BMI1
Nanog

E.

(1)

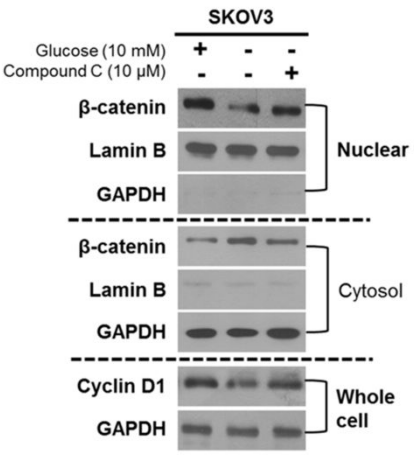
SKOV3
Glucose (10 mM)
Compound C (10 μM)
β-catenin
Lamin B
GAPDH
Nuclear
β-catenin
Lamin B
GAPDH
Cytosol
Cyclin D1
GAPDH
Whole cell

(2)

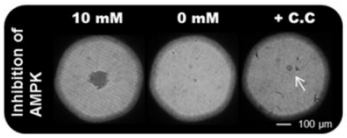
Inhibition of AMPK
10 mM
0 mM
+ C.C
100 μm

(3)

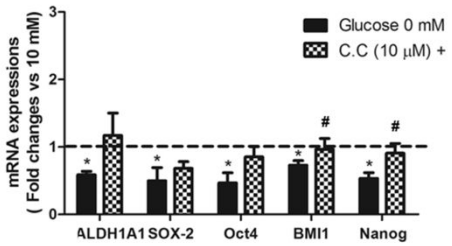
mRNA expressions (Fold changes vs 10 mM)
Glucose 0 mM
C.C (10 μM) +
ALDH1A1
SOX-2
Oct4
BMI1
Nanog

Figure 6. Suppression of ovarian cancer stemness by glucose restriction. To evaluate stemness characteristics in ovarian cancer cells, tumor sphere formation assay were performed and stemness related genes were analyzed by qRT-PCR.

A. (1) Suppression of spheroid formation in SKOV3 by glucose starvation. SKOV3 were cultured in sphere formation media with various concentration of glucose (0, 10 and 20 mM) for three weeks. Phase contrast images of sphere were shown and scale bar represented 100 μm. (2) Suppression of stemness related gene expression by glucose starvation. After 48 h treatment with vaious concentration of glucose (0, 10 and 20 mM), stemness related genes (*ALDH1A1, SOX2, Oct4, BMI1, Nanog*) were evaluated by quantitative real-time PCR (qRT-PCR) and normalized with GAPDH. Data were represented as ± SEM with three independent experiments. * $P< 0.05$ and *** $P < 0.001$. 10 mM of glucose versus 0 mM or 20 mM of glucose containing media.

B. Suppression of β-catenin nuclear expression by glucose restriction. Nuclear fraction was performed after 48 hours treatment with various concentration of glucose containing media, and western blot were conducted with anti- β-catenin,

Lamin B (nuclear marker), and GAPDH (cytoplasmic marker). Cyclin D1 expressions were assessed with whole cell lysate by Western blot.

C. Regulation of β-catenin nuclear expression by GSK3β. Nuclear fraction was performed after pretreatment of GSK3β inhibitors for 3 h and 48 h of treatment with glucose free media. And related molecular events were analyzed by Western blot

D. Regulation of ovarian cancer stemness by GSK3β. Applied with GSK3β inhibitors, (1) tumor spheroid formation and (2) ovarian cancer stemness markers were analyzed. Data were represented as ± SEM with three independent experiments. * $P< 0.05$. 10 mM versus 0 mM of glucose containing meida. $^{\#}$ $P< 0.05$. Glucose free versus Li or SB treatment.

E. Regulation of β-catenin nuclear expression and ovarian cancer stemness by AMPK activation. After pretreatment with C.C, and co-treated with glucose free media for 48 h, (1) nuclear expression of β-catenin and cyclin D1 expressions were analyzed by Western blot. And ovarian cancer stemness phenotypes (2) tumor sphere formation and (3) stemness gene expression were assessed as describe previously. Data were represented as ± SEM with three independent experiments.

*P<0.05, for Glucose 10 mM versus Glucose 0 mM. # P<0.05 for Glucose 0 mM versus C.C in glucose 0 mM.

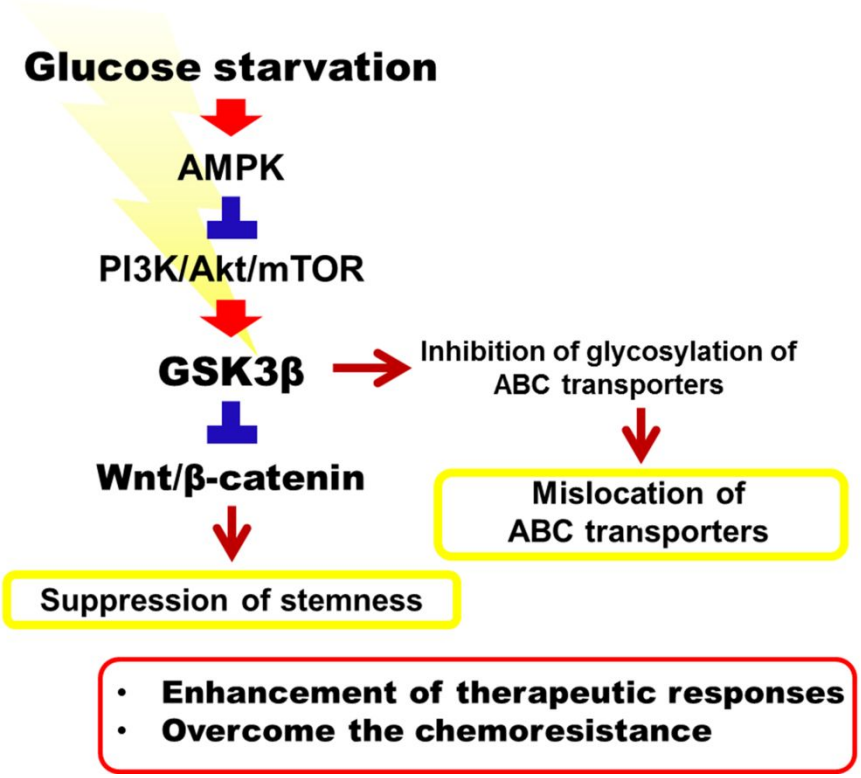

Figure 7. Lack of glucose availabilities impair ABC transporters function via mislocation, resulting from glycosylation defeat. These phenomena are modulated by GSK3β which depends on AMPK. Moreover, GSK3β activation attenuates the phenotypes of ovarian cancer stem-like cells through suppression of Wnt/β-catenin signaling.

4.4. Discussion

We provide evidences that pivotal role of glucose as key modulators of therapeutic resistance in cancer. In this study, we first demonstrated limited glucose availabilities improve therapeutic responses in ovarian cancer via disruption of ATP-binding cassette (ABC) transporters (P-glycoprotein and ABCG2), which described as multi-drug efflux pumps in cancers (Fig 2) (26). Glucose deprivation attenuated the function of ABC transporters, by interruption of glycosylation via GSK3β activation (Fig 4). Further, GSK3β activation suppressed Wnt/β-catenin signaling and attenuated ovarian cancer stem cell-like cells (CSCs) phenotypes, ultimately reduced drug resistance (Fig 5) (44, 45). The action of AMPK regulated GSK3β activation through suppression of Akt and p70S6K in response to glucose mimicking (Fig 6). Dysfunction of ABC transporters and CSC phenotypes by glucose restriction were further shown to be associated with AMPK activation (Fig 6, 7).

Cancers have distinguished features of glucose metabolism and coordinated with that glycan expressions in membrane and unique mucins are suggested tool for diagnosis and monitoring (14). Glycan involve in numerous fundamental biological processed in caner progression and also cellular metabolism, and interruption of protein

glycosylation attenuates its functions and membrane localization (13). In cancer, it has been well documented the impact of ABC transporters in chemoresistance (3, 4, 18, 19). Recent studies suggest that modulation of ABC transporters via glycosylation might improve the therapeutic responses through interfere ABC transporters (14, 15). Dysregulation of ABC transporter by dissecting glycosylation and genetic manipulations enhanced the therapeutic responses (46-48). Notably, these findings are consistent with our observation that glucose restriction improved the cisplatin (CDDP) responses via modulation of ABC transporters by impairing of glycosylation in drug resistant ovarian cancer cells (Fig 3).

According to previous finding, glycan synthase depends on the levels of intracellular glucose and hexosamine biosynthetic pathway which regulated by GSK3β (31). As evidenced hereby, GSK3β was required for membrane association of ABC transporters through a modulator of N-linked glycosylation (Fig 4). Additionally, the action of multi-kinase GSK3β involves in Wnt/β-catenin signaling (34). Glucose starvation suppressed Wnt/β-catenin cascade by GSK3β activation, evidenced by suppression of β-catenin nuclear movement and target gene expressions (Fig 5). Glucose enhance the stability of β-catenin through acetylation and this phenomena associate with cancer progression, and also β-catenin and its regulatory factors are involves in

metabolic homeostasis (49, 50). Base on the fact that Wnt/β-catenin signaling is the key regulator of stem cell differentiation and development (40, 51), this regulation affect on the cancer progression and development of drug resistance by modulating cancer stem cell-like cells (CSC) (39, 52).

Even though herein we provide profound switch of glucose in chemoresistance and CSC phenotypes, metabolic status and requirement of CSCs are controversy (53). Previous report consists with our observations in the glucose requirement of ovarian CSC. Glucose restriction represses side population of ovarian cancer cells, which regulated by ABCG2 activity, via Akt pathway (11). The understanding of systemic metabolism largely unknown in CSCs and also in cancers however, targeting glucose metabolism might indeed have beneficial effect for development therapeutic strategies.

Glucose metabolism has got huge interest as therapeutic approach for chronic diseases including cancer and it has been proposed targeting metabolism might offer novel therapeutic strategies for cancer and a way to overcome to chemoresistance (55, 56). Unless, glucose involves in multiple cellular events, genetic regulation through pentose phosphate pathway, signaling regulation by acetylation and glycosylation, and energy productions, many of studies focused on the energy production. Here we provide the role of glucose in signaling

modulator through protein glycosylation in cancer and related mechanisms. Unfortunately, we could not demonstrate the in vivo experiment, because there are limitations to control glucose levels in living organisms. However, our findings are clearly showed improvement of conventional chemotherapy responses by reducing glucose availabilities. It might be open new therapeutic windows for who were struggle with cancers.

4.5. References

1. Bast RC, Jr., Hennessy B, Mills GB. The biology of ovarian cancer: new opportunities for translation. Nat Rev Cancer. 2009;9(6):415-28.

2. Yap TA, Carden CP, Kaye SB. Beyond chemotherapy: targeted therapies in ovarian cancer. Nat Rev Cancer. 2009;9(3):167-81.

3. Vaughan S, Coward JI, Bast RC, Berchuck A, Berek JS, Brenton JD, et al. Rethinking ovarian cancer: recommendations for improving outcomes. Nat Rev Cancer. 2011;11(10):719-25.

4. Bowtell DD, Bohm S, Ahmed AA, Aspuria PJ, Bast RC, Jr., Beral V, et al. Rethinking ovarian cancer II: reducing mortality from high-grade serous ovarian cancer. Nat Rev Cancer. 2015;15(11):668-79.

5. Coleman RL, Monk BJ, Sood AK, Herzog TJ. Latest research and treatment of advanced-stage epithelial ovarian cancer. Nat Rev Clin Oncol. 2013;10(4):211-24.

6. Lamkin DM, Spitz DR, Shahzad MM, Zimmerman B, Lenihan DJ, Degeest K, et al. Glucose as a prognostic factor in ovarian carcinoma. Cancer-Am Cancer Soc. 2009;115(5):1021-7.

7. Cho H, Lee YS, Kim J, Chung JY, Kim JH. Overexpression of Glucose Transporter-1 (GLUT-1) Predicts Poor Prognosis in Epithelial Ovarian Cancer. Cancer Investigation. 2013;31(9):607-15.

8. Torizuka T, Nobezawa S, Kanno T, Futatsubashi M, Yoshikawa E, Okada H, et al. Ovarian cancer recurrence: role of whole-body positron emission tomography using 2-[fluorine-18]-fluoro-2-deoxy-D-glucose. Eur J Nucl Med Mol I. 2002;29(6):797-803.

9. Gwak H, Haegeman G, Tsang BK, Song YS. Cancer-specific interruption of glucose metabolism by resveratrol is mediated through inhibition of Akt/GLUT1 axis in ovarian cancer cells. Mol Carcinog. 2015;54(12):1529-40.

10. Priebe A, Tan LJ, Kueck WA, He G, Kwok R, Opipari A, et al. Glucose deprivation activates AMPK and induces cell death through modulation of Akt in ovarian cancer cells. Gynecologic Oncology. 2011;122(2):389-95.

11. Liu PP, Liao J, Tang ZJ, Wu WJ, Yang J, Zeng ZL, et al. Metabolic regulation of cancer cell side population by glucose through activation of the Akt pathway. Cell Death Differ. 2014;21(1):124-35.

12. Munoz-Pinedo C, El Mjiyad N, Ricci JE. Cancer metabolism: current perspectives

and future directions. Cell death & disease. 2012;3:e248.
13. Wellen KE, Thompson CB. A two-way street: reciprocal regulation of metabolism and signalling. Nat Rev Mol Cell Bio. 2012;13(4):270-U1.
14. Pinho SS, Reis CA. Glycosylation in cancer: mechanisms and clinical implications. Nat Rev Cancer. 2015;15(9):540-55.
15. Perego P, Gatti L, Beretta GL. The ABC of glycosylation. Nat Rev Cancer. 2010;10(7):523-.
16. Bareiss PM, Paczulla A, Wang H, Schairer R, Wiehr S, Kohlhofer U, et al. SOX2 expression associates with stem cell state in human ovarian carcinoma. Cancer Res. 2013;73(17):5544-55.
17. Lee S, Kim JY, Kim YJ, Seok KO, Kim JH, Chang YJ, et al. Nucleolar protein GLTSCR2 stabilizes p53 in response to ribosomal stresses. Cell Death Differ. 2012;19(10):1613-22.
18. Rein DT, Volkmer A, Beyer IM, Curiel DT, Janni W, Dragoi A, et al. Treatment of chemotherapy resistant ovarian cancer with a MDR1 targeted oncolytic adenovirus. Gynecologic Oncology. 2011;123(1):138-46.
19. Chau WK, Ip CK, Mak ASC, Lai HC, Wong AST. c-Kit mediates chemoresistance and tumor-initiating capacity of ovarian cancer cells through activation of Wnt/beta-catenin-ATP-binding cassette G2 signaling. Oncogene. 2013;32(22):2767-81.
20. Wang YN, Cardenas H, Fang F, Condello S, Taverna P, Segar M, et al. Epigenetic Targeting of Ovarian Cancer Stem Cells. Cancer Research. 2014;74(17):4922-36.
21. Peng S, Maihle NJ, Huang Y. Pluripotency factors Lin28 and Oct4 identify a sub-population of stem cell-like cells in ovarian cancer. Oncogene. 2010;29(14):2153-9.
22. Xu CX, Xu M, Tan L, Yang H, Permuth-Wey J, Kruk PA, et al. MicroRNA miR-214 regulates ovarian cancer cell stemness by targeting p53/Nanog. J Biol Chem. 2012;287(42):34970-8.
23. Lambe M, Wigertz A, Garmo H, Walldius G, Jungner I, Hammar N. Impaired glucose metabolism and diabetes and the risk of breast, endometrial, and ovarian cancer. Cancer causes & control : CCC. 2011;22(8):1163-71.
24. Suh DH, Kim MK, No JH, Chung HH, Song YS. Metabolic approaches to overcoming chemoresistance in ovarian cancer. Annals of the New York Academy of Sciences. 2011;1229:53-60.
25. Gottesman MM, Fojo T, Bates SE. Multidrug resistance in cancer: Role of ATP-dependent transporters. Nat Rev Cancer. 2002;2(1):48-58.
26. Fletcher JI, Haber M, Henderson MJ, Norris MD. ABC transporters in cancer:

more than just drug efflux pumps. Nat Rev Cancer. 2010;10(2):147-56.
27. Gao B, Russell A, Beesley J, Chen XQ, Healey S, Henderson M, et al. Paclitaxel sensitivity in relation to ABCB1 expression, efflux and single nucleotide polymorphisms in ovarian cancer. Sci Rep-Uk. 2014;4.
28. Stordal B, Hamon M, McEneaney V, Roche S, Gillet JP, O'Leary JJ, et al. Resistance to Paclitaxel in a Cisplatin-Resistant Ovarian Cancer Cell Line Is Mediated by P-Glycoprotein. Plos One. 2012;7(7).
29. Koti M, Gooding RJ, Nuin P, Haslehurst A, Crane C, Weberpals J, et al. Identification of the IGF1/PI3K/NF kappaB/ERK gene signalling networks associated with chemotherapy resistance and treatment response in high-grade serous epithelial ovarian cancer. BMC Cancer. 2013;13:549.
30. Birsoy K, Possemato R, Lorbeer FK, Bayraktar EC, Thiru P, Yucel B, et al. Metabolic determinants of cancer cell sensitivity to glucose limitation and biguanides. Nature. 2014;508(7494):108-12.
31. Palorini R, Cammarata FP, Balestrieri C, Monestiroli A, Vasso M, Gelfi C, et al. Glucose starvation induces cell death in K-ras-transformed cells by interfering with the hexosamine biosynthesis pathway and activating the unfolded protein response. Cell Death Dis. 2013;4:e732.
32. Pinho SS, Reis CA. Glycosylation in cancer: mechanisms and clinical implications. Nat Rev Cancer. 2015;15(9):540-55.
33. Wakabayashi-Nakao K, Tamura A, Furukawa T, Nakagawa H, Ishikawa T. Quality control of human ABCG2 protein in the endoplasmic reticulum: ubiquitination and proteasomal degradation. Adv Drug Deliv Rev. 2009;61(1):66-72.
34. Clevers H, Nusse R. Wnt/beta-Catenin Signaling and Disease. Cell. 2012;149(6):1192-205.
35. Li DS. GSK-3 beta as a driving force in ovarian cancer. Cell Res. 2006;16(7):609-.
36. Rask K, Nilsson A, Brannstrom M, Carlsson P, Hellberg P, Janson PO, et al. Wnt-signalling pathway in ovarian epithelial tumours: increased expression of beta-catenin and GSK3 beta. Brit J Cancer. 2003;89(7):1298-304.
37. Gershoni-Baruch R, Patael Y, Dagan, Figer A, Kasinetz L, Kadouri E, et al. Association of the I1307K APC mutation with hereditary and sporadic breast/ovarian cancer: more questions than answers. Brit J Cancer. 2000;83(2):153-5.
38. Arend RC, Londono-Joshi AI, Straughn JM, Buchsbaum DJ. The Wnt/beta-catenin pathway in ovarian cancer: A review. Gynecologic Oncology. 2013;131(3):772-9.

39. Nagaraj AB, Joseph P, Kovalenko O, Singh S, Armstrong A, Redline R, et al. Critical role of Wnt/beta-catenin signaling in driving epithelial ovarian cancer platinum resistance. Oncotarget. 2015;6(27):23720-34.
40. Van Camp J, Beckers S, Zegers D, Van Hul W. Wnt Signaling and the Control of Human Stem Cell Fate. Stem Cell Rev Rep. 2014;10(2):207-29.
41. Kahn M. Can we safely target the WNT pathway? Nat Rev Drug Discov. 2014;13(7):513-32.
42. Takebe N, Harris PJ, Warren RQ, Ivy SP. Targeting cancer stem cells by inhibiting Wnt, notch, and Hedgehog pathways. Nat Rev Clin Oncol. 2011;8(2):97-106.
43. Klaus A, Birchmeier W. Wnt signalling and its impact on development and cancer. Nat Rev Cancer. 2008;8(5):387-98.
44. Hu L, McArthur C, Jaffe RB. Ovarian cancer stem-like side-population cells are tumourigenic and chemoresistant. Brit J Cancer. 2010;102(8):1276-83.
45. Bapat SA, Mali AM, Koppikar CB, Kurrey NK. Stem and progenitor-like cells contribute to the aggressive behavior of human epithelial ovarian cancer. Cancer Research. 2005;65(8):3025-9.
46. Johnatty SE, Beesley J, Paul J, Fereday S, Spurdle AB, Webb PM, et al. ABCB1 (MDR 1) polymorphisms and progression-free survival among women with ovarian cancer following paclitaxel/carboplatin chemotherapy. Clin Cancer Res. 2008;14(17):5594-601.
47. Talekar M, Ouyang Q, Goldberg MS, Amiji MM. Cosilencing of PKM-2 and MDR-1 Sensitizes Multidrug-Resistant Ovarian Cancer Cells to Paclitaxel in a Murine Model of Ovarian Cancer. Molecular Cancer Therapeutics. 2015;14(7):1521-31.
48. Nakagawa H, Wakabayashi-Nakao K, Tamura A, Toyoda Y, Koshiba S, Ishikawa T. Disruption of N-linked glycosylation enhances ubiquitin-mediated proteasomal degradation of the human ATP-binding cassette transporter ABCG2. FEBS J. 2009;276(24):7237-52.
49. Chocarro-Calvo A, Garcia-Martinez JM, Ardila-Gonzalez S, De la Vieja A, Garcia-Jimenez C. Glucose-Induced beta-Catenin Acetylation Enhances Wnt Signaling in Cancer. Mol Cell. 2013;49(3):474-86.
50. Elghazi L, Gould AP, Weiss AJ, Barker DJ, Callaghan J, Opland D, et al. Importance of beta-Catenin in glucose and energy homeostasis. Sci Rep-Uk. 2012;2.
51. Nusse R. Wnt signaling and stem cell control. Cell Res. 2008;18(5):523-7.
52. Gough NR. Focus Issue: Wnt and beta-Catenin Signaling in Development and

Disease. Sci Signal. 2012;5(206).
53. Pasto A, Bellio C, Pilotto G, Ciminale V, Silic-Benussi M, Guzzo G, et al. Cancer stem cells from epithelial ovarian cancer patients privilege oxidative phosphorylation, and resist glucose deprivation. Oncotarget. 2014;5(12):4305-19.
54. Liu PP, Liao J, Tang ZJ, Wu WJ, Yang J, Zeng ZL, et al. Metabolic regulation of cancer cell side population by glucose through activation of the Akt pathway. Cell Death Differ. 2014;21(1):124-35.
55. Zhao Y, Butler EB, Tan M. Targeting cellular metabolism to improve cancer therapeutics. Cell death & disease. 2013;4:e532.
56. Galluzzi L, Kepp O, Vander Heiden MG, Kroemer G. Metabolic targets for cancer therapy. Nat Rev Drug Discov. 2013;12(11):829-46.

Chapter 5. Conclusion

5.1. Conclusion

Ovarian cancer is the most lethal gynecologic oncology in worldwide. Most of patients with ovarian cancer diagnose at the advanced stage and two-third of them experienced disease recurrence and chemoresistance (1, 2). Currently, the primary goal of ovarian cancer treatment is enhanced the sensitivity of conventional chemotherapy and restrained the recurrence (2, 3).

Epidemiological data have been expanded of the concepts that: changes in metabolism influences tumorigenesis, tumor progression and response to therapy (4). Even though clear differences in the metabolic phenotypes between cancers and normal, there are no strong indicators for cancer targeted therapeutic approach based on the notion of the metabolic alterations, so far. Based on the fact that, higher levels of glucose and overexpressions of glucose transporter 1 (GLUT1) have been shown the association with disease recurrence and poor prognosis in ovarian cancer (5, 6). With this signature, disruption of glucose metabolism is suggested as the therapeutic target for ovarian cancer patients.

In current study, we have characterized the selective cytotoxicity of resveratrol (RSV) in ovarian cancer cells through glucose metabolism regulation via GLUT1 modulation. We have

demonstrated that, in contrast to primary normal ovarian epithelial cells, RSV selectively inhibited glucose uptake and induced apoptosis irrespective of p53 status *in vitro*. RSV had no affect on GLUT1 mRNA and protein expressions but interrupted intracellular GLUT1 trafficking to the plasma membrane. Suppressed plasma membrane GLUT1 localization in ovarian cancer was found to be associated with the inhibition of Akt activity by RSV, as confirmed by the action of the Akt inhibitors (LY294002 and Akt inhibitor IV), as well as overexpression of a constitutive active form of Akt. Taken together, these findings suggested that RSV induced apoptosis in ovarian cancer cells by impairing glucose uptake, a process involving Akt-regulated plasma membrane GLUT1 trafficking.

Further, focusing on the utility of glucose metabolism as a therapeutic target, we demonstrated here that resveratrol induced endoplasmic reticulum (ER) stress-mediated apoptosis due to interrupt protein glycosylation in a cancer-specific manner. Our results indicated that resveratrol suppressed hexosamine biosynthetic pathway and interrupted protein glycosylation with GSK3β-activation. Application of either biochemical intermediates of hexosamine pathway or small molecular inhibitors of GSK3β reversed the effects of resveratrol which disrupts protein glycosylation. Furthermore, ER UDPase, ENTPD5 (ectonucleoside triphosphate diphosphohydrolase 5) modulated protein

glycosylation via Akt suppression in response to resveratrol. With inhibition or overexpression of Akt functions, we confirmed the glycosylation activities were dependent on the ENTPD5 expressions and it was charged for the action of Akt in ovarian cancer cells. Resveratrol-mediated disruption of protein glycosylation leads to the induction of cellular apoptosis as indicated by the up-regulation of GADD153, followed by the activation of ER-stress sensors (PERK, IRE1α and ATF6α). Thus, our results provide a novel insight into cancer cell metabolism and protein glycosylation as the therapeutic potential of targeting glucose metabolism for cancers.

In the third chapter, we provide evidence that glucose play a pivotal role in controlling drug resistance in ovarian cancer. Lack of glucose availabilities enhanced cisplatin (CDDP) responses, nonetheless high glucose conditions (20 mM) had opposite effect in ovarian cancer cells. Glucose starvation increased the CDDP responses via interrupted membrane localization of ATP-binding cassette transporters (ABC transporters), result from glycosylation defect. Glycosylation of ABC transporters was regulated by GSK3β through activation of AMPK cascades. Moreover, glucose deficiency attenuated the ovarian cancer stem-like cells phenotypes, sphere forming capacities and stemness related gene expressions, a response to suppression of Wnt/β-catenin signaling by GSK3β activation. Our

findings support that the importance of glucose in cancer, as ABC transporter modulator and novel therapeutic strategies for overcoming chemoresistance.

5.2. References

1. Vaughan S, Coward JI, Bast RC, Berchuck A, Berek JS, Brenton JD, et al. Rethinking ovarian cancer: recommendations for improving outcomes. Nat Rev Cancer. 2011;11(10):719-25.

2. Bowtell DD, Bohm S, Ahmed AA, Aspuria PJ, Bast RC, Jr., Beral V, et al. Rethinking ovarian cancer II: reducing mortality from high-grade serous ovarian cancer. Nat Rev Cancer. 2015;15(11):668-79.

3. Coleman RL, Monk BJ, Sood AK, Herzog TJ. Latest research and treatment of advanced-stage epithelial ovarian cancer. Nat Rev Clin Oncol. 2013;10(4):211-24.

4. Galluzzi L, Kepp O, Vander Heiden MG, Kroemer G. Metabolic targets for cancer therapy (vol 12, pg 829, 2013). Nat Rev Drug Discov. 2013;12(12):965-.

5. Lamkin DM, Spitz DR, Shahzad MM, Zimmerman B, Lenihan DJ, Degeest K, et al. Glucose as a prognostic factor in ovarian carcinoma. Cancer-Am Cancer Soc. 2009;115(5):1021-7.

6. Kurokawa T, Yoshida Y, Kawahara K, Tsuchida T, Okazawa H, Fujibayashi Y, et al. Expression of GLUT-1 glucose transfer, cellular proliferation activity and grade of tumor correlate with [F-18]-fluorodeoxyglucose uptake by positron emission tomography in epithelial tumors of the ovary. International journal of cancer Journal international du cancer. 2004;109(6):926-32.

국문초록

난소암은 가장 치명적인 부인과 종양으로 대부분의 환자가 병변이 진행된 상태에서 발견되며, 이는 암종의 재발 및 항암제 내성과 깊은 연관이 있다. 해서 난소암의 조기 진단 마커의 발견 및 재발로 인한 항암제 내성을 억제하는 것이 중요하다.

종양의 대사 활성은 암종의 악성 병변 및 항암제 반응성과 깊은 연관성이 있다고 제안되고 있고 암종의 대사 활성은 정상세포의 그것과는 뚜렷한 차이를 보임으로 이를 표적하는 약제 개발의 중요성이 대두되고 있다. 하지만, 많은 연구에도 불구하고 현재 암종의 대사 특이성에 관한 깊은 이해가 부족하고 관련 약제의 개발이 더뎌지고 있는 실정이다. 난소암은 당 대사의 특이성을 가지고 있는 암종의 하나로, 당 대사에 의존도가 높고 당 수송체 (glucose transporter 1, GLUT1)의 과발현이 악성 병변 및 불량한 예후와 관련이 있다고 보고된 바 있다.

본 연구에서는 천연 화합물인 resveratrol (RSV)가 당 수송체인 GLUT1의 조절을 통한 난소암의 특이적 세포사멸을 이끄는 것을 확인하였다. RSV의 효과를 확인하기 위해, 정상

난소 표피세포를 배양하여 사용하였고 다양한 난소암 세포주를 이용하였다. RSV 는 난소암 세포 특이적으로 포도당 흡수를 억제하고, 세포사멸을 유도하였다. RSV는 Akt 억제를 통한 GLUT1의 세포막 이동을 억제하였고, 이는 Akt 억제제 (LY294002 와 Akt inhibitor IV) 및 Akt 과발현을 통하여 확인하였다. 해서 RSV는 GLUT1의 조절을 통한 난소암의 당 흡수를 억제, 이를 통한 암세포 특이적 세포사멸을 유도함을 확인하였다.

더 나아가서, 단백질의 당화를 통한 세포신호전달 물질로서의 포도당 역할을 확인하였다. RSV가 유도하는 포도당 흡수 억제는 단백질의 당화를 억제, 극심한 소포체 스트레스 (endoplasmic reticulum (ER) stress)를 유도함으로 세포사멸이 유도됨을 확인하였다. 흥미롭게도 정상세포에서는 RSV가 유도하는 이러한 현상은 정상세포에서는 나타나지 않았으며 세포독성도 나타내지 않았다. RSV는 단백질 당화 초기단계 (hexosamine biosynthetic pathway)에 영향을 주고 이와 관련된 분자적 기전으로는GSK3β의 활성이 관련되어 있었으며, 소포체에 존재하는 UDP 가수분해효소인ENTPD5 (ectonucleoside triphosphate diphosphohydrolase 5) 활성을

억제함으로서 단백질의 당화를 방해함이 확인되었다. 이러한 연구결과를 종합해볼 때, resveratrol은 정상세포에는 영향을 미치지 않으면서 선택적으로 난소암세포의 사멸을 유도됨을 알 수 있다. Resveratrol 또는 이 약제가 유도하는 분자적 기전은 향후 난소암 치료제로서 큰 효과를 기대해 볼 수 있을 것이라 사료된다.

항암제 내성을 극복을 위한 많은 연구가 수행되었음에도 불구하고 이를 조절한다고 기 밝혀진 분자적 물질의 표적 치료제의 효과가 미미하여 난소암의 치료 효과가 크게 증진되지 못하였다. 최근 연구에서 난소암의 당 대사 조절이 치료효과를 증진시킬 수 있다 보고하고 있으나 관련 분자적 기전에 대한 연구는 미미한 실정이다. 본 연구에서는 포도당이 난소암의 항암제 내성과 뚜렷한 연관성이 있는ATP-binding cassette transporters (ABC transporters)의 당화 조절을 통한 이의 활성 및 세포막 이동의 조절을 통하여 기존 항암제의 효과를 증진시킴을 확인하였다. 포도당 억제는ABC transporters의 당화를 억제함으로서 이 단백질들의 발현을 억제시키고 세포막 이동을 방해함을 확인하였다. 이 현상과 더불어 난소암의 표준 치료제인 cisplatin (CDDP)효과를 증진시키는 것

또한 확인되었다. 포도당 억제는 세포내의 대사활성 조절 기작으로 알려진 AMPK 활성을 유도함으로 GSK3β 활성을 도모, ABC transporters의 당화 억제에 기여함이 확인되었다. 이 관련 기작은 난소암의 항암제 내성에 또 다른 특징인 암 줄기세포 (cancer stem-like cells)의 발현 조절에도 기여함이 확인되었다. 연구 결과를 종합하여 볼 때, 포도당 대사 조절은 암세포의 선택적 사멸을 유도할 수 있는 치료법으로 제안될 수 있고 항암제 내성을 극복할 수 있는 대안이 될 것이라 기대된다.